Article

Design, synthesis and biological evaluation of 2-nitroimidazopyrazin-one/-es with antitubercular and antiparasitic activity

Angie M Jarrad, Chee Wei Ang, Anjan Debnath, Hye Jee Hahn, Kyra Woods, Lendl Tan, Melissa L Sykes, Amy J. Jones, Ruby Pelingon, Mark Stuart Butler, Vicky M. Avery, Nicholas P. West, Tomislav Karoli, Mark Arnold Thomas Blaskovich, and Matthew A. Cooper

J. Med. Chem., **Just Accepted Manuscript** • DOI: 10.1021/acs.jmedchem.8b01578 • Publication Date (Web): 23 Nov 2018

Manuscript

Design, synthesis and biological evaluation of 2-nitroimidazopyrazin-one/-es with antitubercular and antiparasitic activity

Angie M. Jarrad[1,§], Chee Wei Ang[1,§], Anjan Debnath[2], Hye Jee Hahn[2], Kyra Woods[3], Lendl Tan[3], Melissa L. Sykes[4], Amy J. Jones[4], Ruby Pelingon[1], Mark S. Butler[1], Vicky M. Avery[4], Nicholas P. West[3], Tomislav Karoli[1, #,] Mark A.T. Blaskovich[1,*] and Matthew A. Cooper[1,*]

[1] Institute for Molecular Bioscience, The University of Queensland, St Lucia, Queensland, 4072, Australia

[2] Center for Discovery and Innovation in Parasitic Diseases, Skaggs School of Pharmacy and Pharmaceutical Sciences, University of California, San Diego, La Jolla, CA 92093 USA

[3] School of Chemistry and Molecular Bioscience, The University of Queensland, St Lucia, Queensland, 4072, Australia

[4] Discovery Biology, Griffith Institute for Drug Discovery, Griffith University, Nathan, Queensland, 4111, Australia

§Authors contributed equally; *joint corresponding authors

Abstract

Tuberculosis and parasitic diseases, such as giardiasis, amebiasis, leishmaniasis and trypanosomiasis, all urgently require improved treatment options. Recently, it has been shown that anti-tubercular bicyclic nitroimidazoles such as pretomanid and delamanid have potential as repurposed therapeutics for the treatment of visceral leishmaniasis. Here we show that pretomanid also possesses potent activity against *Giardia lamblia* and *Entamoeba histolytica*, thus expanding the therapeutic potential of nitroimidazo-

oxazines. Synthetic analogs with the novel nitroimidazopyrazin-one/-e bicyclic nitroimidazole chemotype were designed, synthesized and structure activity relationships generated. Selected derivatives had potent antiparasitic and antitubercular activity whilst maintaining drug-like properties such as low cytotoxicity, good metabolic stability in liver microsomes and high apparent permeability across Caco-2 cells. The kinetic solubility of the new bicyclic derivatives varied, and was found to be a key parameter for future optimization. Taken together, these results suggest promising subclasses of bicyclic nitroimidazoles containing different core architectures have potential for further development.

Introduction

Infectious diseases are an enormous global health burden. The nitroimidazole class of antibiotics, exemplified by metronidazole (**1**, Figure 1), has a long history of use to treat bacterial and parasitic infections.[1] The mode of action of nitroimidazoles involves partial reduction of the nitro group and subsequent decomposition of the compound to give toxic radical species that cause DNA and protein damage.[1] The nitro group is activated by different mechanisms, with multiple enzymes involved in electron transfer reactions in different target organisms, which accounts for the remarkably broad spectra of action of the class. More recently, there have been issues with clinical efficacy that are accompanied, in some cases, by development of resistance, which has prompted re-examination of this old, but still widely used drug class.

New clinical applications of "old" nitroimidazoles and the development of novel nitroimidazoles with a bicyclic core scaffold architecture have significant potential to address the emergent unmet medical need imparted by resistant bacteria and parasites. For example, secnidazole (**2**, Figure 1) was recently approved in the USA for the treatment of bacterial vaginosis, despite being available earlier as a generic in many jurisdictions.[2,3] A pediatric formulation of benznidazole **3** (Figure 1), a 2-nitroimidazole used for treatment of Chagas disease caused by the parasite *Trypanosoma cruzi*, gained FDA approval in 2017

for use in children.[4] The Drugs for Neglected Diseases *initiative* (DND*i*) is currently investigating fexinidazole (**4**, Figure 1) as a candidate for oral treatment of human African trypanosomiasis (HAT), a parasitic infection caused by *Trypanosoma brucei spp.* that is a public health threat to ~70 million people in Africa.[5] Furthermore, bicyclic nitroimidazoles, such as delamanid (**5**, Figure 1) and pretomanid (**6**, PA-824), are promising new antimicrobials being developed for the treatment of tuberculosis (TB),[6] the number one cause of death from infectious diseases and the ninth leading cause of death worldwide.[7] The nitroimidazo-oxazole **5** gained conditional approval in the European Union in 2014 for the treatment of drug resistant TB. This agent was derived from CGI 17341 (**7**)[8,9] and overcame the mutagenic liability of **7** (Figure 1).[10,11] Meanwhile, **6** was developed concurrently with **5**, and is currently in Phase III trials. The PK profile of **6** is superior to **5** and this permits once daily dosing, although **6** is less potent.[12]

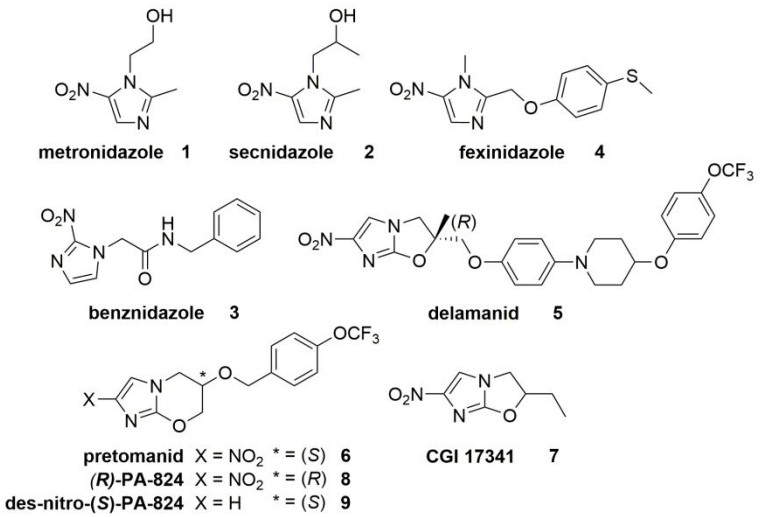

Figure 1. Monocyclic nitroimidazoles **1-4** and the bicyclic variants delamanid (**5**), pretomanid (**6**), CGI 17341 (**7**) and *(R)*-PA-824 (**8**).

Investigations on how **5** and **6** inhibit *M. tuberculosis* under aerobic and anaerobic growth conditions revealed an interesting dual mode of action. Transcriptional profiling of *M. tuberculosis* treated with **6** under aerobic growth conditions, gave a response consistent with both the inhibition of cell wall mycolic acid biosynthesis and also respiratory poisoning.[13] Additionally, it was shown that deazaflavin dependent

nitroreductase (Ddn) catalyzed reduction of **6** to the des-nitro **9** metabolite and that this process generated nitric oxide.[14] Nitric oxide could be detected in *Mycobacterium bovis* cells treated with **6** under both aerobic and anaerobic growth conditions and the rate of NO release in *M. bovis* cells correlated with the anaerobic activities for a series of analogues, supporting the premise that this is the mode of action of this class under anaerobic growth conditions in *M. tuberculosis*.[14] In comparison, **1** is only active against non-replicating *M. tuberculosis* under anaerobic growth conditions (<0.06% oxygen).[15] Nitroimidazoxazine **6** was also investigated for activity against other kinetoplastid organisms in multiple developmental life stages including *L. donovani (*promastigote and amastigote), *T. brucei brucei* (procyclic and bloodstream) and *T. cruzi (*epimastigote and amastigote),[16] with the findings prompting further mode of action studies in *L. donovani*. Compound **8**, the *R*- enantiomer of **6,** was shown to be more effective than the *S*- enantiomer in an in vivo model of visceral leishmaniasis.[16] Recently, an NAD(P)H oxidase was identified as the activating nitroreductase (NTR2) for the nitroimidazo-oxazole/-oxazine.[17] However, the monocyclic sulfone metabolite of **4**, known to be activated by a type I nitroreductase, [18] was only marginally activated by NTR2.[17] These results support the hypothesis that **6** is activated by an alternative mechanism of action in *L. donovani* under these culture conditions and illustrates the biological complexity of the mode of action of various nitroimidazoles.

In the course of development of **5** and **6** as treatments for tuberculosis, over 1000 derivatives were prepared.[19] The structure activity relationships disclosed to date mostly include compounds with modifications to the aryl side chain, with a smaller number of variants that alter the bicyclic core structure (Figure 2A). The nitro group and stereochemistry of the side chain have been shown to be critical for activity as both **8** and *S*-des-nitro-PA-824 (**9**) derivatives were inactive in in vitro cultures at 50 μM.[16] An analog with the nitro group at the 3′ position was shown to be inactive, clarifying that the 2′ position of the nitro group on the **6** bicyclic scaffold is important for activity.[20] Replacement of the benzylic oxygen with nitrogen led to an amino linked series (**10a-b**) with favorable in vitro activity and solubility

properties.[21,22] Modification of the imidazole ring to a pyrazole (**11a**) or triazole (**11b**) was detrimental to *M. tuberculosis* activity, as was replacement of the oxygen heteroatom in the oxazine ring with sulfoxide (**11c**), sulfone (**11d**), amino (**11e**) or methylene (**11f**) groups, although a sulfur (**11g**) heteroatom in the ring was tolerated.[23]

More recent efforts have explored the activity of bicyclic nitroimidazoles against the kinetoplastids *Leishmania* and trypanosomes. DND*i* is currently investigating additional nitro-imidazooxazines for development against visceral leishmaniasis,[24] including DNDI-8219 (**12**) and DNDI-0690 (**13**), 6- and 7-substituted imidazooxazines, as two promising backup candidates.[25,26] Interestingly, nitroimidazothiazine oxides **14a-d** were found to display favorable activity against *T. b. brucei*, an animal infective strain that is commonly used as a model of HAT.[19] Moreover, a "thio-delamanid" derivative (**15**) proved to be efficacious against *T. cruzi*, although it was inactive against *Leishmania*.[27] These studies demonstrate that the selectivity profile toward different parasites can be altered by structural modifications of the bicyclic scaffold and that different subclasses of the bicyclic nitroimidazoles expand the potential therapeutic scope of this antimicrobial class.

We reasoned that bicyclic nitroimidazole derivatives could have potential against an even wider range of organisms than *Leishmania* and trypanosomes. Previously we found that 4(5)-nitroimidazoles (**16**)[28] had potent activity against *Giardia lamblia*, *Entamoeba histolytica*, *Trichomonas vaginalis* and *Clostridium difficile* (Figure 2B) and therefore it was hypothesized that **6** might also have activity against these organisms. Anaerobic protozoa such as *G. lamblia* and *E. histolytica* and the anaerobic bacteria *C. difficile* occupy the gut under reduced oxygen tension and cause diarrheal infections. These organisms spread by the fecal oral route through stable cyst forms for the protozoa or through spores for *C. difficile*. Metronidazole **1** can be used therapeutically for infections caused by these organisms, but alternative treatment options are desirable. Furthermore, cyclizing the 4(5)-nitroimidazoles **16** from the 1′ imidazole

ring position to the carboxamide nitrogen could produce new bicyclic nitroimidazopyrazin-one/-e scaffolds. These could potentially extend the spectra of biological activity to include *M. tuberculosis* and result in altered structure activity relationships against a panel of parasitic organisms. Previous studies have shown that compounds containing the imidazopyrazinone scaffold have a range of different biological activities, including agonism of the $GABA_A$ receptor[29], antagonism of the ionotropic transmembrane receptor,[30,31] modulation of ion channels to control arrhythmia[32] and inhibition of *M. tuberculosis* glutamine synthetase[33]. However, no studies have investigated the antimicrobial activity of a nitrated derivative of this class.

We now report the findings from an evaluation of **6** against a wide range of organisms, and the subsequent design, synthesis and biological evaluation of novel bicyclic nitroimidazoles, nitroimidazopyrazinones (**17**) and nitroimidazopyrazines (**18**) (Figure 2B), derived from the 4(5)-nitroimidazole scaffold **16** previously reported.[28] Given the potential for activity against many different organisms, compounds were screened against a wide range of microorganisms including: *G. lamblia*, *E. histolytica*, *T. b. brucei*, *L. donovani*, *M. tuberculosis*, *C. difficile*, *Cryptoccoccus neoformans*, *Candida albicans* and representative ESKAPE bacteria: *Escherichia coli*, *Staphylococcus aureus*, *Klebsiella pneumoniae*, *Pseudomonas aeruginosa* and *Actinetobacter baumannii*. Derivatives were counter-screened for cytotoxicity against mammalian liver and kidney cell lines. Preferred derivatives with favorable antimicrobial or antiparasitic activity were then evaluated for therapeutic properties including metabolic stability, plasma protein binding and intestinal permeability. Most of the compounds were also assessed for aqueous kinetic solubility. This report presents the first description of structure activity relationships and evaluation of nitroimidazopyrazin-ones/es for antimicrobial and antiparasitic activity with therapeutic potential.

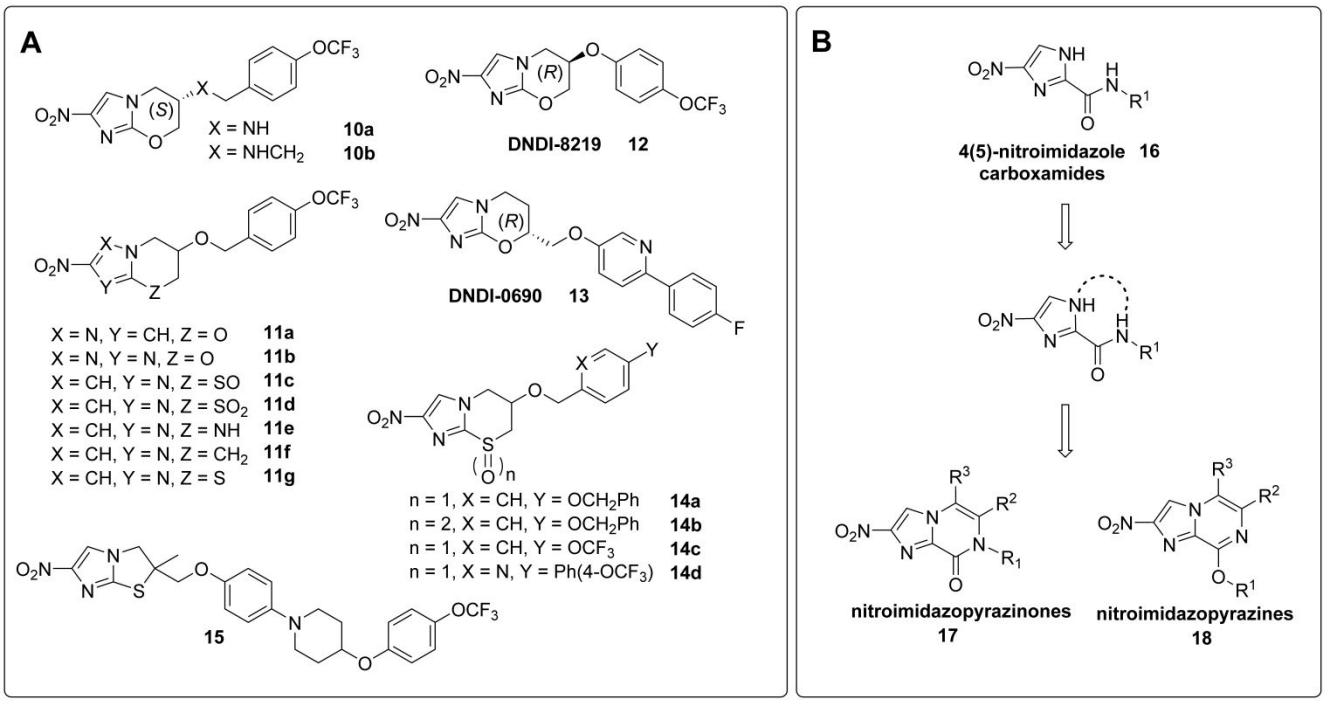

Figure 2. A) Structural variation of bicyclic nitroimidazoles described in the literature and B) the novel nitroimidazopyrazinones and nitroimidazopyrazinones, developed by cyclizing the 4(5)-nitroimidazole framework, described here.

Chemistry

Design and Synthesis of Bicyclic Nitroimidazoles with Variation at R^1, $R^2 = R^3 = H$

In previous work[28] a set of amide-substituted monocyclic nitroimidazoles were prepared and it was hypothesized for this study that linking the amide and imidazole nitrogen could form a bicyclic nitroimidazopyrazinone system, similar to the pretomanid **6** core (Figure 2B). A library of nitroimidazopyrazinones **17a-t** were prepared with different functional groups at R^1 designed to explore a range of physicochemical properties (Scheme 1). Initial biological results indicated that benzylic R^1 groups were favorable for antimicrobial and antiparasitic activity. The library was therefore tailored to contain analogs with a number of different benzyl substituted R^1 groups (**17b-j**), including derivative **17c** with a 4-OCF_3-substituted benzyl group similar to pretomanid, and analogs with substitutions at the 3′ and 2′ positions. Compound **17k** was prepared with $R^1 = CH_2$-(2-pyridyl) to introduce a hydrogen bond

acceptor and to impart more polarity and improve aqueous solubility. A methyl group was introduced at the benzylic position (**17l**) to increase the lipophilicity, bulk and potentially restrict the conformation of the side chain. Two phenethylene derivatives (**17m-n)** were prepared to investigate the effect of spacing the aromatic ring further from the bicyclic core. Derivatives with polar side chain R^1 groups were also synthesized, including ethyl acetate **17o**, ethyl hydroxyl **17p**, morpholine derivatives **17q-r** and the carboxamide group (**17s**). Compound **17t** with R^1 = cyclohexyl group was prepared to investigate the effect of a bulky aliphatic group at this position.

Initially, nitroimidazopyrazinones **17a-f**, **17k-l**, **17n** and **17t** were prepared from 4(5)-nitroimidazole carboxamides **16a-f** , **16k-l**, **16n** and **16t**[28] by cyclizing the 1′ imidazole to the 2′ free amide nitrogen (route 1, Scheme 1). This was achieved by alkylating 4(5)-nitroimidazoles with bromoacetaldehyde diethyl acetal under basic conditions (K_2CO_3) which strongly favored the 4-nitro regioisomer product.[34] Secondly, microwave heating (μW 120°C) of **19a-f**, **19k-l**, **19n** and **19t** under acidic conditions afforded the bicyclic products **17a-f**, **17k-l**, **17n** and **17t**. This synthesis was based on the preparation of des-nitro-imidazopyrazinone **20a**, as previously described by Prévot and Leumann;[35] however, microwave heating at higher temperatures and for shorter periods than conventional reflux facilitated analog generation for both steps. Secondly, inclusion of a cosolvent (aq. 2M HCl :1,4-dioxane 1:1) was necessary to solubilize the secondary amide starting material and achieve conversion to the desired products **17b-f**, **17k-l**, **17n** and **17t**. With this approach, products often precipitated from the reaction mixture and could be isolated in high purity by filtration and washes (H_2O) alone, especially if the intermediate had been purified by chromatography. Alternatively, the products were purified by recrystallization. In the ^{1}H NMR, the imidazopyrazinone R^2 and R^3 proton groups were typically two doublets (J = ~5.9 Hz) each integrating for 1 proton at ~ δ7.4 ppm and ~ δ7.6 ppm, respectively. Furthermore, both NMR (2D HMBC) experiments and an X-ray crystal structure of **17a** confirmed the 2-position of the nitro group (Supporting Information, Figure S1).

A second approach to prepare bicyclic nitroimidazoles **17g-j**, **17m**, **17o** and **17q-s** was developed as shown in route 2, Scheme 1. This method was more convergent as it eliminated the need to prepare 4(5)-nitroimidazole intermediates of each derivative. Route 2 involved alkylation of **17a** with alkyl halides under basic conditions (carbonate base) to form **17g-j**, **17m**, **17o** and **17q-s**. This approach also produced the minor *O*-alkylated regioisomer in some cases. This was considered advantageous because the alternative pyrazine ring was anticipated to have different biological activity and properties. In all cases, use of K_2CO_3 or Cs_2CO_3 in DMF resulted in > 10:1 ratio of the pyrazinone to pyrazine derivatives. Reaction with Ag_2CO_3 in toluene and heating as described in the literature,[36,37] was briefly explored and found to increase the ratio of the minor imidazopyrazine isomer, with pyrazinone:pyrazine ratios of 2:1 for **17g**:**18g** and **17i**:**18i**. Unfortunately, the Ag_2CO_3/toluene method resulted in unreacted starting material and a greater number of side products compared to K_2CO_3 or Cs_2CO_3 in DMF. This complicated the separation of **18g** to the required >95% purity for biological assay. Therefore, isomers **17m** and **18m** were prepared using K_2CO_3 in DMF.

Nitroimidazopyrazines were readily distinguished from nitroimidazopyrazinones as they were more lipophilic, and thus were more strongly retained on C18 silica and more weakly retained on normal phase silica. Furthermore, in the ^{1}H NMR the resonance due to the OC$\underline{H}_2$ of **18i** and **18m** was 0.4–0.6 ppm further downfield than the corresponding resonance due to the NC$\underline{H}_2$ group in the pyrazinone scaffold (eg **18i**/**17i** δ 5.64 vs 5.21 ppm). In the ^{13}C NMR spectrum, the corresponding O$\underline{C}H_2$ resonance was also shifted 17–19 ppm downfield for **18i** and **18m** compared to the corresponding N$\underline{C}H_2$ resonance (eg **18i**/**17i** δ 62.7 vs 45.7 ppm).

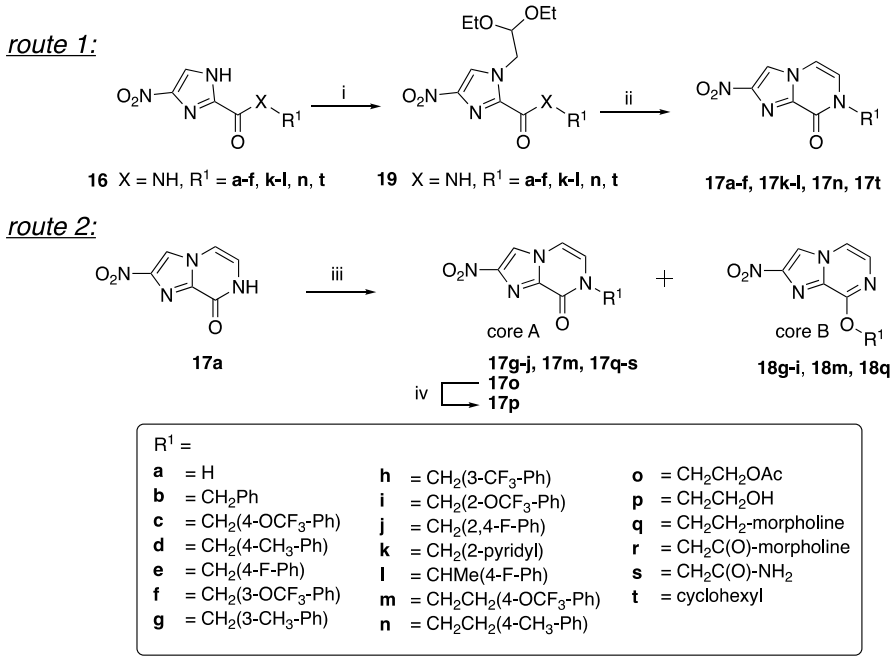

Scheme 1. Synthesis of imidazopyrazin-ones/-es **17a-t**, **18i** and **18m** by route 1) condensation and dehydration via nitroimidazole carboxamide intermediates or route 2) alkylation of **17a**. i) Bromoacetaldehyde diethyl acetal, K_2CO_3, µW 180 °C, 69%–quant. yield, ii) 2M aq. HCl (10 vol), 1,4-dioxane (10 vol), µW 120 ºC, 42–87%, (**17a**: 5% aq. HCl, reflux, 66%); iii) alkyl/benzyl halide, K_2CO_3/Cs_2CO_3, DMF, rt – µW 120 ºC or Ag_2CO_3/toluene, 80 ºC as detailed in the experimental, 3-84% iv) K_2CO_3, MeOH, rt, 45%. Compounds **18g-h** and **18q** were detected but not isolated in pure form.

Des-nitro Derivatives

Des-nitro derivatives **20b-c** were prepared as negative control compounds, essentially as described for the nitrated series above (Scheme 2). It was hypothesized that these compounds should be biologically inactive if the parent compounds had a mechanism of action involving reduction of the nitro group.

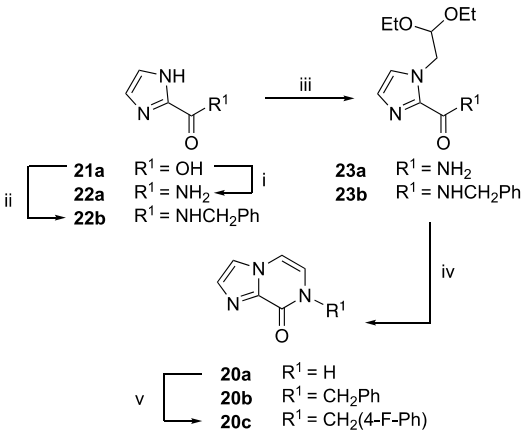

Scheme 2. Synthesis of des-nitro imidazopyrazinones **20b-c**. i) $(COCl)_2$, cat. DMF, DCM, 0 °C → rt, then conc. NH_4OH, 73%[28] ii) $SOCl_2$, reflux, then benzyl amine, 69%; iii) bromoacetaldehyde diethyl acetal, K_2CO_3, μW 120–180 °C, 81–92%; iv) For **20a**: 5% aq. HCl, reflux, 50%; For **20b**: 5% aq. HCl, 80 °C, 39%; v) 4-fluorobenzylamine, K_2CO_3, DMF, rt, 19%.

Design and Synthesis of Nitroimidazopyrazin-ones/es with Modifications at R^2, R^3

We then explored different variations at the R^2 and R^3 positions, established a shortened route to synthesize the imidazopyrazinone core and further investigated the activity of the imidazopyrazine scaffold (Scheme 3). Both core scaffolds were prepared with three different combinations of R^2 and R^3 groups in order to assess how functionalization at these sites could affect activity against different organisms. Since benzyl groups at R^1 were favorable for biological activity, derivatives **24a-e** containing R^2 = Ph and R^3 = H, but including polar substituents (CH_2CH_2OAc or CH_2CH_2OH) at R^1 to counteract the increase in compound lipophilicity, were prepared. The effect of a methyl group at $R^2 = CH_3$, as a small, non-polar substituent (derivatives **25a-m**) was also assessed. For the series with $R^2 = CH_3$, both polar and non-polar substituents at R^1, including $R^1 = CH_2CH_2OAc$, CH_2CH_2OH and several preferred benzyl derivatives were investigated. Lastly, matched pair analogs with $R^2 = R^3 = CH_3$ (**26a-i**) with the preferred benzyl substituents at R^1 were prepared.

The synthesis of the imidazopyrazinone **24a** (R^2 = Ph) was initially performed as in Scheme 3 in a similar manner as described earlier. Intermediate **16a** was alkylated with 2-bromoacetophenone at room temperature with K_2CO_3 as a base catalyst to yield **27a**, which was then purified by silica chromatography. The condensation-dehydration cyclization of **27a** was achieved with 2M aq. HCl and 1,4-dioxane under microwave irradiation to form the phenyl substituted imidazopyrazinone core **24a**. To synthesize the imidazopyrazinone cores with $R^2 = CH_3$ (**25a**) and $R^2 = R^3 = CH_3$ (**26a**), a more concise synthesis was designed that involved a two-step, one-pot tandem alkylation-dehydration reaction (Scheme 3). For **25a** and **26a**, this procedure worked well. The conditions were mild as both steps of the reaction (alkylation and condensation-dehydration) proceeded at room temperature and the products were obtained in high purity after filtration and washes (H_2O and MeOH) of the precipitate (67% yield over two steps). The one pot, two-step methodology was also tested for **24a** (R^2 = phenyl), although conversion and yields were reduced (40% isolated yield with product of 57% purity: Abs% UV254 nm LCMS) due to impurities that formed in both steps because of the different reactivity of the alkylation and condensation-dehydration steps. In addition, product **24a** was slightly soluble in the methanol used in the wash step to remove more non-polar impurities. An intermediate work-up procedure, or optimization of the initial alkylation conditions could be explored to improve this method for **24a**.

Alkylation of imidazopyrazinones **24a**, **25a** and **26a** under basic conditions provided both the *N*- and *O*-alkylated regioisomers that were readily separated by chromatography. Alkylation conditions that used heating in the presence of Cs_2CO_3 generally favored the *O*-alkylated imidazopyrazine product. The method employed here was sufficient to provide both possible isomers for biological evaluation, but further optimization of the reaction conditions could be explored in the future to alter the ratio of *N*- to *O*- alkylated product.[38] Again, the acetate groups were removed using K_2CO_3/MeOH to give the nitroimidazopyrazin-one/-es **24d-e** and **25d-e**.

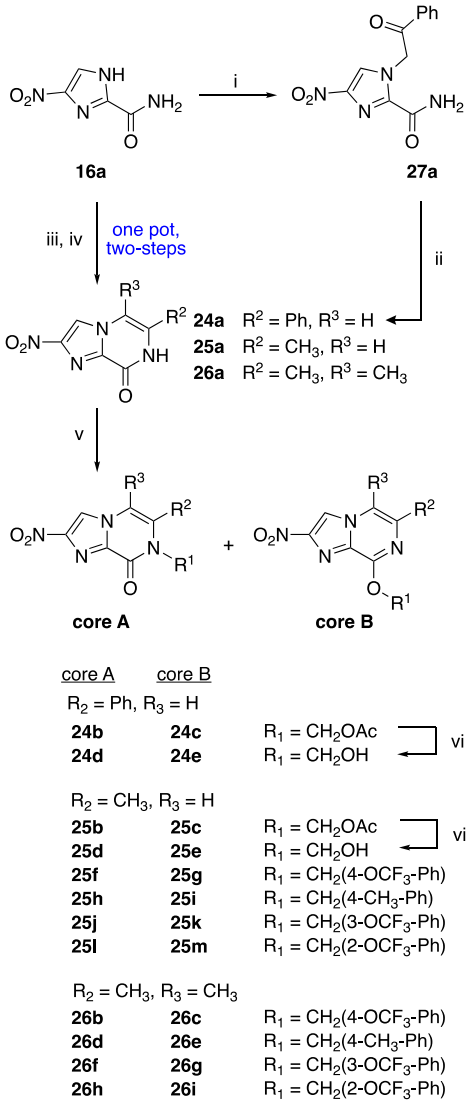

Scheme 3. Synthesis of nitroimidazopyrazinon-one/-es **24a-e**, **25a-m** and **26a-i** with variations at R^2 and R^3. i) 2-Bromoacetophenone, K_2CO_3, DMF, rt, 60%; ii) 2M HCl, 1,4-dioxane, μW 120 ºC, 84%; iii) **25a** & **26a**: α-halo ketone, K_2CO_3, DMF, rt; iv) **25a** & **26a**: 2M HCl, 1,4-dioxane, rt, 40–67% over two steps; v) K_2CO_3 or Cs_2CO_3, DMF, rt – μW 80 ºC, 41–90% yield inclusive of both isomers; vi) K_2CO_3, MeOH, rt, 10–83% yield. Compound **25k** was detected but not isolated.

Results and Discussion

Antiparasitic and Antimicrobial Activity of Pretomanid

Both pretomanid **6** and its enantiomer **8** were found to be ~2-fold more active than metronidazole **1** against *G. lamblia* (Table 1). Both enantiomers also had activity against *E. histolytica*, with **8** active at comparable levels to **1**, and **6** ~2-fold less active than **1**. Compound **6** had moderate activity against *C. difficile* (MIC = 4 μg/mL), which was 8-fold less potent than metronidazole **1** (MIC = 0.5 μg/mL) (Table 1). These results expand the spectrum of action of **6**, which was previously described to inhibit *M. tuberculosis*, *Leishmania spp.* and *Trypanosoma spp.*[16,26] The enantiomers **6**/**8** have been reported to have more significant differences in activities against *L. donovani*, trypanosomes and *M. tuberculosis*.[16] For example, **8** was ~5-fold more active than **6** against *L. donovani* in both the promastigote and amastigote (intracellular macrophage) assays.[16] While **6** had weak activity against *T. cruzi* and *T. b. brucei* in the parasite life stages relevant to mammalian infection, **8** had slightly enhanced activity, similar to the results against *L. donovani*.[16] In contrast, **8** was inactive against *M. tuberculosis*.[39] Compound **8** has previously been shown to bind to the *M. tuberculosis* Ddn enzyme involved in reductive activation of **6**, but it could not be turned over by the enzyme.[39] These differences in selectivity of the enantiomers **6** and **8** likely indicate differences in the mode of action, respective targets, or uptake of compound by the respective organisms. Nonetheless, the results suggest that **6** or newer derivatives may also be repurposed toward enteric parasites. More potent compounds could also potentially be identified in the future by screening a library of pretomanid analogs from the TB alliance/DND*i* collections, given that more than 1000 analogs have been prepared.[19]

Table 1. Activity of pretomanid (6) against enteric pathogens.

Compound	Antiparasitic IC_{50} (μM) (pIC_{50} ± SE)		Antibacterial MIC (μg/mL)
	G. lamblia	*E. histolytica*	*C. difficile*
Metronidazole (1)	7.2 (5.1 ± 0.02)	4.3 (5.4 ± 0.02)	0.5
Pretomanid (6)	3.0 (5.5 ± 0.02)	9.3 (5.0 ± 0.03)	4
(*R*)-PA-824 (8)	3.2 (5.5 ± 0.08)	5.3 (5.3 ± 0.08)	N.D

SAR of Bicyclic Nitroimidazoles with Variation at R^1, $R^2 = R^3 = H$

Given the broad activity of pretomanid **6**, bicyclic nitroimidazoles **17a-t**, **18i** and **18m** were tested against a wide panel of organisms. These organisms included *M. tuberculosis* grown under aerobic (normoxic) and non-replicating (hypoxic) conditions, *G. lamblia* and *E. histolytica*, *L. donovani* (intracellular amastigote assay), *T. b. brucei* and *C. difficile*. To gain a clear understanding of the spectra of action, compounds were also screened against representative ESKAPE bacterial pathogens *S. aureus* (ATCC 43300), *E. coli* (ATCC 25922), *K. pneumoniae* (ATCC 700603), *A. baumannii* (ATCC 19606) and *P. aeruginosa* (ATCC 27853) and fungal pathogens, *C. albicans* (ATCC 90028) and *C. neoformans* (H99 type strain, ATCC 208821) at the Community for Open Antimicrobial Drug Discovery (CO-ADD).[40] The cytotoxicity against mammalian liver HepG2 and kidney HEK293 cell lines was also evaluated.

Gratifyingly, several compounds showed potent activity against *M. tuberculosis*, *G. lamblia* and *T. b. brucei* with the SAR discussed in detail below (Table 2). The *N*- and *O*-alkylated regioisomers had varying profiles, with the nitroimidazopyrazinones **17a-t** consistently lacking activity against *L. donovani*, *E. histolytica* or *C. difficile*. However, nitroimidazopyrazine **18m** was distinguished by its activity against *E. histolytica* (IC_{50} = 7.8 μM, Supporting Information, Table S5) and also *G. lamblia* (IC_{50} = 5.2 μM), despite no activity against *M. tuberculosis* compared to the imidazopyrazinone

derivative **17m**. The screen against ESKAPE and fungal pathogens revealed that these compounds were selective for *M. tuberculosis, G. lamblia* and *T. b. brucei* as they were not active against the other organisms (MIC >32 μg/mL) (Supporting Information, Table S5). Importantly, the majority of the compounds were not cytotoxic at the highest concentration tested (CC_{50} >100 μM) against mammalian liver HepG2 and kidney HEK293 cell lines (CC_{50} > 100 μM) (Supporting Information, Table S5). However, compounds **17b** (R^1 = CH_2Ph) and **17t** (R^1 = cyclohexyl) were moderately cytotoxic against mammalian liver and kidney cell lines (CC_{50} = 98–123 μM) compared to compounds **17a** and **17c-s** (CC_{50} >100 μM). Nitroimidazopyrazine derivatives **18i** and **18m** were also not cytotoxic against mammalian cell lines (CC_{50} >100 μM). This activity profile suggests a specific mechanism of action in *M. tuberculosis*, *G. lamblia* and *T. b. brucei* rather than a general non-specific toxic effect.

Nitroimidazopyrazinones **17b-i** with a monosubstituted benzyl group at R^1 displayed potent activity against *M. tuberculosis* ($MIC_{normoxia}$ = 0.06 –1 μg/mL) at levels up to 2-fold better than pretomanid **6** ($MIC_{normoxia}$ = 0.25–0.5 μg/mL). There was a slight preference for substitution at the 3′ over the 2′ and 4′ positions of the phenyl group (cf. **17f-g** with **17i** and **17c-d**). However, there was otherwise little electronic effect; both electron donating (**17g**, R^1 = CH_2(3-CH_3-Ph)) and withdrawing substituents (**17h**, R^1 = CH_2(3-CF_3-Ph)) had equal activity ($MIC_{normoxia}$ = 0.06 μg/mL). Poor solubility of **17j** in the compound stock solutions was suspected to have contributed to the unexpected weak activity of this disubstituted-fluorine derivative against *M. tuberculosis* and the other organisms. Replacement of the phenyl group (**17b**) with a pyridyl moiety (**17k**) was unfavorable and resulted in a loss of activity against *M. tuberculosis* (**17k** $MIC_{normoxia}$ >32 μg/mL). A methyl substituent at the benzylic position (**17l**) was well tolerated ($MIC_{normoxia}$ = 0.5 μg/mL), but extension of the aromatic linkage with an ethyl bridge in the phenethyl derivatives (**17m-n**) resulted in a 16–32-fold loss of activity against *M. tuberculosis*, with bacteriostatic activity of $MIC_{normoxia}$ = 4-8 μg/mL compared to respective benzyl derivatives **17c-d** with $MIC_{normoxia}$ = 0.125-0.5 μg/mL. None of the derivatives with polar groups at R^1 (**17o-s**) had activity

against *M. tuberculosis* ($MIC_{normoxia}$ >32 μg/mL). Lastly, compound **17t** with an aliphatic cyclohexyl group at R^1 was also inactive ($MIC_{normoxia}$ >32 μg/mL), indicating a preference for an aromatic group rather than non-specific lipophilic group.

In general, compounds with activity against *M. tuberculosis* grown in normoxic conditions were also active against non-replicating *M. tuberculosis* under hypoxic conditions, although generally 2–16-fold less active. By comparison, isoniazid, a compound that inhibits cell wall synthesis in aerobically respiring *M. tuberculosis* (MIC = 0.04 μg/mL), did not inhibit growth in the hypoxic conditions (MIC >5 μg/mL). Metronidazole **1** was inactive (MIC >32 μg/mL) in this hypoxic-recovery assay, indicating the medium was not sufficiently anaerobic to show activity of **1** against *M. tuberculosis*.

The structure activity relationships observed for *G. lamblia* were similar to *M. tuberculosis* and several compounds (**17c-d**, **17f**, **17l-n**) were found to have improved activity (up to 4-fold) relative to metronidazole **1** (IC_{50} = 1.6 to 3.5 μM cf. **1** IC_{50} = 7.2 μM). Interestingly, an expanded range of the derivatives with lipophilic R^1 groups had potent activity against *G. lamblia*. For example, **17m** (R^1 = CH_2CH_2(4-OCF_3-Ph)) and **17n** (R^1 = CH_2CH_2(4-Me-Ph)) had similar activity to the benzyl-substituted analogs **17c-d** against *G. lamblia* (IC_{50} = 1.6–3.2 μM vs 3.4–3.5 μM, respectively). In addition, the cyclohexyl derivative **17t** was potent against *G. lamblia* at equivalent levels to the metronidazole **1** control (**17t** *G. lamblia* IC_{50} = 5.2 μM).

There were also similar trends in the SAR observed against *T. b. brucei* although with a number of differences compared to *M. tuberculosis* and *G. lamblia*. For example, the activity of the benzyl series **17b-i** against *T. b. brucei* was sensitive to the particular nature of the benzyl substitution. For example, **17c** (R^1 = CH_2(4-OCF_3-Ph)) and **17e** (R^1 = CH_2(4-F-Ph)) were active against *T. b. brucei* (IC_{50} = 1.4 and 2.9 μM, respectively), but compounds **17b** (R^1 = CH_2Ph) and **17f** (R^1 = CH_2(3-OCF_3-Ph)) had reduced

activity at the highest concentrations tested (40 and 16 μM, respectively). Another difference observed for *T. b. brucei* was an increased tolerance for polar substituents at R^1. For example, compounds with polar ethyl acetate (**17o**) or morpholino groups (**17q-r**) displayed moderate activity against *T. b. brucei* (IC_{50} = 2.9–6.5 μM), whereas against *M. tuberculosis* and *G. lamblia* these examples were essentially devoid of activity. The unsubstituted imidazopyrazinone compound **17a** with H at R^1 displayed some activity against *T. b. brucei* (97% inhibition at 40 μM) but was insufficiently active at 20 μM to determine an IC_{50} value. The cyclohexyl derivative **17t** also had good activity against *T. b. brucei* (IC_{50} = 1.4 μM), similarly to *G. lamblia*. These examples demonstrate that it is possible to identify compounds with selective antiparasitic activity, although all compounds with *M. tuberculosis* activity tended to display some activity towards parasites. The selectivity observed for the particular organisms may be due to differences in the compound activation or uptake of the compounds and is an area of ongoing investigation.

Table 2. Activity of imidazopyrazinones and imidazopyrazinones with variation at R^1, $R^2 = R^3 = H$**.**

Compound			Molecular weight (g/mol)	Antibacterial MIC (μg/mL)		Antiparasitic IC_{50} (μM) ($pIC_{50} \pm SE$)[d]	
No.	**Core**	**R^1**		*M. tuberculosis*[a] *normoxia*	*M. tuberculosis*[a] *hypoxia*	*G. lamblia*[b]	*T. b. brucei*[c]
Metronidazole 1			171.2	>32	>32	7.2 (5.1 ± 0.02)	>40 (<4.4)
Pretomanid 6			359.3	0.25-0.5	1	3.0 (5.5 ± 0.02)	19 (4.7 ± 2.4)
17a	A	H	180.1	>32	>32	>25 (<4.6)	97% I @ 40 μM
17b	A	CH_2Ph	270.2	0.5-1	4-8	5.0 (5.3 ± 0.05)	73%I @ 40 μM
17c	A	CH_2(4-OCF_3-Ph)	354.2	0.5	1-4	3.5 (5.5 ± 0.01)	1.4 (5.9 ± 0.08)
17d	A	CH_2(4-CH_3-Ph)	284.3	0.125	1-4	3.4 (5.5 ± 0.03)	>40 (<4.4)
17e	A	CH_2(4-F-Ph)	288.2	1	2	6.4 (5.2 ± 0.07)	2.9 (5.5 ± 0.41)
17f	A	CH_2(3-OCF_3-Ph)	354.2	0.125	0.5-2	1.7 (5.8 ± 0.03)	38% I @ 16 μM

Compound			Molecular weight (g/mol)	Antibacterial MIC (μg/mL)		Antiparasitic IC_{50} (μM) ($pIC_{50} \pm SE$)[d]	
No.	**Core**	**R^1**		*M. tuberculosis*[a] *normoxia*	*M. tuberculosis*[a] *hypoxia*	*G. lamblia*[b]	*T. b. brucei*[c]
17g	A	CH_2(3-CH_3-Ph)	284.3	0.06	70-90% I @ 0.125-8 μg/mL	9.0 (5.0 ± 0.03)	5.4 (5.3 ± 0.23)
17h	A	CH_2(3-CF_3-Ph)	338.2	0.06	70-90% I @ 0.06-16 μg/mL	7.1 (5.1 ± 0.03)	5.3 (5.3 ± 0.18)
17i	A	CH_2(2-OCF_3-Ph)	354.2	1	8	8.2 (5.1 ± 0.03)	6.0 (5.2 ± 1.5)
17j	A	CH_2(2,4-F-Ph)	306.2	16-32	>32	>50 (<4.3)	>40 (<4.4)
17k	A	CH_2(2-pyridyl)	271.2	>32	>32	14 (4.8 ± 0.05)	9.7 (5.0 ± 0.18)
17l	A	CHMe(4-F-Ph)	302.3	0.5	4-6.3	2.1 (5.7 ± 0.03)	94% I @ 40 μM
17m	A	CH_2CH_2(4-OCF_3-Ph)	368.3	8* (70%I)	>32	1.6 (5.8 ± 0.04)	44%I @ 40 μM
17n	A	CH_2CH_2(4-CH_3-Ph)	298.3	4* (78%I)	>32	3.2 (5.5 ± 0.04)	>40 (<4.4)
17o	A	CH_2CH_2OAc	266.2	>32	>32	65 (4.2 ± 0.03)	6.5 (5.2 ± 0.22)
17p	A	CH_2CH_2OH	224.2	>32	>32	>50 (<4.3)	87%I @ 40 μM
17q	A	CH_2CH_2-morpholine	293.3	>32	>32	~50 (~4.3)	2.9 (5.5 ± 0.14)
17r	A	CH_2CO-morpholine	307.3	>32	>32	>50 (<4.3)	4.1 (5.4 ± 6.8)
17s	A	CH_2CONH_2	237.2	>32	>32	>50 (<4.3)	>40 (<4.4)
17t	A	cyclohexyl	262.3	>32	>32	5.2 (5.3 ± 0.03)	1.4 (5.9 ± 0.13)
18i	B	CH_2(2-OCF_3-Ph)	354.2	>32	>32	12 (4.9 ± 0.05)	>40 (<4.4)
18m	B	CH_2CH_2(4-OCF_3-Ph)	368.3	>32	>32	5.2 (5.3 ± 0.03)	N.D

[a] H37Rv, *M. tuberculosis*-normoxia primary screen at 32 μg/mL n = 3, *M. tuberculosis*-hypoxia primary screen at 32 μg/mL n = 1–3, MIC-normoxia/hypoxia of active compounds n = 3–6. Isoniazid control *M. tuberculosis*-normoxia MIC = 0.04 μg/mL, *M. tuberculosis*-hypoxia

MIC >5 μg/mL; [b] WB; [c] pentamidine control IC_{50} = 0.002 μM, diminazine aceturate IC_{50} = 0.062 μM, puromycin IC_{50} = 0.05 μM, n = 2; [d] the percentage inhibition (%I) at the highest concentration tested is reported for compounds that were not sufficiently active to determine an IC_{50}. *Increasing concentrations of compound did not inhibit growth further.

Comparison of Bicyclic Antimicrobial Activity to Monocyclic 4- and 4(5)-Nitroimidazole Carboxamide Analogs

Given the activity of the bicyclic derivatives against *M. tuberculosis*, we screened a number of previously reported[28] 4-nitroimidazole carboxamides **28b-k** and 4(5)-nitroimidazole carboxamides **16a**, **16c**, **16e** and **16f**, along with intermediates **16b** and **16d** prepared for this study, against *M. tuberculosis* under normoxic and hypoxic growth conditions. This would allow us to compare the SAR between the monocyclic and bicyclic series. Note that the 2-nitro group of the imidazopyrazinones occupies the equivalent position of the nitro group in the 4-nitroimidazole series (Figure 3). Interestingly, none of the 4- or 4(5)- monocyclic nitroimidazoles tested were active against *M. tuberculosis* grown aerobically at 32 μg/mL (Supporting Information, Table S6). Under hypoxic growth conditions, weak activity was observed for **28j** and **16c** (60-75% inhibition at 32 μg/mL), but this also correlated with increased cytotoxicity against the mammalian kidney cell line for these compounds (Supporting Information, Table S6). Therefore, the rigid, bicyclic nature of **17b-f** appears necessary for antitubercular activity, especially against actively dividing *M. tuberculosis* cells, but is not essential for activity against other parasites. A comparison of the activity of the 4- and 4(5)- nitroimidazole carboxamide series with that of the bicyclic derivatives is summarized in Figure 3.

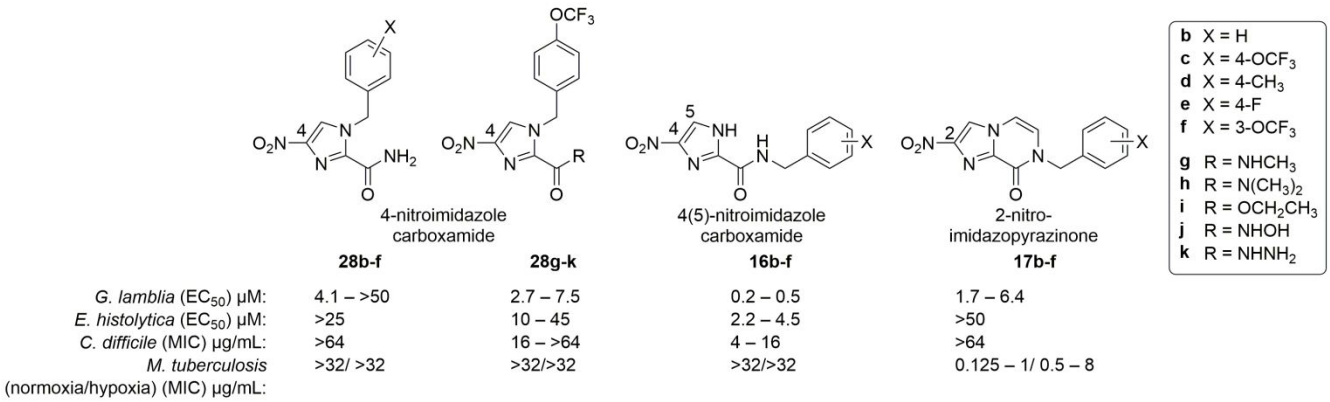

Figure 3. 4-Nitroimidazoles **28b-k** and 4(5)-nitroimidazole carboxamide **16b-f**, compared to imidazopyrazinones **17b-f**.

Evaluation of Des-nitro Derivatives for Biological Activity

Two des-nitro derivatives **20b-c** were prepared as negative control compounds, to confirm that the proposed mode of action relies on reduction of the nitro group. The des-nitro imidazopyrazinone derivatives **20b-c** were tested for activity and indeed, were found to be inactive against *M. tuberculosis*, *G. lamblia*, *T. b. brucei* and *E. histolytica* (complete profiling results are detailed in the Supporting Information, Table S7). This result is consistent with the inactivity of a des-nitro pretomanid analog **9** against *M. tuberculosis* under both aerobic and anaerobic growth (MIC >160 μM and >500 μM, respectively),[41] and supports a critical role for the nitro group in the mechanism of action of nitroimidazopyrazinones.

SAR of Bicyclic Nitroimidazoles with Variation at R^2 = Ph or CH_3, R^3 = H or CH_3

Compounds **24a-e**, **25a-m** and **26a-i** with R^2 = Ph or CH_3 and R^3 = H or CH_3 were evaluated for antiparasitic and antimicrobial in the same manner as described for **17a-t**, **18i**, **18m** (Table 3). Both the R^2 and R^3 sites were found to influence activity against different pathogens to varying degrees. Interestingly, the modifications R^2 and R^3 on the imidazopyrazinone series was found to be particularly beneficial for activity against *T. b. brucei*. A number of imidazopyrazinones were active against *T. b. brucei* between 0.2 and 0.9 μM (**24a-b**, **25b**, **25f**, **25h**, **26b**, **26d, 26f** and **26h**). While some of the

pyrazine matched pairs generally lost activity, several compounds (**24c, 25m, 26e, 26g** and **26i**) maintained activity in the 1.2–2.2 μM range. Furthermore, when $R^1 = CH_2CH_2OAc$, compound **24b** (R^2 = Ph) and **25b** ($R^2 = CH_3$) showed 7.6–10-fold improvement compared to **17o** (R^2 = H). This benefit was also clear for the derivatives with benzyl substitutions at R^1. For example, compound **17f** ($R^1 = CH_2$(3-OCF_3-Ph), R^2 = H, R_3= H) showed incomplete inhibition at 16 μM, while the matched pairs **25j** ($R^2 = CH_3$, R^3= H) and **26f** ($R^2 = CH_3$, R^3= CH_3) inhibited *T. b. brucei* at 1.1 and 0.40 μM, respectively. This last example also demonstrates a slight preference for methyl group substitutions at both R^2 and R^3 on the pyrazinone ring, as this resulted in activity that was consistently about two-fold improved.

The methyl and phenyl groups explored at R^2 and R^3 did not result in any overall improvement or loss of activity against *G. lamblia*, as the activity was generally in the same range. As observed for imidazopyrazine **18m**, the expanded series of imidazopyrazine derivatives also had activity against *G. lamblia*. When R^2 = Ph, R^3 = H, the pyrazine derivatives **24c** and **24e** performed better than the pyrazinone analogs **24b** and **24d** against *G. lamblia*. However, similar activity was observed when $R^2 = CH_3$, R^3 = H (e.g. matched pair **25h** and **25i**) and $R^2 = CH_3$, $R^3 = CH_3$ (e.g. matched pair **26d** and **26e**), although the pyrazine was slightly worse by two-fold for a few derivatives.

Activity against *E. histolytica* was also improved for the imidazopyrazinone series when R^2= CH_3 and R^3= CH_3. Both imidazopyrazinones (e.g **26b** and **26f**) and imidazopyrazines (e.g **26c** and **26g**) were active, with a slight preference for the imidazopyrazinone core. Despite this improvement, none of the derivatives had activity comparable to metronidazole **1**, with the active derivatives having only moderate to weak activity (10–34 μM). This suggests distinct requirements for activity in *E. histolytica* compared to *T. b. brucei* and *G. lamblia*. Nonetheless, it is possible that further modification of the scaffold may lead to identification of an optimal "sweet spot" for activity against *E. histolytica*.

Modifications explored at R^2 and R^3 were mostly detrimental for activity against *M. tuberculosis*. Activity against *M. tuberculosis* activity was abolished when $R^2 = CH_3$ or Ph and $R^3 = H$. Consistent with the previous SAR study, all of the imidazopyrazines were found to be inactive (MIC >32 μg/mL). Nonetheless, activity was retained for three imidazopyrazinone examples (**26b**, **26d** and **26f**) when $R^2 = R^3 = CH_3$ and R^1 was a benzyl group. Compounds **26b**, **26d** and **26f** also displayed activity against *M. tuberculosis* under hypoxic growth conditions and against *G. lamblia*, *E. histolytica* and *T. b. brucei*. These results indicate that it is possible to identify compounds with broad spectrum activity against both *M. tuberculosis* and parasites.

Continuing the trend previously observed for compounds **17a-t**, **18i** and **18m**, none of the additional imidazopyrazin-ones/-es synthesized had appreciable activity against ESKAPE bacteria or fungal pathogens (MIC ≥ 32 μg/mL) (Supporting Information, Table S8). Both the nitroimidazopyrazinones and nitroimidazopyrazines series were also not cytotoxic against mammalian liver and kidney cell lines (CC_{50} >100 μM, **24d** >75 μM due to compound limitations), except for **26f** that displayed moderate cytotoxicity in both cell lines (CC_{50} = 26–80 μM) (Supporting Information, Table S8).

To summarize, the SAR of the R^2, R^3 sites was determined for both the nitroimidazopyrazinone and nitroimidazopyrazine series. Several compounds with potent activity against *M. tuberculosis*, *G. lamblia* and *T. b. brucei* were identified. Further work confirming the target/mode of action in *M. tuberculosis*, *G. lamblia* and *T. b. brucei* could aid in explaining the differences in activity. Additional studies to measure the reduction potential may provide insight into the differences in the activity between the nitroimidazopyrazinones and nitroimidazopyrazines.

Table 3. SAR exploring the differences between the R^2 and R^3 groups for the imidazopyrazinone (core A) versus the imidazopyrazine (core B).

Compound					Molecular weight (g/mol)	Antibacterial MIC (μg/mL)		Antiparasitic IC_{50} (μM) (pIC_{50} ± SE)[e]		
No.	**Core**	**R^1**	**R^2**	**R^3**		*M. tuberculosis*[a] *normoxia*	*M. tuberculosis*[a] *hypoxia*	*G. lamblia*[b]	*E. histolytica*[c]	*T. b brucei*[d]
Metronidazole 1					171.2	>32	>32	7.2 (5.1 ± 0.02)	4.3 (5.4 ± 0.02)	>40 (<4.4)
Pretomanid 6					359.3	0.25-0.5	1	3.0 (5.5 ± 0.02)	9.3 (5.0 ± 0.03)	19 (4.7 ± 2.4)
24a	A	H	Ph	H	256.2	>32	>32	10 (5.0 ± 0.03)	>25 (<4.6)	0.22 (6.7 ± 0.071)
24b	A	CH_2CH_2OAc			342.3	>32	>32	11 (5.0 ± 0.05)	34 (4.5 ± 0.1)	0.86 (6.1 ± 0.085)
24c	B				342.3	>32	>32	1.9 (5.7 ± 0.05)	>50 (<4.3)	1.5 (5.8 ± 0.085)
24d	A	CH_2CH_2OH			300.3	>32	>32	38 (4.4 ± 0.03)	>50 (<4.3)	N.D.
24e	B				300.3	>32	>32	5.2 (5.3 ± 0.05)	>50 (<4.3)	1.1 (6.0 ± 0.12)
25a	A	H	CH_3	H	194.2	>32	>32	~50 (~4.3)	>50 (<4.3)	3.6 (5.4 ± 0.20)
25b	A	CH_2CH_2OAc			280.2	>32	>32	~50 (~4.3)	41% I @ 50 μM	0.65 (6.2 ± 0.021)
25c	B				280.2	>32	>32	21 (4.7 ± 0.06)	42% I @ 50 μM	>40 (<4.4)
25d	A	CH_2CH_2OH			238.2	>32	>32	>50 (<4.3)	>50 (<4.3)	4.6 (5.3 ± 0.092)
25e	B				238.2	>32	>32	80% I @ 50 μM	>50 (<4.3)	56% I @ 40 μM

Compound					Molecular weight (g/mol)	Antibacterial MIC (μg/mL)		Antiparasitic IC_{50} (μM) (pIC_{50} ± SE)[e]		
No.	**Core**	**R^1**	**R^2**	**R^3**		*M. tuberculosis*[a] *normoxia*	*M. tuberculosis*[a] *hypoxia*	*G. lamblia*[b]	*E. histolytica*[c]	*T. b brucei*[d]
25f	A	CH_2(4-OCF_3-Ph)			368.3	>32	>32	5.8 (5.2 ± 0.04)	>50 (<4.3)	0.41 (5.4 ± 0.057)
25g	B				368.3	>32	>32	7.4 (5.1 ± 0.03)	9.5 (5 ± 0.07)	>40 (<4.4)
25h	A	CH_2(4-CH_3-Ph)			298.3	>32	>32	4.4 (5.4 ± 0.03)	10 (5.0 ± 1.0)	0.56 (6.3 ± 0.028)
25i	B				298.3	N.D.	N.D.	5.7 (5.2 ± 0.03)	30 (4.5 ± 0.1)	N.D.
25j	A	CH_2(3-OCF_3-Ph)			368.3	>32	>32	2.8 (5.6 ± 0.01)	16 (4.8 ± 0.1)	1.1 (5.9 ± 0.021)
25l	A	CH_2(2-OCF_3-Ph)			368.3	>32	>32	3.3 (5.5 ± 0.01)	9.1 (5 ± 0.08)	2.1 (5.7 ± 0.29)
25m	B				368.3	>32	>32	5.7 (5.2 ± 0.02)	>50 (<4.3)	1.2 (5.9 ± 0.13)
26a	A	H	CH_3	CH_3	208.2	>32	>32	~50 (~4.3)	>50 (<4.3)	2.6 (5.6 ± 0.17)
26b	A	CH_2(4-OCF_3-Ph)			382.3	1	4	4.2 (5.4 ± 0.04)	10 (5 ± 0.1)	0.24 (5.7 ± 0.0071)
26c	B				382.3	>32	>32	8.6 (5.1 ± 0.04)	17 (4.8 ± 0.09)	10 (5.0 ± 0.20)
26d	A	CH_2(4-CH_3-Ph)			312.3	2	4	5.2 (5.3 ± 0.02)	33 (4.5 ± 0.04)	0.25 (6.6 ± 0.0071)
26e	B				312.3	>32	>32	5.8 (5.2 ± 0.02)	>50 (<4.3)	2.2 (5.6 ± 0.31)
26f	A	CH_2(3-OCF_3-Ph)			382.3	1	16-32	1.7 (5.8 ± 0.01)	15 (4.8 ± 0.03)	0.40 (6.4 ± 0.0071)

Compound					Molecular weight (g/mol)	Antibacterial MIC (μg/mL)		Antiparasitic IC_{50} (μM) (pIC_{50} ± SE)[e]		
No.	**Core**	**R^1**	**R^2**	**R^3**		*M. tuberculosis*[a] *normoxia*	*M. tuberculosis*[a] *hypoxia*	*G. lamblia*[b]	*E. histolytica*[c]	*T. b brucei*[d]
26g	B				382.3	>32	>32	3.9 (5.4 ± 0.01)	27 (4.6 ± 0.02)	1.4 (5.9 ± 0.24)
26h	A	CH_2(2-OCF_3-Ph)			382.3	>32	>32	5.3 (5.3 ± 0.03)	18 (4.7 ± 0.02)	0.78 (6.1 ± 0.090)
26i	B				382.3	>32	>32	>50 (<4.3)	>50 (<4.3)	1.9 (5.7 ± 0.27)

[a] H37Rv, *M.tuberculosis*-normoxia primary screen at 32 μg/mL n = 3, *M. tuberculosis*-hypoxia primary screen at 32 μg/mL n = 1–3, MIC-normoxia/hypoxia of active compounds n = 3–6. Isoniazid control *M. tuberculosis*-normoxia MIC = 0.04 μg/mL, *M. tuberculosis*-hypoxia MIC >5 μg/mL; [b] WB; [c] HM1:IMSS; [d] pentamidine control IC_{50} = 0.002 μM, diminazine aceturate IC_{50} = 0.062 μM, puromycin IC_{50} = 0.05 μM, n = 2; [e] the percentage inhibition (%I) at the highest concentration tested is reported for compounds that were not sufficiently active to determine an IC_{50}.

Microsomal Stability, Plasma Stability and Plasma Protein Binding

A set of ten compounds was selected for initial assessment of drug-like properties (microsomal stability, plasma stability and plasma protein binding (PPB)) based on their potency and structural diversity (Table 4). It was also envisioned that these studies would provide clarity as to whether there was a clear benefit to either the nitroimidazopyrazinone or nitroimidazopyrazine series from the perspective of ADMET properties. Nitroimidazopyrazinones were stable in human liver microsomes (HLM) after 2 h of incubation, regardless of the structural differences in R^1, R^2 and R^3. However, **18i**, **25g** and **26c** from the nitroimidazopyrazine series only showed moderate stability in HLM, independent of differences at R^1, R^2, and R^3, with 44-69% of compound remaining after 2 h (Table 4).

To further understand how the metabolic stability could impact in vivo efficacy studies, metabolic stability was evaluated in CD-1 mouse liver microsomes (MLM) because the CD-1 mouse strain is intended to be used for future in vivo efficacy studies. As for HLM, the majority of the nitroimidazopyrazinones **17c-f**, **17i** and **25f** displayed excellent stabilities toward MLM. However, one of the imidazopyrazinone analogs, **26b** ($R^2 = R^3 = CH_3$) showed significant degradation after 2 h, with only 3.6% of intact compound remaining (compared to 92% in HLM) (Table 4). Comparison of **25f** with **26b**, which differ by the presence of a hydrogen or methyl group at R^3 respectively, indicated that the methyl group at R^3 was responsible for the high intrinsic clearance of **26b** in MLM. Nitroimidazopyrazines, **18i**, **25g** and **26c** were also not stable in MLM (<0.5–8% remaining), suggesting a metabolic liability of this series.

Compound stability in both human and mouse (CD-1) plasma was assessed for compounds **17c-f**, **25f-g** and **26b-c** (Table 4). All of the examples had >90% of compound remaining after 2 h at 37 °C, similar to pretomanid **6**. Therefore, both the nitroimidazopyrazinones and nitroimidazopyrazines series were stable in human and mouse plasma, despite the instability of nitroimidazopyrazines observed in liver microsomes.

Plasma protein binding affects compound bioavailability and tissue distribution in vivo. Therefore, to understand PPB for the nitroimidazopyrazines and nitroimidazopyrazines series, selected potent compounds (**17c**, **17e-f**, **25f-g** and **26b**) were evaluated for PPB using the ultrafiltration method (Table 4). Most of the tested compounds, except **17e** (82% bound) had high PPB at >95%, which might limit the concentration of free compounds at the site of infection. However, as many approved and clinical drugs, including **6**, tend to have high PPB, this parameter is not recommended to be optimized in early drug design.[42]

Table 4. In vitro physicochemical properties for representative compounds.

Compound	Core	R^1	R^2	R^3	Microsomal stability (% remaining at 2 h)		Plasma stability (% remaining at 2 h)		Plasma protein binding (%)
					Human	Mouse (CD-1)	Human	Mouse (CD-1)	
Pretomanid 6					97 ± 5.0	92 ± 2.7	96 ± 6.9	96 ± 1.9	97 ± 1.1
17c	A	CH_2(4-OCF_3-Ph)	H	H	>99	>99	>99	>99	98 ± 0.4
17d	A	CH_2(4-CH_3-Ph)			97 ± 1.1	96 ± 6.0	>99	>99	N.D
17e	A	CH_2(4-F-Ph)			99	>99	98 ± 1.4	>99	82 ± 0.3
17f	A	CH_2(3-OCF_3-Ph)			>99	>99	>99	97 ± 2.2	99 ± 0.2
17i	A	CH_2(2-OCF_3-Ph)			>99	>99	N.D	N.D	N.D
18i	B	CH_2(2-OCF_3-Ph)			51 ± 18	<0.5	N.D	N.D	N.D
25f	A	CH_2(4-OCF_3-Ph)	CH_3	H	>99	>99	92 ± 4.1	99 ± 4.8	98 ± 0.4
25g	B	CH_2(4-OCF_3-Ph)			69 ± 4.3	7.9 ± 4.0	94 ± 4.7	>99	>99
26b	A	CH_2(4-OCF_3-Ph)	CH_3	CH_3	92 ± 1.1	3.6 ± 0.1	97 ± 1.4	>99	99 ± 0.1
26c	B	CH_2(4-OCF_3-Ph)			44 ± 0.98	<0.5	>99	>99	N.D

Values are presented as mean of three replicates ± SD. N.D represents not determined. Microsome stability verapamil control = 2% (MLM), 9% (HLM) remaining at 30 min; plasma stability eucatropine control = 28% (mouse), 21% (human) remaining at 2 h; plasma protein binding sulfamethoxazole control = 68% bound.

Caco-2 Intestinal Epithelium Permeability

An in vitro Caco-2 monolayer bidirectional assay was used to evaluate intestinal epithelium permeability and to predict the oral absorption of the nitroimidazopyrazinone series.[43] Three derivatives (**17c**, **17f** and **26b**) were selected based on potency against *M. tuberculosis*, *G. lamblia* and *T. b. brucei* and to permit direct comparison of $R_2 = R_3 = H$ (**17c**) versus $R_2 = R_3 = CH_3$ (**26b**). Pleasingly, compounds **17c**, **17f** and **26b** were highly permeable (Table 5). The apparent permeability coefficient (P_{app}) apical to basal (A to B) had values of >20 × 10^{-6} cm/s, similar to pretomanid **6** and propranolol, with the latter used as a positive control for high permeability. No metabolism of the compounds by Caco-2 cells was observed. This was evident from the high recovery of tested nitroimidazopyrazinones obtained in both directions,

similar to the control propranolol (A to B measured). Nitroimidazopyrazinones **17c**, **17f** and **26b** and **6** also showed a low efflux ratio of <2 (cf. digoxin efflux ratio >360 as it is a substrate for P-gp). Therefore, the tested bicyclic nitroimidazoles do not appear to be substrates of efflux transporters. These results suggest that **17c**, **17f** and **26b** have desirable therapeutic properties and may display good oral absorption properties in vivo.

Table 5. Caco-2 permeability of selected analogs.

Compound	Core	R^1	R^2	R^3	P_{app} (10^{-6} cm/s)		Mean recovery (%)		Efflux ratio
					A to B	B to A	A to B	A to B	
Pretomanid 6*					29	22	81	101	0.74
Fenoterol					0.27	N.D	92	N.D	N.D
Propranolol					21	N.D	70	N.D	N.D
Digoxin					<0.020	8.4	<72	88	>360
17c	A	CH_2(4-OCF_3-Ph)	H	H	25	22	83	97	0.88
17f	A	CH_2(3-OCF_3-Ph)	H	H	24	24	88	99	1.0
26b	A	CH_2(4-OCF_3-Ph)	CH_3	CH_3	21	20	83	97	0.95

N.D represents not determined. * Comparable results with the literature.[22]

Kinetic Solubility

Compound solubility impacts in vivo absorption, efficacy and dosing and is thus an important parameter to optimize in drug development. For example, the recently approved TB drug, delamanid has limited solubility which requires twice daily dosing,[44] and new bicyclic analogs with improved solubility would be of great interest. According to the generic criteria for hits and leads in infectious diseases identified by Japanese Global Health Innovative Technology (GHIT) Fund and its key partners, a lead should have acceptable physicochemical properties, with solubility at least >10 μM in phosphate-buffered saline pH 7.4 (PBS).[45]

The kinetic solubility of 48 compounds from the nitroimidazopyrazin-one/e libraries in water and PBS buffer (pH 7.4) was determined using LC-UV (Figure 4, for full data see Supporting Information, Table S9). The solubility of the derivatives varied over a wide range reflective of the different properties that the R^1 side chain can impart. As anticipated, polar groups at R^1 such as morpholine (**17r**: CH_2CO-morpholine, **17q**: CH_2CH_2-morpholine), amide (**17s**: CH_2CONH_2) and alcohol groups (**17p**: CH_2CH_2OH) had >30-fold (ΔLogS ~ 1.6 units) better solubility than benzyl derivatives (**17b-j**). The nitroimidazopyrazinones had equivalent or improved solubility relative to the nitroimidazopyrazine series and this is also reflected in their lower logP values. Encouragingly, when the solubility versus activity was compared, a number of compounds with antitrypanosomal activity (*T. b. brucei* $IC_{50} \leq 10$ μM) had good solubility at >100 μM (equivalent to log*S* >-4), including two potential hits **24b** and **25b** with IC_{50} <1 μM. The most potent compound **24a** achieved moderate aqueous solubility (27 μM in water; 17 μM in PBS), whereas **26b** and **26d** with comparable activity were poorly soluble (<10 μM, or log*S* <-5 in water and PBS) (Figure 4). These results demonstrate the potential to achieve desirable solubility and activity profile by modifying the R^1 group of the bicyclic nitroimidazoles.

However, compounds with potent activity against *M. tuberculosis*, *G. lamblia* and *E. histolytica* generally had poor solubility. Most of the potent compounds against *M. tuberculosis* showed poor solubility with <10 μM in both water and PBS, which might require complicated formulations for in vivo efficacy. This indicates the importance of lipophilicity at the R^1 side chain, which is potentially required for penetration of these molecules through the mycobacterial cell walls. Although changing R^1 to CH_2-pyridinyl decreased activity against *M. tuberculosis*, this derivative (**17k**) had significantly improved water solubility (176 μM in water; 184 μM in PBS) and decreased lipophilicity (ΔLogP -0.94 units). Exploring other heterocyclic analogs may provide the desired balance of potency and solubility, which has been a successful strategy in the literature to identify analogs of pretomanid **6** with improved solubility.[46,47]

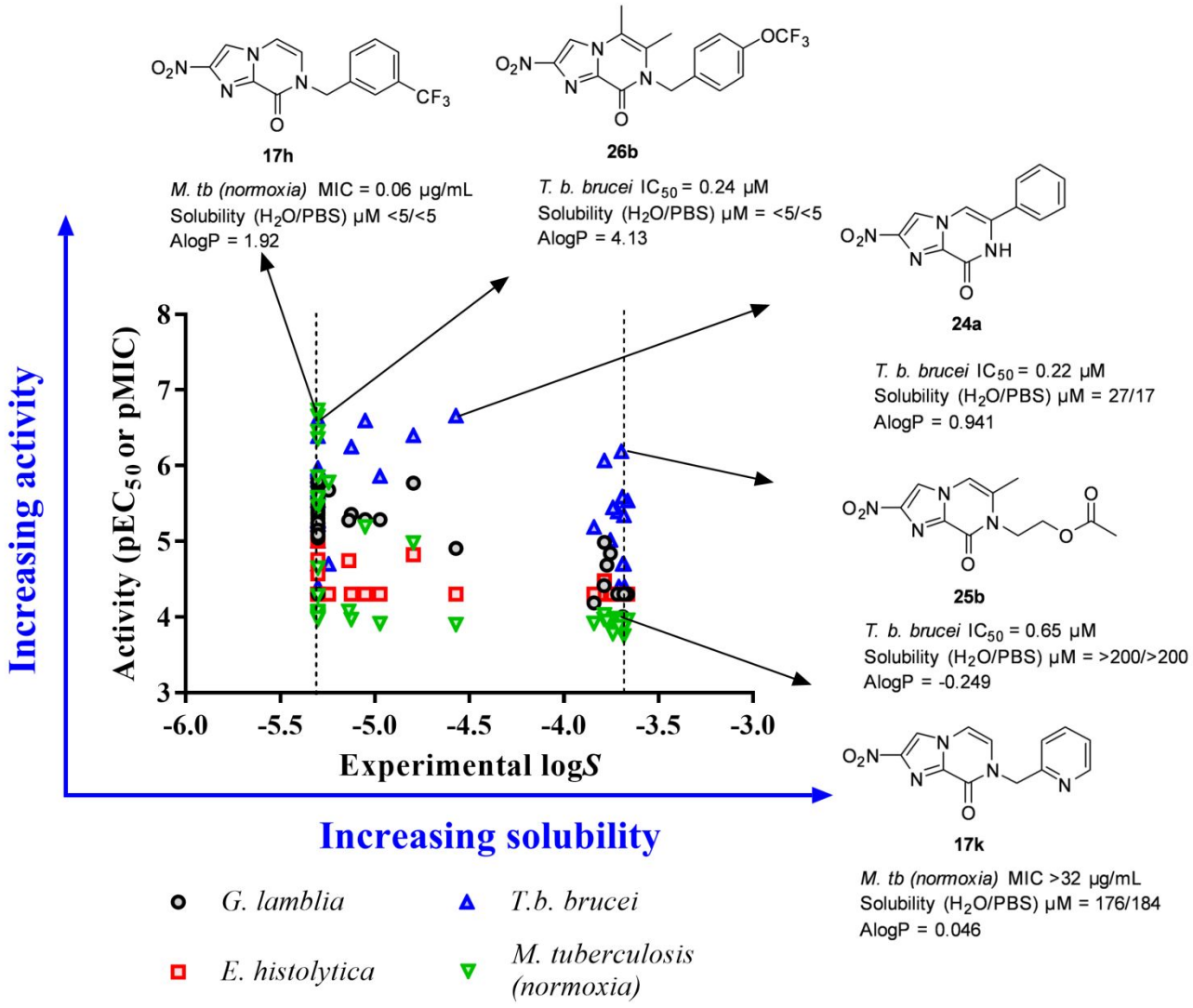

Figure 4. Comparison of activity vs aqueous solubility data. Several compounds e.g. **25b** active against *T. b. brucei* (in blue) had good solubility (>100 µM or log*S* > -4). Most of the potent compounds, e.g. **17h**, against the other organisms displayed poor solubility (log*S* ≤ -5). Dashed lines represent the minimum and maximum range of solubility determined experimentally.

Conclusion

In this study pretomanid **6** was shown to have potent activity against enteric pathogens including *G. lamblia*, *E. histolytica* and *C. difficile*. These results expand the current understanding of the spectrum of action of **6** from mycobacterium and *Leishmania* to include anaerobic protozoan parasites and an anaerobic Gram-positive bacterium. The in vitro activity of **6** against *G. lamblia* and *E. histolytica* at equivalent levels to metronidazole **1**, suggests that this class of compounds and other subclasses of bicyclic nitroimidazoles could be a beneficial avenue to explore for the development of new nitroimidazole based therapeutics against these pathogens.

The activity of **6** against enteric pathogens inspired the synthesis and biological evaluation of two new bicyclic scaffolds; nitroimidazopyrazin-one/-es derived from the monocyclic 4(5)-nitroimidazole carboxamide framework previously reported. A modular synthetic approach enabled the exploration of bicyclic imidazopyrazinone derivatives with different substitutions at R^1, R^2 and R^3, along with the isomeric *O*-alkylated nitroimidazopyrazine core scaffold. Through these studies, compounds with potent activity against *M. tuberculosis, G. lamblia* and *T. b. brucei* were identified. Several compounds also displayed moderate activity against *E. histolytica*. To our knowledge, this is the first example of a nitroimidazopyrazinone heterocyclic core with potent antiparasitic activity against *M. tuberculosis* under both normoxic and hypoxic growth conditions as well as promising antiparasitic activity against *G. lamblia* and *T. b. brucei*. The bicyclic core was essential for antitubercular activity.

This study highlights the potential to prepare new subclasses of bicyclic nitroimidazoles with varied ring systems to gain different selectivity profiles toward *M. tuberculosis* and a range of parasitic organisms. All of the compounds with *M. tuberculosis* activity also displayed activity towards at least some of the parasites tested. However, we showed that the activity profile of the series could be tuned towards

parasites away from *M. tuberculosis*, which may be relevant for treating parasitic diseases without inducing resistance in *M. tuberculosis* in co-exposed patients. For example, nitroimidazopyrazinones and nitroimidazopyrazines, particularly **24c**, **24e** (R^2 = Ph) and **25h**, **25j**, **25l-m** (R^2 = CH_3), were active against *G. lamblia* (IC_{50} = 1.9–5.7 μM, respectively) and *T. b. brucei* (IC_{50} = 0.56–2.1 μM, respectively) but not *M. tuberculosis* (MIC >32 μg/mL).

In general, these new subclasses displayed desirable therapeutic properties. Low cytotoxicity against mammalian cell lines was observed generally (CC_{50} >100 μM) for both series. In addition, many of the potent derivatives were stable in human and mouse liver microsomes, although the imidazopyrazine series was metabolized, particularly in MLM, and when R^2 and R^3 were methyl substituents. Selected derivatives also gave similar results to **6** in plasma stability, plasma protein binding and Caco-2 intestinal permeability assays. Like other early stage anti-tubercular leads including bicyclic nitroimidazoles, solubility was identified as an important parameter for future optimization. While a number of active compounds against *T. b. brucei* had moderate solubility, the most potent anti-tubercular compounds had poor aqueous kinetic solubility (<10 μM). Optimization of the R^1, R^2 and R^3 sites, particularly the R^1 site, to arrive at more potent compounds, while maintaining desirable drug-like properties and improving the solubility will be explored in future studies.

This study lays the foundation for future work focused on determining and optimizing the efficacy of selected derivatives in in vivo models of *M. tuberculosis*, *G. lamblia* and *T. b. brucei* and understanding their mode of action in various microorganisms. These studies are expected to provide further insight into nitroimidazole activation and guide the development of bicyclic nitroimidazoles with therapeutic potential against both *M. tuberculosis* and a wide range of parasitic organisms.

Experimental

General Information. Reagents and anhydrous solvents were used as received. Reactions requiring anhydrous conditions were performed under an inert atmosphere of nitrogen. Reactions were monitored by TLC or LCMS. Analytical TLC was performed on Merck TLC aluminum sheets pre-coated with Silica Gel 60 F-254 and compounds were visualized using UV_{254} lamp and potassium permanganate stain. Melting points were determined using a Gallenkamp melting point apparatus and are corrected to a standard curve of the measured and literature melting points of vanillin, acetyl salicylic acid, 3-phenoxybenzoic acid and caffeine standards. Analytical LCMS was performed on a Shimadzu LCMS using 0.05% formic acid in water as solvent A and 0.05% formic acid in acetonitrile as solvent B. Standard conditions unless otherwise specified: Column Zorbax Eclipse XDB-Phenyl, 3.0×100mm, 3.5 µ. Alternative column: Waters Atlantis T3, 3.0 × 100mm, 3 µ. Detection: PDA UV, ELSD and electrospray MS. Compounds were purified by MPLC (Biotage Isolera or Grace Reveleris X2 chromatography systems) or by HPLC (Agilent Preparative HPLC 1260 Infinity Series). Commercially available cartridges were used for MPLC chromatography (Biotage SNAP cartridge HP-Silica 10 g, 25 g or 50 g, Reveleris 4 g or 12 g Silica (40 µm) cartridge or Reveleris C18 Reversed-Phase 12 g cartridge). Column for HPLC: Agilent XDB Phenyl 5 µm, 30 x 100 mm. All products tested for biological activity were obtained in >95% purity as determined by HPLC using UV at 254 nm, ESIMS and ELSD detection. NMR data were collected and calibrated in DMSO-d_6 or $CDCl_3$ with 0.05% TMS at 298K on a Varian Unity 400 MHz or Bruker Avance-600 MHz spectrometer. Where appropriate, ^{1}H-coupling constants were examined using resolution enhancement with MestReNova software. High resolution mass spectrometry (HRMS) was performed on a Bruker MicroTOF mass spectrometer using (+)-ESI calibrated to HCOONa. For compounds purified by reverse phase chromatography, the exact concentration of the compounds for assay was determined by the quantitative NMR integration 'PULCON' experiment.[48] These settings were used for all PULCON experiments: relaxation delay of 30

s, 8 scans, 2 dummy scans, 90° pulse and temperature at 298 K. The mass calculated from PULCON experiments was used to calculate the reaction percentage yields.

General Procedure A: Alkylation of imidazole and imidazopyrazinones

To a stirred solution of imidazole/imidazopyrazinone (1 eq) in anh. DMF (15–30 vol) was added K_2CO_3 or Cs_2CO_3 (3 eq) followed by alkyl or benzyl halide (1.2–1.5 eq). The reaction was stirred at rt or heated in a microwave reactor at 80–180 °C for 15 min and monitored by LCMS. If necessary, an additional portion of alkylating agent (0.5–1.5 eq) was added and the reaction was heated at μW 120–180 °C for a further 15 min to consume the imidazole starting material. Work-up procedure A: the reaction was poured into H_2O and extracted with EtOAc. The combined organic layers were washed with brine, dried over $MgSO_4$ and filtered. Volatiles were removed in vacuo to give the crude product. Work-up procedure B: The reaction was poured into water, the precipitate collected by filtration, washed with water and dried in vacuo.

General Procedure B: Alkylation of imidazopyrazinones

To a stirred suspension of imidazopyrazinone (1 eq) in toluene (20 vol) was added Ag_2CO_3 (1.2 eq) followed by benzyl halide (2 eq). The reaction was heated at 80 °C overnight and monitored by LCMS. General aqueous work up: the reaction was poured into H_2O and extracted with EtOAc. The combined organic layers were washed with brine, dried over $MgSO_4$ and filtered. Volatiles were removed in vacuo to give the crude product.

General Procedure C: Ring closure to synthesize imidazopyrazinones

To a stirred solution of 4-nitroimidazole (1 eq) in 1,4-dioxane (10 vol) was added 2 M aq. HCl (10 vol). The reaction was heated at 120 °C for 30 min in the microwave. Work-up procedure A: The crystalline solid was collected by vacuum filtration. The precipitate was washed with water and dried in vacuo to

give a solid. Work-up procedure B: After heating the reaction, the volatiles were evaporated in vacuo to yield a crude material that was purified by recrystallization or chromatography.

General Procedure D: Deprotection of acetate protecting group

Anh. K_2CO_3 (1.5 eq) was added to a stirred suspension of ethyl acetate imidazopyrazinone (1 eq) in MeOH (20 vol). After 1 hr, volatiles were removed under a stream of N_2. The solid was suspended with H_2O, filtered, washed with water and dried under vacuum. Work-up procedure B: the reaction was acidified with a 5% solution of TFA in MeOH. The suspension was then concentrated onto C18 silica gel and purified by MPLC.

General Procedure E: Two step, one pot synthesis of imidazopyrazinones

Alkylating agent (1.2–1.5 eq) was added slowly to a stirred suspension of **13a** (1 eq), anh. K_2CO_3 (3 eq) in anh. DMF (15 vol). The reaction was stirred at rt until complete (10 min–5 h). 2M aq. HCl (15 vol), was then added slowly to control effervescence (CO_2). The reaction was then stirred at rt (overnight to 4 days), or for **22a** heated with microwave irradiation until the cyclization was complete. The solid precipitate was collected by vacuum filtration, washed with water and MeOH and then dried in vacuo.

***N*-Benzyl-5-nitro-1*H*-imidazole-2-carboxamide; 16b**

Prepared according to Jarrad et al.[28] Amine: benzylamine (300 μL, 2.74 mmol). The crude material was purified over silica gel by MPLC (Biotage 20–100% EtOAc in pet. spirits gradient) to yield a colorless solid (399 mg, 71%). LCMS: R_t = 3.13 min, 99 A% @ 254 nm, $[M - H]^-$ = 245.0. ^{1}H NMR (600 MHz, DMSO-d_6) δ 14.31 (s, 1H), 9.45 (t, J = 6.4 Hz, 1H), 8.46 (s, 1H), 7.31 (d, J = 4.4 Hz, 4H), 7.27 – 7.20 (m, 1H), 4.43 (d, J = 6.4 Hz, 2H). ^{13}C NMR (150 MHz, DMSO-d_6) δ 157.2, 146.8, 139.7, 139.1, 128.3, 127.4, 126.9, 121.6, 42.3. HRMS (ESI): m/z calcd for $C_{11}H_{10}N_4NaO_3$ $[M + Na]^+$, 269.0645; found, 269.0639.

_N_-(4-Methylbenzyl)-5-nitro-1_H_-imidazole-2-carboxamide; 16d

Prepared according to Jarrad et al.[28] Amine: 4-methylbenzylamine (155 μL, 1.37 mmol). The crude material was purified over silica gel by MPLC (Grace Reveleris X2, 20–100% EtOAc in pet. spirits gradient) to obtain a yellow solid (201 mg, 68%). LCMS: R_t = 3.27 min, 99 A% @ 254 nm, $[M - H]^-$ = 259.0. ^{1}H NMR (600 MHz, DMSO-d_6) δ 14.30 (s, 1H), 9.37 (t, J = 6.4 Hz, 1H), 8.43 (s, 1H), 7.20 (d, J = 8.2 Hz, 2H), 7.11 (d, J = 7.8 Hz, 2H), 4.37 (d, J = 6.4 Hz, 2H), 2.26 (s, 3H). ^{13}C NMR (150 MHz, DMSO-d_6) δ 157.2, 146.8, 140.0, 136.1, 135.9, 128.8, 127.4, 121.8, 42.0, 20.7. HRMS (ESI): m/z calcd for $C_{12}H_{12}N_4NaO_3$ $[M + Na]^+$, 283.0802; found, 283.0794.

2-Nitroimidazo[1,2-*a*]pyrazin-8(7*H*)-one; 17a

To a stirred suspension of **19a** (551 mg, 2.02 mmol) in H_2O (11 mL) was added 5% aq. HCl (1.44 mL, 1 eq). The reaction was refluxed for 4.5 h. The solvent was removed in vacuo. The crude product was purified by recrystallization (slurry equilibration with hot MeOH) to give fine off-white needles (241 mg, 66%). Mp = 350 °C (decomposed). LCMS: R_t = 1.49 min, 99 A% @ 254 nm, $[M + H]^+$ = 180.8. ^{1}H NMR (600 MHz, DMSO-d_6) δ 11.58 (s, 1H), 8.81 (s, 1H), 7.50 (d, J = 5.6 Hz, 1H), 7.07 (d, J = 5.7 Hz, 1H). ^{13}C NMR (150 MHz, DMSO-d_6) δ 153.2, 147.6, 135.5, 119.8, 116.6, 107.1. The position of the nitro group was confirmed by HMBC and X-ray crystallography. X-ray diffraction data were collected on Oxford Diffraction Gemini Ultra dual source (Mo and Cu) CCD Diffractometer with Cu radiation (λ = 1.54184 Å), T = 190(2) K. Additional crystallographic data and HMBC data are available in the Supporting Information, Figure S1 and Tables S1-S3. HRMS (ESI): *m/z* calcd for $C_{12}H_8N_8NaO_6$ $[2M + Na]^+$, 383.0459; found, 383.0454.

7-Benzyl-2-nitroimidazo[1,2-*a*]pyrazin-8(7*H*)-one; 17b

Compound **19b** (150 mg, 0.414 mmol) was reacted according to general procedure C, work-up procedure B. The crude material was purified by recrystallization (hot slurry from DCM/MeOH) to yield a tan solid

(88 mg, 78%). Mp = 298–299 °C (decomposed). LCMS: R_t = 3.17 min, 99 A% @ 254 nm, $[M + H]^+$ = 271.0. ^{1}H NMR (600 MHz, DMSO-d_6) δ 8.81 (s, 1H), 7.60 (d, J = 5.9 Hz, 1H), 7.42 (d, J = 5.9 Hz, 1H), 7.37 – 7.34 (m, 4H), 7.32 – 7.24 (m, 1H), 5.13 (s, 2H). ^{13}C NMR (150 MHz, DMSO-d_6) δ 152.8, 148.0, 136.5, 135.2, 128.7, 127.8, 127.7, 123.6, 116.7, 107.4, 50.2. HRMS (ESI): *m/z* calcd for $C_{13}H_{10}N_4NaO_3$ $[M + Na]^+$, 293.0645; found, 293.0640.

2-Nitro-7-(4-(trifluoromethoxy)benzyl)imidazo[1,2-*a*]pyrazin-8(7*H*)-one; 17c

Compound **19c (**300 mg, 0.672 mmol) was reacted according to general procedure C, work-up procedure A, to yield a lemon yellow crystalline solid (207 mg, 87%). Mp = 264–266 °C (decomposed). LCMS: R_t = 3.47 min, 99 A% @ 254 nm, $[M + H]^+$ = 355.0. ^{1}H NMR (600 MHz, DMSO-d_6) δ 8.82 (s, 1H), 7.62 (d, J = 5.9 Hz, 1H), 7.52 – 7.47 (m, 2H), 7.46 (d, J = 5.9 Hz, 1H), 7.39 – 7.33 (m, 2H), 5.16 (s, 2H).^{13}C NMR (150 MHz, DMSO-d_6) δ 152.8, 148.0, 147.7, 136.0, 135.1, 129.7, 123.5, 121.2, 120.0 (q, J = 257.6 Hz), 116.6, 107.5, 49.6. HRMS (ESI): *m/z* calcd for $C_{14}H_9F_3N_4NaO_4$ $[M + Na]^+$, 377.0468; found, 377.0467.

7-(4-Methylbenzyl)-2-nitroimidazo[1,2-*a*]pyrazin-8(7*H*)-one; 17d

Compound **19d** (100 mg, 0.266 mmol) was reacted according to general procedure C, work-up procedure B. The crude material was purified by recrystallization (slurry equilibration with hot DCM/MeOH) to yield a tan solid (53 mg, 70%). Mp = 311–312 °C (decomposed). LCMS: R_t = 3.30 min, 99 A% @ 254 nm, $[M + H]^+$ = 285.1. ^{1}H NMR (600 MHz, DMSO-d_6) δ 8.80 (s, 1H), 7.58 (d, J = 5.9 Hz, 1H), 7.39 (d, J = 5.9 Hz, 1H), 7.27 – 7.22 (m, 2H), 7.18 – 7.13 (m, 2H), 5.07 (s, 2H), 2.27 (s, 3H). ^{13}C NMR (151 MHz, DMSO-d_6) δ 152.7, 148.0, 137.1, 135.1, 133.5, 129.2, 127.8, 123.5, 116.6, 107.4, 49.9, 20.7. HRMS (ESI): *m/z* calcd for $C_{14}H_{13}N_4O_3$ $[M + H]^+$, 285.0982; found, 285.0973.

7-(4-Fluorobenzyl)-2-nitroimidazo[1,2-*a*]pyrazin-8(7*H*)-one; 17e

Compound **19e** (384 mg, 1.01 mmol) was reacted according to the general procedure C, work-up procedure A, to yield a yellow crystalline solid (249 mg, 86%). Mp = 297 °C (decomposed). LCMS: R_t = 3.23 min, 98 A% @ 254 nm, $[M + H]^+$ = 289.0. ^{1}H NMR (600 MHz, DMSO-d_6) δ 8.81 (s, 1H), 7.60 (d, J = 5.9 Hz, 1H), 7.44 (d, J = 5.9 Hz, 1H), 7.44 – 7.39 (m, 2H), 7.23 – 7.15 (m, 2H), 5.11 (s, 2H). ^{13}C NMR (150 MHz, DMSO-d_6) δ 161.7 (d, J = 243.9 Hz), 152.8, 148.0, 135.1, 132.7, 130.0 (d, J = 8.6 Hz), 123.4, 116.6, 115.4 (d, J = 20.1 Hz), 107.4, 49.5. HRMS (ESI): *m/z* calcd for $C_{13}H_9FN_4NaO_3$ $[M + Na]^+$, 311.0551; found, 311.0551.

2-Nitro-7-(3-(trifluoromethoxy)benzyl)imidazo[1,2-*a*]pyrazin-8(7*H*)-one; 17f

Compound **19f** (100 mg, 0.224 mmol) was reacted according to general procedure C, work-up procedure B. The crude material was purified by recrystallization (DCM/EtOH) with hot filtration to obtain a colorless pearlescent solid (33 mg, 42%). Mp = 230–231 °C (decomposed). LCMS: R_t = 3.45 min, 99 A% @ 254 nm, $[M + H]^+$ = 355.0. ^{1}H NMR (600 MHz, DMSO-d_6) δ 8.82 (s, 1H), 7.61 (d, J = 5.8 Hz, 1H), 7.49 (t, J = 7.9 Hz, 1H), 7.45 (d, J = 5.9 Hz, 1H), 7.41 – 7.38 (m, 1H), 7.37 (ddd, J = 7.5, 1.6, 0.7 Hz, 1H), 7.33 – 7.28 (m, 1H), 5.17 (s, 2H). ^{13}C NMR (150 MHz, DMSO-d_6) δ 152.9, 148.5, 148.0, 139.3, 135.2, 130.7, 126.7, 123.5, 120.3, 120.2, 120.1 (q, J = 257.2 Hz), 116.7, 107.6, 49.8. HRMS (ESI): *m/z* calcd for $C_{14}H_9F_3N_4NaO_4$ $[M + Na]^+$, 377.0468; found, 377.0471.

7-(3-Methylbenzyl)-2-nitroimidazo[1,2-*a*]pyrazin-8(7*H*)-one; 17g

Compound **17a** (70 mg, 0.389 mmol) was reacted according to general procedure B. The crude material contained imidazopyrazinone (major) and imidazopyrazine (minor) isomers in a ratio of 2:1 as detected by LC-MS (UV 254 nm). The crude was partially purified over silica gel by MPLC (Biotage Isolera, 0-6% DCM/MeOH), then purified over C18-reversed phase silica (Grace Reveleris X2, A: H_2O + 0.1% TFA, B: ACN + 0.1% TFA, 0–100% B) to yield imidazopyrazinone **17g** as white powder (11 mg, 7%) and imidazopyrazine **18g** as white powder (9 mg, 7%). **Major isomer imidazopyrazinone 17g**: LCMS:

R_t = 3.25 min, 99 A% @ 254 nm, $[M+H]^+$ = 285.1. ^{1}H NMR (600 MHz, DMSO-d_6) δ 8.81 (s, 1H), 7.59 (d, *J* = 5.9 Hz, 1H), 7.40 (d, *J* = 5.9 Hz, 1H), 7.24 (t, *J* = 7.6 Hz, 1H), 7.18 – 7.09 (m, 3H), 5.09 (s, 2H), 2.28 (s 3H). ^{13}C NMR (150 MHz, DMSO-d_6) δ 152.7, 148.0, 137.9, 136.4, 135.1, 128.5, 128.4, 128.2, 124.8, 123.5, 116.6, 107.3, 50.1, 20.9. HRMS (ESI): *m/z* calc for $C_{14}H_{12}N_4O_3Na$ $[M+Na]^+$: 307.0802, found 307.0800. Characterization data of **18g** is listed below following Compounds 17a-t.

2-Nitro-7-(3-(trifluoromethyl)benzyl)imidazo[1,2-*a*]pyrazin-8(7*H*)-one; 17h

Compound **17a** (70 mg, 0.389 mmol) was reacted with Cs_2CO_3 and 3-(trifluoromethyl)benzyl bromide (1.2 eq) according to general procedure A at μW 100 °C (15 min), work-up B. The crude material containing imidazopyrazinone (major) and imidazopyrazine (minor) isomers were detected in a ratio of 10.1:1 by LC-MS (UV 254 nm). The crude material was purified over silica gel by MPLC (Biotage Isolera, 0-5% DCM/MeOH) to give final products imidazopyrazinone **17h** as white powder (11 mg, 7%) and imidazopyrazine **18h** as white powder (9 mg, 7%). **Major isomer imidazopyrazinone 17h** (cream powder, 72 mg, 55%): LCMS: R_t = 2.95 min, 99 A% @ 254 nm, $[M+H]^+$ = 339.1; ^{1}H NMR (600 MHz, DMSO-d_6) δ 8.82 (s, 1H), 7.77 (d, *J* = 1.7 Hz, 1H), 7.67 (dd, *J* = 12.3, 7.4 Hz, 2H), 7.63 – 7.58 (m, 2H), 7.48 (d, *J* = 5.9 Hz, 1H), 5.22 (s, 2H); ^{13}C NMR (150 MHz, DMSO-d_6) δ 152.9, 148.0, 137.9, 135.2, 131.9, 129.7, 129.3 (q, *J* = 31.8 Hz), 124.5, 124.5, 124.1 (q, *J* = 272.2 Hz), 123.5, 116.7, 107.6, 49.9.HRMS (ESI): *m/z* calc for $C_{14}H_9F_3N_4O_3Na$ $[M+Na]^+$: 361.0519, found 361.0517. Characterization data of **18h** is listed below following Compounds 17a-t.

2-Nitro-7-(2-(trifluoromethoxy)benzyl)imidazo[1,2-*a*]pyrazin-8(7*H*)-one; 17i

Compound **17a** (70 mg, 0.389 mmol) was reacted according to general procedure B. The crude material contained imidazopyrazinone (major) and imidazopyrazine (minor) isomers in a ratio of 1.9:1 as detected by LC-MS (UV 254 nm). The crude material was purified over C18-reversed phase silica (Grace Reveleris X2, A: H_2O + 0.1% TFA, B: ACN + 0.1% TFA, 30–80% B) to give final product: **Major**

isomer imidazopyrazinone 17i (cream powder, 20 mg, 5%): LCMS: R_t = 2.95 min, 98 A% @ 254 nm, $[M+H]^+$ = 355.1; ^{1}H NMR (600 MHz, DMSO-d_6) δ 8.84 (s, 1H), 7.63 (d, J = 5.9 Hz, 1H), 7.47 (ddd, J = 8.2, 7.1, 1.8 Hz, 1H), 7.42 (dt, J = 8.2, 1.6 Hz, 1H), 7.39 – 7.27 (m, 3H), 5.21 (s, 2H); ^{13}C NMR (150 MHz, DMSO-d_6) δ 152.7, 148.0, 146.2, 135.1, 129.7, 129.5, 128.5, 127.6, 123.6, 120.5, 120.2 (q, J = 257.1 Hz), 116.7, 107.5, 45.7. HRMS (ESI): *m/z* calc for $C_{14}H_9F_3N_4O_4Na$ $[M+Na]^+$: 377.0468, found 377.0469. Mixed fractions were combined and purified over silica gel by MPLC (Biotage Isolera, 0-6% DCM/MeOH) to yield **minor isomer imidazopyrazine 18i** (white powder, 11 mg, 3%). Characterization data of **18i** is listed below following Compounds 17a-t.

7-(2,4-Difluorobenzyl)-2-nitroimidazo[1,2-*a*]pyrazin-8(7*H*)-one; 17j

Compound **17a** (50 mg, 0.278 mmol) was reacted with Cs_2CO_3 and 2,4-difluorobenzyl bromide (1.2 eq) according to general procedure A at rt for 1 h, with work-up procedure B. The crude product was purified by recrystallization (slurry equilibration with hot DCM/EtOH) to yield the final product imidazopyrazinone **17j** as a white powder (64 mg, 75%). LCMS: R_t = 2.79 min, 99 A% @ 254 nm, $[M+H]+$ = 307.1; ^{1}H NMR (600 MHz, DMSO-d_6) δ 8.82 (s, 1H), 7.61 (d, J = 5.9 Hz, 1H), 7.43 (td, J = 8.7, 6.5 Hz, 1H), 7.37 (d, J = 5.9 Hz, 1H), 7.30 (ddd, 10.7, 9.3, 2.6 Hz, 1H), 7.10 – 7.06 (m, 1H), 5.14 (s, 2H); ^{13}C NMR (150 MHz, DMSO-d_6) δ 161.9 (dd, J = 246.9, 12.2 Hz), 160.3 (dd, J = 247.9, 12.2 Hz), 152.7, 148.0, 135.0, 131.5 (dd, J = 10.3, 5.6 Hz), 123.6, 119.5 (dd, J = 15.2, 3.9 Hz), 116.7, 111.6 (dd, J = 21.4, 3.2 Hz), 107.4, 104.0 (t, J = 25.7 Hz), 44.6 (d, J = 3.2 Hz). HRMS (ESI): *m/z* calc for $C_{13}H_8F_2N_4O_3Na$ $[M+Na]^+$: 329.0457, found 329.0449.

2-Nitro-7-(pyridin-2-ylmethyl)imidazo[1,2-*a*]pyrazin-8(7*H*)-one.1TFA; 17k

Compound **19k** (150 mg, 0.413 mmol) was reacted according to general procedure C, work-up procedure B. The crude material was purified over C18 silica gel by MPLC (Grace Reveleris X2, A: H_2O + 0.1% TFA, B: ACN + 0.1% TFA, 5–30% B) to yield a colorless powder (88 mg, 56%). LCMS: R_t = 2.61 min,

99 A% @ 254 nm, $[M + H]^+$ = 272.0. ^{1}H NMR (600 MHz, DMSO-d_6) δ 8.85 (s, 1H), 8.53 (dt, J = 4.8, 1.4, 1H), 7.86 (td, J = 7.7, 1.8 Hz, 1H), 7.63 (d, J = 5.9 Hz, 1H), 7.44 (dd, J = 10.1, 6.9 Hz, 2H), 7.40 – 7.34 (m, 1H), 5.26 (s, 2H). ^{13}C NMR (150 MHz, DMSO-d_6) δ 155.0, 152.8, 148.6, 148.0, 137.8, 135.1, 124.6, 123.1, 122.1, 116.6, 107.1, 51.8. HRMS (ESI): *m/z* calcd for $C_{12}H_9N_5O_3$ $[M + H]^+$, 272.0778; found, 272.0782.

7-(1-(4-Fluorophenyl)ethyl)-2-nitroimidazo[1,2-*a*]pyrazin-8(7*H*)-one; 17l

Compound **19l** (100 mg, 0.254 mmol) was reacted according to general procedure C, work-up procedure B. The crude material was purified by recrystallization (DCM/EtOH) with hot filtration to yield a colorless pearlescent solid (34 mg, 45%). Mp = 275–277 °C (decomposed). LCMS: R_t = 3.31 min, 99 A% @ 254 nm, $[M + H]^+$ = 303.0. ^{1}H NMR (600 MHz, DMSO-d_6) δ 8.77 (s, 1H), 7.57 (d, J = 6.1 Hz, 1H), 7.47 – 7.41 (m, 2H), 7.24 – 7.19 (m, 3H), 6.15 (q, J = 7.1 Hz, 1H), 1.71 (d, J = 7.2 Hz, 3H). ^{13}C NMR (150 MHz, DMSO-d_6) δ 161.6 (d, J = 244.4 Hz), 152.6, 148.0, 136.2 (d, J = 2.90 Hz), 134.9, 129.3 (d, J = 8.49 Hz), 119.8, 116.4, 115.5 (d, J = 21.3 Hz), 107.8, 51.6, 18.4. HRMS (ESI): *m/z* calcd for $C_{14}H_{11}FN_4NaO_3$ $[M + Na]^+$, 325.0707; found, 325.0718.

2-Nitro-7-(4-(trifluoromethoxy)phenethyl)imidazo[1,2-*a*]pyrazin-8(7*H*)-one; 17m

Imidazopyrazinone **17a** (75 mg, 0.42 mmol), K_2CO_3 and 1-(2-bromoethyl)-4-(trifluoromethoxy)benzene (1.2 eq) were reacted according to general procedure A (μW 80 °C, 30 min). The crude material contained imidazopyrazinone (major) and imidazopyrazine (minor) isomers in a 10:1 ratio (^{1}H NMR integration). The major imidazopyrazinone isomer **17m** was obtained by purification of the crude residue over C18 silica gel (Grace Reveleris X2, A: H_2O + 0.1% TFA, B: ACN + 0.1% TFA, 40–100% B) to yield a cream solid (33 mg, 22%). Purification of mixed fractions over silica gel by MPLC (Grace Reveleris X2, 0–7% MeOH in DCM gradient) yielded an additional portion of imidazopyrazinone **17m** as a cream solid (34 mg, 22%) and the imidazopyrazine isomer **18m** as a colorless solid (6 mg, 4%). **Major isomer**

imidazopyrazinone 17m: LCMS: R_t = 3.51 min, 99 A% @ 254 nm, 95 A% @ 200 nm, $[M + H]^+$ = 369.0. ^{1}H NMR (600 MHz, DMSO-d_6) δ 8.79 (s, 1H), 7.54 (d, J = 5.8 Hz, 1H), 7.41 – 7.35 (m, 2H), 7.29 (d, J = 8.0 Hz, 2H), 7.27 (d, J = 5.9 Hz, 1H), 4.13 (t, J = 7.5 Hz, 2H), 3.00 (t, J = 7.5 Hz, 2H). ^{13}C NMR (150 MHz, DMSO-d_6) δ 152.6, 148.0, 147.0, 137.4, 135.0, 130.7, 123.6, 121.1, 120.1 (q, J = 257.1 Hz), 116.5, 106.8, 48.6, 33.3. HRMS (ESI): *m/z* calcd for $C_{15}H_{12}F_3N_4O_4$ $[M + H]^+$, 369.0805; found, 369.0814. Characterization data of **18m** is listed below following Compounds 17a-t.

7-(4-Methylphenethyl)-2-nitroimidazo[1,2-*a*]pyrazin-8(7*H*)-one; 17n

Compound **19n** (100 mg, 0.273 mmol) was reacted according to general procedure C, work-up procedure B. The crude material was purified by recrystallization (DCM/acetone) with hot filtration to yield a pearlescent tan solid (45 mg, 59%). Mp = 262–264 °C. LCMS: R_t = 3.38 min, 99 A% @ 254 nm, $[M + H]^+$ = 299.1. ^{1}H NMR (600 MHz, DMSO-d_6) δ 8.78 (s, 1H), 7.52 (d, J = 5.8 Hz, 1H), 7.26 (d, J = 5.9 Hz, 1H), 7.12 (d, J = 7.8 Hz, 2H), 7.09 (d, J = 7.8 Hz, 2H), 4.10 (dd, J = 8.4, 6.7 Hz, 2H), 2.92 (t, J = 7.5 Hz, 2H), 2.25 (s, 3H). ^{13}C NMR (150 MHz, DMSO-d_6) δ 152.6, 148.0, 135.5, 135.0, 134.7, 129.1, 128.7, 123.7, 116.4, 106.7, 49.0, 33.7, 20.7. HRMS (ESI): *m/z* calcd for $C_{15}H_{15}N_4O_3$ $[M + H]^+$, 299.1139; found, 299.1132.

2-(2-Nitro-8-oxoimidazo[1,2-*a*]pyrazin-7(8*H*)-yl)ethyl acetate; 17o

Imidazopyrazinone **17a** (70 mg, 0.39 mmol), K_2CO_3 and 2-bromoethylacetate (1.5 eq) were reacted according to general procedure A (μW 80 °C, 30 min). Imidazopyrazinone isomer was detected as the major regioisomer, with a 10: 1 imidazopyrazinone:imidazopyrazine ratio, by LCMS (UV 254 nm). The reaction was poured into H_2O (20 mL) and the precipitate filtered to yield a cream solid (72 mg, 69%). LCMS: R_t = 2.18 min, 99 A% @ 254 nm, $[M + H]^+$ = 267.0. ^{1}H NMR (600 MHz, DMSO-d_6) δ 8.81 (s, 1H), 7.58 (d, J = 5.9 Hz, 1H), 7.35 (d, J = 5.9 Hz, 1H), 4.33 – 4.27 (m, 2H), 4.19 – 4.14 (m, 2H), 1.97

(s, 3H). ^{13}C NMR (150 MHz, DMSO-d_6) δ 170.2, 152.8, 147.9, 134.9, 124.0, 116.5, 106.8, 61.3, 46.7, 20.6. HRMS (ESI): *m/z* calcd for $C_{10}H_{10}N_4NaO_5$ $[M + Na]^+$, 289.0543; found, 289.0545.

7-(2-Hydroxyethyl)-2-nitroimidazo[1,2-*a*]pyrazin-8(7*H*)-one; 17p

Compound **17o** (45 mg, 0.17 mmol) was reacted according to general procedure D. The product was purified over C18 silica gel by MPLC (Grace Reveleris X2, A: H_2O + 0.1% TFA, B: ACN + 0.1% TFA, 5–22% B) to yield a pale lemon powder (18 mg, 45%). LCMS: R_t = 1.79 min, 99 A% @ 254 nm, $[M + H]^+$ = 225.0. ^{1}H NMR (600 MHz, DMSO-d_6) δ 8.81 (s, 1H), 7.55 (d, *J* = 5.9 Hz, 1H), 7.29 (d, *J* = 5.8 Hz, 1H), 4.90 (t, *J* = 5.7 Hz, 1H), 3.96 (t, *J* = 5.5 Hz, 2H), 3.66 (q, *J* = 5.6 Hz, 2H). ^{13}C NMR (150 MHz, DMSO-d_6) δ 152.8, 147.9, 135.1, 124.7, 116.3, 106.2, 58.4, 50.3. HRMS (ESI): *m/z* calcd for $C_8H_8N_4NaO_4$ $[M + Na]^+$, 247.0438; found, 247.0435.

4-(2-(2-Nitro-8-oxoimidazo[1,2-*a*]pyrazin-7(8*H*)-yl)ethyl)morpholin-4-ium 2,2,2-trifluoroacetate; 17q

Imidazopyrazinone **17a** (75 mg, 0.42 mmol), 4-(2-chloroethyl)morpholine hydrochloride (1.5 eq), potassium iodide (0.06 eq), K_2CO_3 (3 eq) and anh. DMF (20 vol) were reacted according to general procedure A (μW 120 ºC, 15 min). To achieve conversion of the imidazopyrazinone starting material, further portions of potassium iodide (0.09 eq), 4-(2-chloroethyl)morpholine hydrochloride (1.5 eq) and anh. K_2CO_3 (1.5 eq) were added and the reaction heated in the microwave for a further 30 min at 120 ºC and then for 15 min at 150 ºC. The reaction was then evaporated to dryness to give crude material containing imidazopyrazinone (major) and imidazopyrazine (minor) isomers in a 13:1 ratio by LCMS (UV 254 nm). The crude solid was purified over C18 silica gel by MPLC (Grace Reveleris X2, A: H_2O + 0.1% TFA, B: ACN + 0.1% TFA, 5–15% B) to yield imidazopyrazinone **17q** as a sticky solid (143 mg, 84%) and imidazopyrazine **18q** as a red residue (6 mg, 5%). **Major isomer imidazopyrazinone 17q**: LCMS: R_t = 1.58 min, 99 A% @ 254 nm, $[M + H]^+$ = 294.1. ^{1}H NMR (600 MHz, DMSO-d_6) δ 9.94

(br s, 1H), 8.86 (s, 1H), 7.67 (d, J = 5.9 Hz, 1H), 7.37 (d, J = 5.9 Hz, 1H), 4.31 (t, J = 6.2 Hz, 2H), 4.12 – 3.89 (m, 2H), 3.85 – 3.32 (m, 4H), 3.29 – 2.95 (m, 2H), 2.92 – 2.60 (m, 2H). ^{13}C NMR (150 MHz, DMSO-d_6) δ 153.6, 148.0, 135.0, 123.2, 116.6, 107.7, 63.3, 54.3, 52.4, 51.5, 51.0, 41.4. HRMS (ESI): *m/z* calcd for $C_{12}H_{16}N_5O_4$ $[M + H]^+$, 294.1197; found, 294.1197. Characterization data of **18q** is listed below following Compounds 17a-t.

7-(2-Morpholino-2-oxoethyl)-2-nitroimidazo[1,2-*a*]pyrazin-8(7*H*)-one; 17r

Imidazopyrazinone **17a** (75 mg, 0.42 mmol), K_2CO_3 and 4-(chloroacetyl)morpholine (1.2 eq), were reacted according to general procedure A (rt, 2.5 hr). The reaction volatiles were removed in vacuo. Imidazopyrazinone isomer was detected 99: 1 ratio by LCMS (UV 254 nm). A solid precipitated from ACN: (H_2O + 0.1% TFA) mixture and was filtered. The solid was then washed with water (500 µL) and ACN (500 µL) and volatiles removed in vacuo to yield a tan pearlescent solid (80 mg, 63%). LCMS: R_t = 2.44 min, 99 A% @ 254 nm, $[M + H]^+$ = 308.1. ^{1}H NMR (600 MHz, DMSO-d_6) δ 8.85 (s, 1H), 7.59 (d, J = 5.9 Hz, 1H), 7.24 (d, J = 5.9 Hz, 1H), 4.89 (s, 2H), 3.66 (t, J = 4.8 Hz, 2H), 3.59 (t, J = 4.9 Hz, 2H), 3.54 (t, J = 4.9 Hz, 2H), 3.45 (t, J = 4.9 Hz, 2H), 3.33 (s, 1H). ^{13}C NMR (150 MHz, DMSO-d_6) δ 164.8, 152.8, 148.0, 134.8, 124.7, 116.8, 106.6, 66.0, 65.9, 48.7, 44.6, 41.9. HRMS (ESI): *m/z* calcd for $C_{12}H_{13}N_5NaO_5$ $[M + Na]^+$, 330.0809; found, 330.0819.

2-(2-Nitro-8-oxoimidazo[1,2-*a*]pyrazin-7(8*H*)-yl)acetamide; 17s

Imidazopyrazinone **17a** (75 mg, 0.42 mmol), K_2CO_3 and 2-bromoacetamide (1.2 eq) were reacted according to general procedure A at rt for 1.5 h. Imidazopyrazinone isomer was detected 32: 1 ratio by HPLC (UV 254 nm). The reaction was then filtered and the precipitate was washed with water (4 x 250 µL) and MeOH (2 x 250 µL). The crude material was purified over C18 silica gel by MPLC (Grace Reveleris X2, A: H_2O + 0.1% TFA, B: ACN + 0.1% TFA, 5–25% B) to yield a tan solid (5 mg, 4%). LCMS: R_t = 1.75 min, 99 A% @ 254 nm, $[M + H]^+$ = 238.0. ^{1}H NMR (600 MHz, DMSO-d_6) δ 8.84 (s,

1H), 7.66 (br s, 1H), 7.57 (d, *J* = 5.9 Hz, 1H), 7.31 (br s, 1H), 7.30 (d, *J* = 5.8 Hz, 1H), 6.57 (s, 0.3H), 4.52 (s, 2H). A broad singlet that was exchangeable with water was observed at 6.57 ppm integrating for 0.3H. This has previously been observed for this class of compounds and is proposed to be due to protonation of the imidazopyrazinone core. ^{13}C NMR (150 MHz, DMSO-d_6) δ 168.2, 152.9, 148.0, 135.1, 124.8, 116.6, 106.6, 49.9. HRMS (ESI): *m/z* calcd for $C_8H_7N_5NaO_4$ $[M + Na]^+$, 260.0390; found, 260.0392.

7-Cyclohexyl-2-nitroimidazo[1,2-*a*]pyrazin-8(7*H*)-one; 17t

Compound **19t** (79 mg, 0.22 mmol) was reacted according to general procedure C, work-up procedure B. The crude material was purified by recrystallization (DCM/EtOH) to yield a cream colored crystalline solid (42 mg, 68%). Mp = 275–277 °C (decomposed). LCMS: R_t = 3.20 min, 99 A% @ 254 nm, $[M + H]^+$ = 263.1. ^{1}H NMR (600 MHz, DMSO-d_6) δ 8.76 (s, 1H), 7.58 (d, *J* = 6.0 Hz, 1H), 7.43 (d, *J* = 6.1 Hz, 1H), 4.66 (tt, *J* = 12.1, 3.8 Hz, 1H), 1.83 (d, *J* = 13.6 Hz, 2H), 1.74 (d, *J* = 12.0 Hz, 2H), 1.64 (qd, *J* = 12.3, 3.6 Hz, 3H), 1.41 (qt, *J* = 12.5, 3.4 Hz, 2H), 1.20 (qt, *J* = 12.5, 4.0 Hz, 1H). ^{13}C NMR (150 MHz, DMSO-d_6) δ 152.3, 148.0, 135.0, 119.8, 116.2, 107.1, 53.3, 30.8, 25.3, 24.7. HRMS (ESI): *m/z* calcd for $C_{12}H_{14}N_4NaO_3$ $[M + Na]^+$, 285.0958; found, 285.0953.

8-((3-Methylbenzyl)oxy)-2-nitroimidazo[1,2-*a*]pyrazine; 18g

Minor isomer imidazopyrazine 18g was isolated from **17g**. LCMS: R_t = 3.58 min, 99 A% @ 254 nm, $[M+H]^+$ = 285.1; ^{1}H NMR (600 MHz, DMSO-d_6) δ 9.02 (t, *J* = 1.8 Hz, 1H), 8.25 (dt, *J* = 3.8, 1.7 Hz, 1H), 7.65 (dt, *J* = 4.0, 1.8 Hz, 1H), 7.36 – 7.28 (m, 3H), 7.20 (dd, *J* = 6.8, 3.5 Hz, 1H), 5.55 – 5.51 (m, 2H), 3.42 (s, 1H), 2.34 (d, *J* = 2.1 Hz, 3H). Impurities were detected by ^{1}H NMR and this compound was not subjected to biological evaluation.

2-Nitro-8-((3-(trifluoromethyl)benzyl)oxy)imidazo[1,2-*a*]pyrazine; 18h

Minor isomer imidazopyrazine 18h was isolated from **17h**. LCMS: R_t = 3.22 min, 99 A% @ 254 nm, $[M+H]^+$ = 339.1; ^{1}H NMR (600 MHz, $CDCl_3$) δ 8.31 (s, 1H), 7.81 – 7.76 (m, 2H), 7.76 – 7.72 (m, 1H), 7.63 – 7.58 (m, 2H), 7.54 – 7.48 (m, 1H), 5.67 (s, 2H). Impurities were detected by ^{1}H NMR and this compound was not subjected to biological evaluation.

2-Nitro-8-((2-(trifluoromethoxy)benzyl)oxy)imidazo[1,2-*a*]pyrazine; 18i

Minor isomer imidazopyrazine 18i was isolated from **17i**. LCMS: R_t = 3.25 min, 99 A% @ 254 nm, $[M+H]^+$ = 355.1; ^{1}H NMR (600 MHz, DMSO-d_6) δ 9.04 (s, 1H), 8.27 (d, J = 4.7 Hz, 1H), 7.76 – 7.72 (m, 1H), 7.66 (d, J = 4.7 Hz, 1H), 7.60 – 7.53 (m, 1H), 7.51 – 7.44 (m, 2H), 5.64 (s, 2H); ^{13}C NMR (150 MHz, DMSO-d_6) δ 153.8, 148.2, 146.7, 131.2, 130.6, 130.1, 128.3, 128.0, 127.7, 120.7, 120.2 (q, J = 258.3 Hz), 116.5, 115.0, 62.7.δ HRMS (ESI): *m/z* calc for $C_{14}H_9F_3N_4O_4Na$ $[M+Na]^+$: 377.0468, found 377.0470.

2-Nitro-8-(4-(trifluoromethoxy)phenethoxy)imidazo[1,2-*a*]pyrazine; 18m

Minor isomer imidazopyrazine 18m was isolated from **17m**. LCMS: R_t = 3.76 min, 99 A% @ 254 nm, $[M + H]^+$ = 369.1. ^{1}H NMR (600 MHz, DMSO-d_6) δ 9.01 (s, 1H), 8.22 (d, J = 4.7 Hz, 1H), 7.62 (d, J = 4.7 Hz, 1H), 7.52 – 7.46 (m, 2H), 7.34 – 7.29 (m, 2H), 4.73 (t, J = 6.7 Hz, 2H), 3.20 (t, J = 6.7 Hz, 2H). ^{13}C NMR (150 MHz, DMSO-d_6) δ 154.3, 148.2, 147.0, 137.7, 130.8, 128.2, 121.1, 120.1 (q, J = 256.2 Hz), 116.0, 114.9, 67.1, 33.5. HRMS (ESI): *m/z* calcd for $C_{15}H_{12}F_3N_4O_4$ $[M + H]^+$, 369.0805; found, 369.0799.

4-(2-((2-Nitroimidazo[1,2-*a*]pyrazin-8-yl)oxy)ethyl)morpholin-4-ium 2,2,2-trifluoroacetate; 18q

Minor isomer imidazopyrazine 18q was isolated from **17q**. LCMS: R_t = 2.31 min, 97 A% @ 254 nm, $[M + H]^+$ = 294.1. ^{1}H NMR (600 MHz, DMSO-d_6) δ 9.08 (s, 1H), 8.31 (d, J = 4.7 Hz, 1H), 7.67 (d, J =

4.7 Hz, 1H), 4.85 (br s, 2H), 4.27 – 3.02 (m, 10H). Impurities were detected in the ^{1}H NMR analysis and therefore the compound was not subjected to biological analysis.

1-(2,2-Diethoxyethyl)-4-nitro-1*H*-imidazole-2-carboxamide; 19a

Imidazole-2-carboxamide **16a** (650 mg, 3.38 mmol) was reacted according to general procedure A with K_2CO_3, bromoacetaldehyde diethyl acetal (2 × 1.5 eq) at μW 180 °C (2 × 15 min). The crude material was triturated with pet. spirits (3 × 3 mL) and dried in vacuo to yield an orange solid (710 mg, 77%). LCMS: R_t = 3.04 min, 88 A% @ 254 nm, $[M + H - EtOH]^+$ = 227.0. ^{1}H NMR (400 MHz, $CDCl_3$) δ 7.93 (s, 1H), 7.93 (br s, 1H), 5.62 (br s, 1H), 4.73 (dd, *J* = 5.2, 4.5 Hz, 1H), 4.64 (d, *J* = 5.0 Hz, 2H), 3.75 (dq, *J* = 9.4, 7.1 Hz, 2H), 3.53 (dq, *J* = 9.4, 7.0 Hz, 2H), 1.19 (t, *J* = 7.0 Hz, 6H). ^{13}C NMR (150 MHz, $CDCl_3$) δ 159.5, 145.3, 136.2, 125.4, 100.5, 64.2, 51.8, 15.2. HRMS (ESI): *m/z* calcd for $C_{10}H_{16}N_4NaO_5$ $[M + Na]^+$, 295.1013; found, 295.1010.

***N*-Benzyl-1-(2,2-diethoxyethyl)-4-nitro-1*H*-imidazole-2-carboxamide; 19b**

Imidazole-2-carboxamide **16b** (150 mg, 0.609 mmol) was reacted according to general procedure A with K_2CO_3 and bromoacetaldehyde diethyl acetal (1.5 eq, 2nd portion = 0.5 eq) at μW 150 °C (30 min, followed by 15 min) to yield a waxy yellow solid (219 mg, 99%). LCMS: R_t = 3.72 min, 97 A% @ 254 nm, $[M + H - EtOH]^+$ = 317.1. ^{1}H NMR (400 MHz, $CDCl_3$) δ 7.91 (s, 1H), 7.68 (t, *J* = 4.5 Hz, 1H), 7.40 – 7.27 (m, 5H), 4.75 (dd, *J* = 5.3, 4.5 Hz, 1H), 4.68 (d, *J* = 4.8 Hz, 2H), 4.57 (d, *J* = 6.1 Hz, 2H), 3.75 (dq, *J* = 9.0, 7.3 Hz, 2H), 3.54 (dq, *J* = 9.4, 6.9 Hz, 2H), 1.19 (t, *J* = 7.1 Hz, 6H). ^{13}C NMR (150 MHz, $CDCl_3$) δ 157.5, 145.2, 136.9, 136.8, 128.8, 128.0, 127.9, 125.2, 100.6, 64.2, 51.6, 43.4, 15.2. HRMS (ESI): *m/z* calcd for $C_{17}H_{22}N_4NaO_5$ $[M + Na]^+$, 385.1482; found, 385.1480.

1-(2,2-Diethoxyethyl)-4-nitro-*N*-(4-(trifluoromethoxy)benzyl)-1*H*-imidazole-2-carboxamide; 19c

Imidazole-2-carboxamide **16c** (125 mg, 0.332 mmol) was reacted according to general procedure A with K_2CO_3 and bromoacetaldehyde diethyl acetal (2 × 1.5 eq) at μW 180 °C (2 × 15 min). The crude residue was purified over silica gel by MPLC (Biotage, 12–100% EtOAc in pet. spirits gradient) to yield a pale yellow waxy solid (112 mg, 76%). LCMS: R_t = 3.40 min, 99 A% @ 254 nm, $[M - H]^-$ = 445.0. ^{1}H NMR (600 MHz, $CDCl_3$) δ 7.92 (s, 1H), 7.75 (br t, 1H), 7.39 – 7.33 (m, 2H), 7.20 (m, 2H), 4.74 (dd, *J* = 5.1, 4.5 Hz, 1H), 4.67 (d, *J* = 4.8 Hz, 2H), 4.57 (d, *J* = 6.2 Hz, 2H), 3.75 (dq, *J* = 9.4, 7.0 Hz, 2H), 3.53 (dq, *J* = 9.4, 7.0 Hz, 2H), 1.18 (t, *J* = 7.0 Hz, 6H). ^{13}C NMR (150 MHz, $CDCl_3$) δ 157.8, 148.9, 145.4, 136.8, 136.0, 129.5, 125.4, 121.5, 120.6 (q, *J* = 256.5 Hz), 100.7, 64.3, 51.7, 42.7, 15.3. HRMS (ESI): *m/z* calcd for $C_{18}H_{21}F_3N_4NaO_6$ $[M + Na]^+$, 469.1305; found, 469.1316.

1-(2,2-Diethoxyethyl)-*N*-(4-methylbenzyl)-4-nitro-1*H*-imidazole-2-carboxamide; 19d

Imidazole-2-carboxamide **16d** (75 mg, 0.29 mmol) was reacted according to general procedure A with K_2CO_3 and bromoacetaldehyde diethyl acetal (2 × 1.5 eq) at μW 150 °C (2 × 30 min) to yield a yellow oil which was used without further purification (116 mg with 43 mol% residual DMF by ^{1}H NMR, 98%). LCMS: R_t = 3.80 min, 97 A% @ 254 nm, $[M + H - EtOH]^+$ = 331.1. ^{1}H NMR (600 MHz, $CDCl_3$) δ 7.92 (s, 1H), 7.67 (d, *J* = 5.7 Hz, 1H), 7.25 – 7.19 (m, 2H), 7.19 – 7.14 (m, 2H), 4.76 (t, *J* = 4.9 Hz, 1H), 4.68 (d, *J* = 4.9 Hz, 2H), 4.54 (d, *J* = 6.1 Hz, 2H), 3.77 (dq, *J* = 9.4, 7.0 Hz, 2H), 3.55 (dq, *J* = 9.4, 7.0 Hz, 2H), 2.35 (s, 3H), 1.19 (t, *J* = 7.0 Hz, 5H). ^{13}C NMR (151 MHz, $CDCl_3$) δ 157.5, 145.2, 137.6, 136.9, 133.9, 129.5, 128.0, 125.2, 100.6, 64.2, 51.6, 43.2, 21.1, 15.2. HRMS (ESI): *m/z* calcd for $C_{18}H_{24}N_4NaO_5$ $[M + Na]^+$, 399.1639; found, 399.1643.

1-(2,2-Diethoxyethyl)-*N*-(4-fluorobenzyl)-4-nitro-1*H*-imidazole-2-carboxamide; 19e

Imidazole-2-carboxamide **16e** (311 mg, 1.18 mmol) was reacted according to general procedure A with K_2CO_3 and bromoacetaldehyde diethyl acetal (2 × 1.5 eq) at μW 180 °C (2 × 15 min). The crude residue was purified over silica gel by MPLC (Biotage, 10–60% EtOAc in pet. spirits gradient) to yield a pale

yellow oil (411 mg, 92%). LCMS: R_t = 3.76 min, 99 A% @ 254 nm, $[M + H - EtOH]^+$ = 335.0. ^{1}H NMR (400 MHz, $CDCl_3$) δ 7.91 (s, 1H), 7.70 (br s, 1H), 7.35 – 7.27 (m, 2H), 7.09 – 6.98 (m, 2H), 4.74 (dd, *J* = 5.2, 4.4 Hz, 1H), 4.67 (d, *J* = 4.8 Hz, 2H), 4.60 – 4.50 (m, 2H), 3.75 (dq, *J* = 9.4, 7.0 Hz, 2H), 3.54 (dq, *J* = 9.4, 7.0 Hz, 2H), 1.18 (t, *J* = 7.0 Hz, 6H). ^{13}C NMR (150 MHz, $CDCl_3$) δ 162.4 (d, *J* = 245.19 Hz), 157.6, 145.3, 136.8, 132.8 (d, *J* = 3.8 Hz), 129.7 (d, *J* = 8.1 Hz), 125.2, 115.7 (d, *J* = 21.6 Hz), 100.6, 64.2, 51.6, 42.7, 15.2. HRMS (ESI): *m/z* calcd for $C_{17}H_{21}F_1N_4NaO_5$ $[M + Na]^+$, 403.1388; found, 403.1389.

1-(2,2-Diethoxyethyl)-4-nitro-*N*-(3-(trifluoromethoxy)benzyl)-1*H*-imidazole-2-carboxamide; 19f

Imidazole-2-carboxamide **16f** (75 mg, 0.23 mmol) was reacted according to general procedure A with K_2CO_3 and bromoacetaldehyde diethyl acetal (2 × 1.5 eq) at μW 150 °C (2 × 30 min) to yield an orange solid which was used without further purification (108 mg, quant.). LCMS: R_t = 3.88 min, 95 A% @ 254 nm, $[M + H - EtOH]^+$ = 401.1. ^{1}H NMR (600 MHz, $CDCl_3$) δ 7.94 (s, 1H), 7.81 (t, *J* = 6.1 Hz, 1H), 7.39 (t, *J* = 7.9 Hz, 1H), 7.30 – 7.24 (m, 1H), 7.21 – 7.14 (m, 2H), 4.75 (dd, *J* = 5.2, 4.5 Hz, 1H), 4.69 (d, *J* = 4.8 Hz, 2H), 4.60 (d, *J* = 6.3 Hz, 2H), 3.76 (dq, *J* = 9.4, 7.1 Hz, 2H), 3.54 (dq, *J* = 9.4, 7.0 Hz, 2H), 1.19 (t, *J* = 7.0 Hz, 6H). ^{13}C NMR (150 MHz, $CDCl_3$) δ 157.7, 149.5, 145.2, 139.5, 136.6, 130.2, 126.1, 125.3, 120.4 (q, *J* = 260.9 Hz), 120.4, 120.2, 100.5, 64.2, 51.6, 42.7, 15.1. HRMS (ESI): *m/z* calcd for $C_{18}H_{21}F_3N_4NaO_6$ $[M + Na]^+$, 469.1305; found, 469.1306.

1-(2,2-Diethoxyethyl)-4-nitro-*N*-(pyridin-2-ylmethyl)-1*H*-imidazole-2-carboxamide; 19k

Imidazole-2-carboxamide **16k** (150 mg, 0.607 mmol) was reacted according to general procedure A with K_2CO_3 and bromoacetaldehyde diethyl acetal (1.5 eq, 2nd portion = 0.5 eq) at μW 150 °C (30 min, followed by 15 min) to yield a red oil which was used without further purification (153 mg, 69%). LCMS: R_t = 3.13 min, 97 A% @ 254 nm, $[M + H - EtOH]^+$ = 318.1. ^{1}H NMR (600 MHz, DMSO-d_6) δ 9.41 (t, *J* = 6.1 Hz, 1H), 8.52 (s, 1H), 8.51 (ddd, *J* = 4.7, 1.7, 1.0 Hz, 1H), 7.76 (td, *J* = 7.7, 1.8 Hz, 1H), 7.32 (d,

J = 8.3 Hz, 1H), 7.27 (ddd, *J* = 7.6, 4.9, 1.1 Hz, 1H), 4.79 (t, *J* = 5.2 Hz, 1H), 4.60 (d, *J* = 5.2 Hz, 2H), 4.53 (d, *J* = 6.1 Hz, 2H), 3.61 (dq, *J* = 9.7, 7.0 Hz, 2H), 3.41 (dq, *J* = 9.7, 7.0 Hz, 2H), 1.02 (t, *J* = 7.0 Hz, 6H). ^{13}C NMR (150 MHz, DMSO-d_6) δ 157.9, 157.7, 148.9, 144.4, 137.7, 136.7, 126.4, 122.2, 120.9, 100.0, 62.8, 50.3, 44.1, 15.1. HRMS (ESI): *m/z* calcd for $C_{16}H_{22}N_5O_5$ $[M + H]^+$, 364.1615; found, 364.1622.

1-(2,2-Diethoxyethyl)-*N*-(1-(4-fluorophenyl)ethyl)-4-nitro-1*H*-imidazole-2-carboxamide; 19l

Imidazole-2-carboxamide **16l** (75 mg, 0.27 mmol) was reacted according to general procedure A with K_2CO_3 and bromoacetaldehyde diethyl acetal (1.5 eq, 2nd portion = 1 eq) at µW 150 °C (2 × 30 min) to yield a yellow oil (113 mg, quant) which was used without further purification. LCMS: R_t = 3.80 min, 97 A% @ 254 nm, $[M + H - EtOH]^+$ = 349.1. ^{1}H NMR (600 MHz, $CDCl_3$) δ 7.92 (s, 1H), 7.60 (d, *J* = 8.2 Hz, 1H), 7.37 – 7.31 (m, 2H), 7.08 – 7.01 (m, 2H), 5.20 (p, *J* = 7.2 Hz, 1H), 4.74 – 4.66 (m, 2H), 4.65 – 4.56 (m, 1H), 3.77 – 3.69 (m, 2H), 3.52 (dq, *J* = 9.4, 7.0 Hz, 2H), 1.60 (d, *J* = 7.0 Hz, 3H), 1.17 (dt, *J* = 12.1, 7.0 Hz, 6H). ^{13}C NMR (150 MHz, $CDCl_3$) δ 162.1 (d, *J* = 245.3 Hz), 156.8, 145.2, 138.1 (d, *J* = 3.0 Hz), 136.8, 127.8 (d, *J* = 8.2 Hz), 125.3, 115.6 (d, *J* = 21.8 Hz), 100.5, 64.1, 51.6, 48.5, 21.9, 15.1. HRMS (ESI): *m/z* calcd for $C_{18}H_{23}FN_4NaO_5$ $[M + Na]^+$, 417.1545; found, 417.1537.

1-(2,2-Diethoxyethyl)-*N*-(4-methylphenethyl)-4-nitro-1*H*-imidazole-2-carboxamide; 19n

Imidazole-2-carboxamide **16n** (75 mg, 0.27 mmol) was reacted according to general procedure A with K_2CO_3 and bromoacetaldehyde diethyl acetal (2 × 1.5 eq) at µW 150 °C (2 × 30 min) to yield a yellow oil which was used without further purification (112 mg, quant.). LCMS: R_t = 3.85 min, 98 A% @ 254 nm, $[M + H - EtOH]^+$ = 345.1. ^{1}H NMR (600 MHz, $CDCl_3$) δ 7.90 (s, 1H), 7.46 (t, *J* = 6.2 Hz, 1H), 7.19 – 7.03 (m, 4H), 4.72 (t, *J* = 4.9 Hz, 1H), 4.64 (d, *J* = 4.9 Hz, 2H), 3.76 (dq, *J* = 9.4, 7.0 Hz, 2H), 3.64 (dt, *J* = 7.7, 6.5 Hz, 2H), 3.53 (dq, *J* = 9.4, 7.0 Hz, 2H), 2.91 – 2.85 (m, 2H), 2.34 (s, 3H), 1.19 (t, *J* = 7.0 Hz, 6H). ^{13}C NMR (150 MHz, $CDCl_3$) δ 157.6, 145.1, 136.9, 136.2, 135.1, 129.4, 128.6, 125.1, 100.7, 64.2,

51.6, 40.8, 35.3, 21.0, 15.2. HRMS (ESI): *m/z* calcd for $C_{19}H_{26}N_4NaO_5$ $[M + Na]^+$, 413.1795; found, 413.1797.

_N_-Cyclohexyl-1-(2,2-diethoxyethyl)-4-nitro-1_H_-imidazole-2-carboxamide; 19t

Imidazole-2-carboxamide **16t** (75 mg, 0.31 mmol) was reacted according to general procedure A with K_2CO_3 and bromoacetaldehyde diethyl acetal (1.5 eq, 2nd portion = 1 eq) at μW 150 °C (2 × 30 min) to yield an orange solid (107 mg, 96%) which was used without further purification. LCMS: R_t = 3.78 min, 97 A% @ 254 nm, $[M + H]^+$ = 309.1. ^{1}H NMR (600 MHz, $CDCl_3$) δ 7.90 (s, 1H), 7.24 (d, *J* = 8.5 Hz, 1H), 4.75 (t, *J* = 5.0 Hz, 1H), 4.65 (d, *J* = 5.0 Hz, 2H), 3.88 (tdt, *J* = 11.9, 8.2, 3.9 Hz, 1H), 3.76 (dq, *J* = 9.3, 7.1 Hz, 2H), 3.54 (dq, *J* = 9.3, 7.0 Hz, 2H), 2.02 – 1.96 (m, 2H), 1.83 – 1.77 (m, 2H), 1.72 – 1.62 (m, 1H), 1.44 – 1.35 (m, 2H), 1.35 – 1.25 (m, 3H), 1.19 (t, *J* = 7.0 Hz, 6H). ^{13}C NMR (150 MHz, $CDCl_3$) δ 156.8, 145.1, 137.2, 125.1, 100.7, 64.2, 51.7, 48.8, 32.9, 25.3, 25.0, 15.2. HRMS (ESI): *m/z* calcd for $C_{16}H_{26}N_4NaO_5$ $[M + Na]^+$, 377.1795; found, 377.1794.

Imidazo[1,2-*a*]pyrazin-8(7*H*)-one; 20a

To a stirred suspension of imidazole **23a** (168 mg, 0.741 mmol) in H_2O (20 vol.) was added 5% w/v HCl (530 μL, 1 eq). The solution was heated to reflux for 2 h, cooled to rt and concentrated *in vacuo* to dryness. The solid was purified by recrystallization (slurry equilibration with hot MeOH) to yield beige crystals (50 mg, 50%). Mp = 307–308 °C (decomposed). LCMS (Waters Atlantis): R_t = 1.75 min, 99 A% @ 254 nm, $[M + H]^+$ = 136.1 ^{1}H NMR (400 MHz, DMSO-d_6) δ 8.20 (d, *J* = 1.7 Hz, 1H), 8.01 (d, *J* = 1.7 Hz, 1H), 7.75 (d, *J* = 5.6 Hz, 1H), 7.23 (t, *J* = 5.6 Hz, 1H). ^{13}C NMR (150 MHz, DMSO-d_6) δ 151.3, 135.1, 126.3, 119.7, 118.3, 107.2. HRMS calcd for $C_{12}H_{10}N_6NaO_2$ $[2M + Na]^+$, 293.0757; found, 293.0764. The proton spectra was consistent with literature.[35]

7-Benzylimidazo[1,2-*a*]pyrazin-8(7*H*)-one; 20b

To a stirred suspension of compound **23b** (120 mg, 0.378 mmol) in H_2O (20 vol.) was added 5% aq. HCl (270 µL, 1 eq). The reaction was heated at 80 °C for 3 days before further addition of 5% aq. HCl (135 µL, 0.5 eq). The reaction mixture was then washed with EtOAc (3 × 5 mL followed by 3 × 10 mL). The aqueous layer was then evaporated to dryness. The crude material was purified over C18 silica gel by MPLC (Grace Reveleris X2. A: H_2O + 0.1% TFA, B: ACN + 0.1% TFA, 10–30% B) to yield a colorless solid (47 mg, 39%). LCMS: R_t = 2.14 min, 98 A% @ 254 nm, $[M + H]^+$ = 226.0. ^{1}H NMR (600 MHz, DMSO-d_6) δ 7.93 (d, J = 1.2 Hz, 1H), 7.69 – 7.65 (m, 2H), 7.40 – 7.27 (m, 6H), 5.14 (s, 2H). ^{13}C NMR (151 MHz, DMSO-d_6) δ 152.1, 136.7, 136.0, 130.3, 128.5, 127.6, 127.6, 121.6, 117.8, 107.4, 49.8. HRMS (ESI): *m/z* calcd for $C_{13}H_{11}N_3NaO$ $[M + Na]^+$, 248.0794; found, 249.0799.

7-(4-Fluorobenzyl)imidazo[1,2-*a*]pyrazin-8(7*H*)-one; 20c

Imidazopyrazinone **20a** (100 mg, 0.740 mmol), K_2CO_3 and 4-fluorobenzyl bromide (1.2 eq), were reacted according to general procedure A at rt for 45 min. The imidazopyrazinone regioisomer was detected as the preferred isomer (24: 1 ratio) by HPLC (UV 254 nm). The crude material was purified by recrystallization (EtOH) to yield a colorless solid (34 mg, 19%). Mp = 168–169 °C. LCMS: R_t = 2.94 min, 99 A% @ 254 nm, $[M + H]^+$ = 244.1. ^{1}H NMR (400 MHz, DMSO-d_6) δ 7.84 – 7.78 (m, 1H), 7.61 (d, J = 5.8 Hz, 1H), 7.52 – 7.46 (m, 1H), 7.45 – 7.36 (m, 2H), 7.24 (d, J = 5.9 Hz, 1H), 7.22 – 7.12 (m, 2H), 5.09 (s, 2H). ^{13}C NMR (150 MHz, DMSO-d_6) δ 161.6 (d, J = 243.2 Hz), 153.0, 137.0, 133.4 (d, J = 3.0 Hz), 132.7, 129.9 (d, J = 8.5 Hz), 120.4, 117.6, 115.4 (d, J = 21.7 Hz), 107.5, 49.1. HRMS (ESI): *m/z* calcd for $C_{13}H_{11}FN_3O$ $[M + H]^+$, 244.0881; found, 244.0884.

***N*-(Benzyl)-1*H*-imidazole-2-carboxamide; 22b**

1*H*-Imidazole-2-carboxylic acid **21a** (1.08 g, 9.60 mmol) was refluxed in $SOCl_2$ (10 mL) under N_2 for 22 h. Volatiles were removed in vacuo and residual $SOCl_2$ was removed by co-evaporation with toluene to give the crude acid chloride intermediate. Benzylamine (478 µL, 4.38 mmol) was added drop wise to

acid chloride (476 mg, 3.65 mmol) suspended in anh. THF (13 mL) under an atmosphere of N_2. The light brown precipitate was filtered and washed with THF to yield a tan solid (685 mg, 79%) that was used without further purification. LCMS: R_t = 2.68 min, 99 A% @ 254 nm, $[M + H]^+$ = 202.1. ^{1}H NMR (600 MHz, $CDCl_3$) δ 8.97 (t, *J* = 5.7 Hz, 1H), 7.49–7.04 (m, 7H), 4.43 (d, *J* = 6.2 Hz, 2H). ^{13}C NMR (150 MHz, $CDCl_3$) δ 158.3, 140.9, 139.5, 134.0, 128.1, 127.1, 126.6, 119.6 (br), 41.8.

1-(2,2-Diethoxyethyl)-1*H*-imidazole-2-carboxamide; 23a

Imidazole-2-carboxamide **22a** (650 mg, 5.85 mmol) was reacted according to general procedure A with K_2CO_3, bromoacetaldehyde diethyl acetal (2 × 1.5 eq) at μW 120 °C (2 × 15 min) to yield a yellow solid that was used without further purification (1.08 g, 81%). LCMS: R_t = 2.65 min, 99 A% @ 254 nm, $[M + H- EtOH]^+$ = 182.1. ^{1}H NMR (400 MHz, $CDCl_3$) δ 7.23 (br s, 1H), 7.12 (d, *J* = 1.1 Hz, 1H), 7.01 (d, *J* = 1.1 Hz, 1H), 5.33 (br s, 1H), 4.84 – 4.60 (m, 1H), 4.53 (d, *J* = 5.3 Hz, 2H), 3.73 (dq, *J* = 9.4, 7.0 Hz, 2H), 3.48 (dq, *J* = 9.4, 7.0 Hz, 2H), 1.16 (t, *J* = 7.0 Hz, 6H). ^{13}C NMR (150 MHz, $CDCl_3$) δ 161.1, 137.8, 127.6, 126.7, 101.8, 64.0, 51.0, 15.2. NMR data was consistent with literature.[35]

***N*-Benzyl-1-(2,2-diethoxyethyl)-1*H*-imidazole-2-carboxamide; 23b**

Imidazole-2-carboxamide **22b** (201 mg, 0.846 mmol) was reacted according to general procedure A with K_2CO_3, bromoacetaldehyde diethyl acetal (1 eq, 2nd portion = 0.2 eq) at μW 180 °C (2 × 15 min). Crude product was obtained as a yellow oil (246 mg, 92%) which was used without further purification. LCMS: R_t = 2.37 min, 89 A% @ 254 nm, $[M + H]^+$ = 318.2. ^{1}H NMR (600 MHz, $CDCl_3$) δ 7.79 (t, *J* = 6.3 Hz, 1H), 7.40 – 7.34 (m, 4H), 7.34 – 7.30 (m, 1H), 7.14 (d, *J* = 1.0 Hz, 1H), 7.01 (d, *J* = 1.0 Hz, 1H), 4.79 (t, *J* = 5.5 Hz, 1H), 4.61 (d, *J* = 6.3 Hz, 2H), 4.60 (d, *J* =5.5 Hz, 2H), 3.77 (dq, *J* = 9.4, 7.0 Hz, 2H), 3.52 (dq, *J* = 9.4, 7.0 Hz, 2H), 1.20 (t, *J* = 7.0 Hz, 6H). ^{13}C NMR (100 MHz, $CDCl_3$) δ 159.0, 138.5, 137.9,

128.7, 127.7, 127.5, 127.4, 126.3, 101.9, 64.0, 50.8, 43.1, 15.2. HRMS (ESI): *m/z* calcd for $C_{34}H_{46}N_6NaO_6$ $[2M + Na]^+$, 657.3371; found, 657.3392.

2-Nitro-6-phenylimidazo[1,2-*a*]pyrazin-8(7*H*)-one; 24a

Compound **27a** (230 mg, 0.839 mmol) was reacted according to general procedure C to yield a crystalline yellow solid (181 mg, 84%). Mp = 342 °C (decomposed). LCMS: R_t = 3.05 min, 99 A% @ 254 nm, $[M + H]^+$ = 257.0. ^{1}H NMR (600 MHz, DMSO-d_6) δ 11.97 (s, 1H), 8.79 – 8.73 (s, 1H), 7.83 (s, 1H), 7.71 – 7.64 (m, 2H), 7.57 – 7.48 (m, 3H). ^{13}C NMR (150 MHz, DMSO-d_6) δ 153.6, 147.9, 134.6, 132.1, 130.7, 129.9, 129.0, 126.8, 116.7, 104.6. HRMS (ESI): *m/z* calcd for $C_{12}H_8N_4NaO_3$ $[M + Na]^+$, 279.0489; found, 279.0482.

2-Nitro-6-phenylimidazo[1,2-*a*]pyrazin-8(7*H*)-one; 24a

Imidazole-2-carboxamide **13a** (450 mg, 2.34 mmol) was reacted according to general procedure E with 2-bromoacetophenone (1.2 eq) in anh. DMF (20 vol). HCl (2M aq., 20 vol) was then added slowly and reaction was then heated (μW 120 °C for 1 h, 150 °C for 15 min) and the product isolated to yield a brown solid (242 mg, 40%). LCMS: R_t = 3.02 min, 98 A% @ 254 nm, $[M + H]^+$ = 257.0. ^{1}H NMR (600 MHz, DMSO-d_6) δ 11.99 (s, 1H), 8.77 (s, 1H), 7.83 (s, 1H), 7.69 – 7.67 (m, 2H), 7.55 – 7.50 (m, 3H). Proton spectrum consistent with preparation using 4-nitroimidazole **21a** as starting material.

2-((2-Nitro-6-phenylimidazo[1,2-*a*]pyrazin-8-yl)oxy)ethyl acetate; 24b and 2-(2-nitro-8-oxo-6-phenylimidazo[1,2-*a*]pyrazin-7(8*H*)-yl)ethyl acetate; 24c

Imidazopyrazinone **24a** (280 mg, 1.09 mmol) was reacted according to general procedure A with K_2CO_3 and 2-bromoethylacetate (2 × 1.5 eq) with heating (2 × μW 80 °C, 30 min). The crude material contained imidazopyrazinone (minor) and imidazopyrazine (major) isomers in a 1:5.7 ratio by NMR. The crude material was purified over C18 silica gel by MPLC (Grace Reveleris, A: H_2O + 0.1% TFA, B: ACN +

0.1% TFA, 20–100% B) to yield imidazopyrazine as a yellow solid (231 mg, 62%) and imidazopyrazinone as a yellow solid (19 mg, 5%). **Minor isomer imidazopyrazinone 24b**: LCMS: R_t = 2.59 min, 99 A% @ 254 nm, $[M + H]^+$ = 343.0. ^{1}H NMR (600 MHz, DMSO-d_6) δ 8.74 (s, 1H), 7.60 – 7.52 (m, 5H), 7.50 (s, 1H), 4.10 – 4.02 (m, 4H), 1.89 (s, 3H). ^{13}C NMR (150 MHz, DMSO-d_6) δ 170.0, 153.3, 148.1, 134.6, 134.1, 131.3, 129.9, 129.8, 128.8, 116.1, 106.8, 60.7, 43.4, 20.6. HRMS (ESI): *m/z* calcd for $C_{16}H_{14}N_4Na_1O_5$ $[M + Na]^+$, 365.0856; found, 365.0858. **Major isomer imidazopyrazine 24c**: LCMS: R_t = 2.93 min, 99 A% @ 254 nm, $[M + H]^+$ = 343.0. ^{1}H NMR (600 MHz, DMSO-d_6) δ 8.95 (s, 1H), 8.86 (s, 1H), 8.03 – 7.98 (m, 2H), 7.57 – 7.51 (m, 2H), 7.49 – 7.43 (m, 1H), 4.89 – 4.84 (m, 2H), 4.53 – 4.48 (m, 2H), 2.05 (s, 3H). ^{13}C NMR (150 MHz, DMSO-d_6) δ 170.3, 153.0, 148.4, 136.8, 135.0, 129.5, 129.2, 128.9, 125.7, 115.1, 111.9, 65.0, 62.0, 20.7. HRMS (ESI): *m/z* calcd for $C_{16}H_{14}N_4Na_1O_5$ $[M + Na]^+$, 365.0856; found, 365.0861.

7-(2-Hydroxyethyl)-2-nitro-6-phenylimidazo[1,2-*a*]pyrazin-8(7*H*)-one; 24d

Compound **24b** (19 mg, 55 μmol) was reacted according to general procedure D. After 25 min volatiles were removed under a stream of N_2. The residue was diluted with H_2O (2 mL) then extracted with EtOAc (3 × 2 mL) followed by DCM (3 × 2 mL). The organic layer was further diluted with EtOAc (14 mL), washed with brine (20 mL), dried with anh. $MgSO_4$ and filtered. Volatiles were removed in vacuo to give a yellow residue which was purified over silica gel by MPLC (Grace Reveleris X2, 4–15% MeOH in DCM) then over C18 silica gel by MPLC (Grace Reveleris, A: H_2O + 0.1% TFA, B: ACN + 0.1% TFA, 15–40% B) to yield a yellow-brown solid (3.8 mg, 17%). LCMS: R_t = 2.52 min, 99 A% @ 254 nm, $[M + H]^+$ = 301.1. ^{1}H NMR (600 MHz, DMSO-d_6) δ 8.73 (s, 1H), 7.59 – 7.51 (m, 5H), 7.46 (s, 1H), 4.77 (s, 1H), 3.85 (t, J = 6.3 Hz, 2H), 3.43 (br t, J = 6.7 Hz, 2H). ^{13}C NMR (150 MHz, DMSO-d_6) δ 153.2, 148.0, 135.1, 134.4, 131.7, 129.9, 129.7, 128.6, 115.9, 106.5, 57.5, 46.6. HRMS (ESI): *m/z* calcd for $C_{14}H_{12}N_4Na_1O_4$ $[M + Na]^+$, 323.0751; found, 323.0759.

2-((2-Nitro-6-phenylimidazo[1,2-*a*]pyrazin-8-yl)oxy)ethan-1-ol; 24e

Compound **24c** (146 mg, 0.427 mmol) was reacted according to general procedure D, work-up procedure B. The crude material was purified by MPLC (Grace Reveleris X2, A: H_2O + 0.1% TFA, B: ACN + 0.1% TFA, 30–100% B) to yield a bright yellow solid (13 mg, 10%). LCMS: R_t = 3.36 min, 98 A% @ 254 nm, $[M + H]^+$ = 301.0. ^{1}H NMR (600 MHz, DMSO-d_6) δ 8.94 (s, 1H), 8.83 (s, 1H), 8.04 – 7.98 (m, 2H), 7.57 – 7.51 (m, 2H), 7.49 – 7.43 (m, 1H), 4.69 – 4.64 (m, 2H), 3.91 – 3.86 (m, 2H). ^{13}C NMR (150 MHz, DMSO-d_6) δ 153.4, 148.3, 137.0, 135.1, 129.6, 129.1, 128.9, 125.7, 115.0, 111.6, 68.7, 58.9. HRMS (ESI): *m/z* calcd for $C_{14}H_{12}N_4NaO_4$ $[M + Na]^+$, 323.0751; found, 323.0756.

6-Methyl-2-nitroimidazo[1,2-*a*]pyrazin-8(7*H*)-one; 25a

Imidazole-2-carboxamide **16a** (1.50 g, 7.79 mmol) was reacted according to general procedure E with chloroacetone (1.3 eq) to yield a yellow solid (1.01 g, 67%). LCMS: R_t = 2.35 min, 99 A% @ 254 nm, $[M + H]^+$ = 195.0. ^{1}H NMR (600 MHz, DMSO-d_6) δ 11.66 (s, 1H), 8.76 (s, 1H), 7.34 – 7.29 (m, 1H), 2.12 (d, J = 1.2 Hz, 3H). ^{13}C NMR (150 MHz, DMSO-d_6) δ 153.4, 147.7, 134.4, 129.5, 116.2, 103.9, 15.7. HRMS (ESI): *m/z* calcd for $C_{14}H_{12}N_8NaO_6$ $[2M + Na]^+$, 411.0772; found, 411.0782.

2-(6-Methyl-2-nitro-8-oxoimidazo[1,2-*a*]pyrazin-7(8*H*)-yl)ethyl acetate; 25b and 2-((6-methyl-2-nitroimidazo[1,2-*a*]pyrazin-8-yl)oxy)ethyl; 25c

Compound **25a** (150 mg, 0.773 mmol) was reacted according to general procedure A with K_2CO_3 and 2-bromoethyl acetate (2 × 2 eq) with heating (2 × μW 80 °C, 30 min). The crude material contained imidazopyrazinone (major) and imidazopyrazine (minor) isomers in a 2.4:1 ratio by NMR. The crude solid was purified over silica gel by MPLC (Grace Reveleris X2, 0–10% MeOH in DCM gradient) to yield imidazopyrazinone as a yellow solid (140 mg, 48%) and imidazopyrazine as a yellow solid (57 mg, 21%). **Major isomer imidazopyrazinone 25b**: LCMS: R_t = 2.80 min, 99 A% @ 254 nm, $[M + H]^+$ = 281.1. ^{1}H NMR (600 MHz, DMSO-d_6) δ 8.76 (s, 1H), 7.45 (q, J = 1.2 Hz, 1H), 4.27 (t, J = 5.6 Hz, 2H),

4.21 (t, J = 5.5 Hz, 2H), 2.35 (d, J = 1.2 Hz, 3H), 1.98 (s, 3H). ^{13}C NMR (150 MHz, DMSO-d_6) δ 170.2, 153.4, 147.9, 133.8, 131.2, 115.7, 104.8, 61.1, 42.4, 20.6, 16.8. HRMS (ESI): *m/z* calcd for $C_{11}H_{13}N_4O_5$ $[M + H]^+$, 281.0880; found, 281.0878. **Minor isomer imidazopyrazine 25c**: LCMS: R_t = 3.23 min, 99 A% @ 254 nm, $[M + H]^+$ = 281.1. ^{1}H NMR (600 MHz, DMSO-d_6) δ 8.96 (s, 1H), 8.06 (q, J = 1.1 Hz, 1H), 4.70 – 4.65 (m, 2H), 4.46 – 4.41 (m, 2H), 2.33 (d, J = 1.1 Hz, 3H), 2.05 (s, 3H). ^{13}C NMR (151 MHz, DMSO) δ 170.4, 152.8, 148.1, 136.9, 129.0, 114.4, 112.4, 64.8, 62.0, 20.7, 20.4. HRMS (ESI): *m/z* calcd for $C_{11}H_{13}N_4O_5$ $[M + H]^+$, 281.0880; found, 281.0890.

7-(2-Hydroxyethyl)-6-methyl-2-nitroimidazo[1,2-*a*]pyrazin-8(7*H*)-one; 25d

Imidazopyrazinone **25b** (50 mg, 0.18 mmol) was reacted according to general procedure D, work-up procedure B. The crude material was purified over C18 silica gel by MPLC (Grace Reveleris, A: H_2O + 0.1% TFA, B: ACN + 0.1% TFA, 5–25% B) to yield a yellow solid (35 mg, 83%). LCMS: R_t = 2.42 min, 99 A% @ 254 nm, $[M + H]^+$ = 239.0. ^{1}H NMR (600 MHz, DMSO-d_6) δ 8.75 (s, 1H), 7.42 (q, J = 1.2 Hz, 1H), 4.95 (t, J = 5.8 Hz, 1H), 4.02 (t, J = 5.7 Hz, 2H), 3.64 (q, J = 5.7 Hz, 2H), 2.36 (d, J = 1.2 Hz, 3H). ^{13}C NMR (150 MHz, DMSO-d_6) δ 153.3, 147.9, 134.0, 132.0, 115.5, 104.3, 58.1, 45.9, 17.3. HRMS (ESI): *m/z* calcd for $C_{18}H_{20}N_8NaO_8$ $[2M + Na]^+$, 499.1296; found, 499.1296.

2-((6-Methyl-2-nitroimidazo[1,2-*a*]pyrazin-8-yl)oxy)ethan-1-ol; 25e

Imidazopyrazine **25c** (20 mg, 71 μmol) was reacted according to general procedure D, work-up procedure B. The crude material was purified over C18 silica gel by MPLC (Grace Reveleris, A: H_2O + 0.1% TFA, B: ACN + 0.1% TFA, 10–30% B) to yield a yellow solid product (11 mg, 67%). LCMS: R_t = 2.78 min, 99 A% @ 254 nm, $[M + H]^+$ = 239.0. ^{1}H NMR (600 MHz, DMSO-d_6) δ 8.94 (s, 1H), 8.03 (q, J = 1.1 Hz, 1H), 5.00 (t, J = 5.5 Hz, 1H), 4.51 – 4.46 (m, 2H), 3.84 – 3.78 (m, 2H), 2.32 (d, J = 1.1 Hz, 3H). ^{13}C NMR (150 MHz, DMSO-d_6) δ 153.3, 148.1, 137.1, 129.2, 114.3, 112.0, 68.6, 58.9, 20.5. HRMS (ESI): *m/z* calcd for $C_{18}H_{20}N_8NaO_8$ $[2M + Na]^+$, 499.1296; found, 499.1315.

6-Methyl-2-nitro-7-(4-(trifluoromethoxy)benzyl)imidazo[1,2-*a*]pyrazin-8(7*H*)-one; 25f and 6-methyl-2-nitro-8-((4-(trifluoromethoxy)benzyl)oxy)imidazo[1,2-*a*]pyrazine; 25g

Compound **25a** (150 mg, 0.773 mmol), K_2CO_3, and 1-(bromomethyl)4-(trifluoromethoxy)benzene (1.2 eq) were reacted according to general procedure A at rt for 3 h, work-up B. The crude material contained imidazopyrazinone (major) and imidazopyrazine (minor) isomers in a 7.2:1 ratio by NMR. The crude solid was purified over silica gel by MPLC (Grace Reveleris X2, 0–7% MeOH in DCM gradient) to yield imidazopyrazinone as an off-white solid (197 mg, 69%) and imidazopyrazine as a colorless solid (27 mg, 9%). **Major isomer imidazopyrazinone 25f**: LCMS: R_t = 3.52 min, 99 A% @ 254 nm, $[M + H]^+$ = 369.0. ^{1}H NMR (600 MHz, DMSO-d_6) δ 8.81 (s, 1H), 7.50 (q, J = 1.2 Hz, 1H), 7.40 – 7.36 (m, 2H), 7.36 – 7.32 (m, 2H), 5.31 (s, 2H), 2.21 (d, J = 1.2 Hz, 3H). ^{13}C NMR (150 MHz, DMSO-d_6) δ 153.7, 148.0, 147.4, 136.1, 134.0, 131.0, 128.3, 121.4, 120.1 (q, J = 256.4 Hz), 115.9, 105.2, 45.3, 16.6. HRMS (ESI): *m/z* calcd for $C_{15}H_{12}F_3N_4O_4$ $[M + H]^+$, 369.0805; found, 369.0803. **Minor isomer imidazopyrazine 25g**: LCMS: R_t = 3.86 min, 99 A% @ 254 nm, $[M + H]^+$ = 369.1. ^{1}H NMR (600 MHz, DMSO-d_6) δ 8.96 (s, 1H), 8.08 (q, J = 1.1 Hz, 1H), 7.72 – 7.66 (m, 2H), 7.46 – 7.41 (m, 2H), 5.58 (s, 2H), 2.36 (d, J = 1.1 Hz, 3H). ^{13}C NMR (151 MHz, DMSO) δ 152.7, 148.2, 148.2, 137.0, 135.3, 130.6, 129.1, 121.1, 120.1 (q, J = 257.1 Hz), 114.4, 112.5, 67.2, 20.4. HRMS (ESI): *m/z* calcd for $C_{15}H_{12}F_3N_4NaO_4$ $[M + Na]^+$, 391.0625; found, 391.0629.

6-Methyl-7-(4-methylbenzyl)-2-nitroimidazo[1,2-*a*]pyrazin-8(7*H*)-one; 25h and 6-methyl-8-((4-methylbenzyl)oxy)-2-nitroimidazo[1,2-*a*]pyrazine; 25i

Compound **25a** (150 mg, 0.773 mmol) was reacted according to general procedure method A with Cs_2CO_3 and 4-methylbenzyl bromide (1.2 eq) with heating (μW 80 °C for 10 min, then 90 °C at 10 min) followed by rt overnight, work up B. The crude material contained imidazopyrazinone (major) and imidazopyrazine (minor) isomers in a ratio of 1.8:1 by LC-MS (UV 254 nm). The crude product was

purified over silica gel by MPLC (Biotage Isolera, 0-4% DCM/MeOH) to give imidazopyrazinone as light yellow powder (150 mg, 65%) and imidazopyrazine as a light orange solid (21 mg, 9%). **Major isomer imidazopyrazinone 25h**: LCMS: R_t = 2.92 min, 99 A% @ 254 nm, $[M+H]^+$ = 299.1. ^{1}H NMR (600 MHz, DMSO-d_6) δ 8.79 (s, 1H), 7.48 (d, *J* = 1.3 Hz, 1H), 7.17 – 7.08 (m, 4H), 5.24 (s, 2H), 2.27 (s, 3H), 2.20 (d, *J* = 1.3 Hz, 3H); ^{13}C NMR (150 MHz, DMSO-d_6) δ 153.6, 148.0, 136.4, 133.9, 133.5, 131.1, 129.2, 126.1, 115.8, 105.0, 45.5, 20.6, 16.5. HRMS (ESI): *m/z* calc for $C_{15}H_{14}N_4O_3Na$ $[M+Na]^+$: 321.0958, found 321.0957. **Minor isomer imidazopyrazine 25i**: LCMS: R_t = 3.26 min, 99 A% @ 254 nm, $[M+H]^+$ = 299.1; ^{1}H NMR (600 MHz, DMSO-d_6) δ 8.94 (d, *J* = 0.9 Hz, 1H), 8.06 (t, *J* = 1.1 Hz, 1H), 7.43 (d, *J* = 7.8 Hz, 2H), 7.23 (d, *J* = 7.7 Hz, 2H), 5.49 (s, 2H), 2.36 (d, *J* = 1.1 Hz, 3H), 2.32 (s, 3H); ^{13}C NMR (150 MHz, DMSO-d_6) δ 152.9, 148.1, 137.7, 137.0, 132.7, 129.1, 129.0, 128.7, 114.3, 112.3, 68.1, 20.8, 20.4. HRMS (ESI): *m/z* calc for $C_{15}H_{14}N_4O_3Na$ $[M+Na]^+$: 321.0958, found 321.0958.

6-Methyl-2-nitro-7-(3-(trifluoromethoxy)benzyl)imidazo[1,2-*a*]pyrazin-8(7*H*)-one; 25j

Compound **25a** (120 mg, 0.618 mmol), Cs_2CO_3, and 1-(bromomethyl)-3-(trifluoromethoxy)benzene (1.2 eq) was reacted according to general procedure A with heating (μW 80 °C) for 10 min, work-up B. The crude material contained imidazopyrazinone (major) and imidazopyrazine (minor) isomers in a ratio of 4.3:1 by LC-MS (UV 254 nm). The crude product was purified over silica gel by MPLC (Biotage Isolera, 2-4% DCM/MeOH) to give imidazopyrazinone as white powder **(**122 mg, 54%) and imidazopyrazine as white solid. **Major isomer imidazopyrazinone 25j**: LCMS: R_t = 3.49 min, 99 A% @ 254 nm, $[M+H]^+$ = 368.8. ^{1}H NMR (600 MHz, DMSO-d_6) δ 8.80 (s, 1H), 7.51 – 7.45 (m, 2H), 7.32 – 7.23 (m, 3H), 5.33 (s, 2H), 2.20 (d, J = 1.3 Hz, 3H). ^{13}C NMR (150 MHz, DMSO-d_6) δ 153.7, 148.6, 147.9, 139.5, 134.0, 130.9, 130.7, 125.2, 120.0 (q, *J* = 256.9 Hz), 119.6, 119.1, 115.9, 105.2, 45.4, 16.6. HRMS (ESI): *m/z* calc for $C_{15}H_{11}F_3N_4O_4Na$ $[M+Na]^+$: 391.0624, found 391.0625. **Minor isomer imidazopyrazine 25k**: LCMS: R_t = 3.79 min, 65 A% @ 254 nm, $[M+H]^+$ = 368.8; Impurity detected at R_t = 4.03 min, 35 A% @ 254 nm, $[M+H]^+$ = 737.2. This compound was not subjected to biological evaluation.

6-Methyl-2-nitro-7-(2-(trifluoromethoxy)benzyl)imidazo[1,2-*a*]pyrazin-8(7*H*)-one; 25l and 6-methyl-2-nitro-8-((2-(trifluoromethoxy)benzyl)oxy)imidazo[1,2-*a*]pyrazine; *25m*

Compound **25a** (120 mg, 0.618 mmol), Cs_2CO_3, and 2-(trifluoromethoxy)benzyl bromide (1.2 eq) were reacted according to general procedure A with heating (μW 80 °C) for 10 min, work-up B. The crude material contained imidazopyrazinone (major) and imidazopyrazine (minor) isomers in a ratio of 1.3:1 by LC-MS (UV 254 nm). The crude product was purified over silica gel by MPLC (Biotage Isolera, 0-4% DCM/MeOH) to yield imidazopyrazinone as white powder (76 mg, 33%) and imidazopyrazine as cream powder (cream powder, 18 mg, 8%). **Major isomer imidazopyrazinone 25l**: LCMS: R_t = 3.48 min, 99 A% @ 254 nm, $[M+H]^+$ = 369.0; ^{1}H NMR (600 MHz, DMSO-d_6) δ 8.83 (s, 1H), 7.54 (d, J = 1.3 Hz, 1H), 7.49 – 7.42 (m, 2H), 7.36 – 7.30 (m, 1H), 7.11 (dt, J = 7.8, 1.0 Hz, 1H), 5.30 (s, 2H), 2.18 (d, J = 1.2 Hz, 3H. ^{13}C NMR (150 MHz, DMSO-d_6) δ 153.6, 148.0, 145.6, 133.9, 130.8, 129.2, 128.7, 127.9, 127.1, 120.8, 120.2 (q, J = 257.4 Hz), 116.0, 105.4, 41.3, 16.2. HRMS (ESI): *m/z* calc for $C_{15}H_{11}F_3N_4O_4Na$ $[M+Na]^+$: 391.0625, found 391.0613. **Minor isomer imidazopyrazine 25m**: LCMS: R_t = 3.78 min, 99 A% @ 254 nm, $[M+H]^+$ = 369.0; ^{1}H NMR (600 MHz, DMSO-d_6) δ 8.96 (s, 1H), 8.09 (d, J = 1.3 Hz, 1H), 7.75 (dd, J = 7.6, 1.7 Hz, 1H), 7.57 (td, J = 7.9, 1.8 Hz, 1H), 7.51 – 7.44 (m, 2H), 5.63 (s, 2H), 2.36 (d, J = 1.1 Hz, 3H); ^{13}C NMR (150 MHz, DMSO-d_6) δ 152.5, 148.2, 146.8, 136.9, 131.4, 130.6, 128.9, 128.3, 127.7, 120.6, 120.1 (q, J= 256.4 Hz), 114.4, 111.6, 62.5, 20.3. HRMS (ESI): *m/z* calc for $C_{15}H_{11}F_3N_4O_4Na$ $[M+Na]^+$: 391.0625, found 391.0621.

5,6-Dimethyl-2-nitroimidazo[1,2-*a*]pyrazin-8(7*H*)-one; 26a

Imidazole-2-carboxamide **16a** (750 mg, 3.89 mmol) was reacted according to general procedure E with 3-bromo-2-butanone (1.5 eq) to yield a yellow solid (477 mg, 67%). LCMS: R_t = 2.57 min, 99 A% @ 254 nm, $[M + H]^+$ = 209.1. ^{1}H NMR (600 MHz, DMSO-d_6) δ 11.55 (s, 1H), 8.82 (s, 1H), 2.32 (q, J = 1.0

Hz, 3H), 2.16 (q, *J* = 1.0 Hz, 3H). ^{13}C NMR (150 MHz, DMSO-d_6) δ 152.8, 147.9, 134.6, 124.6, 115.2, 111.0, 14.7, 12.5. HRMS (ESI): *m/z* calcd for $C_{16}H_{16}N_8NaO_6$ $[2M + Na]^+$, 439.1085; found, 439.1090.

6-Methyl-2-nitro-7-(4-(trifluoromethoxy)benzyl)imidazo[1,2-*a*]pyrazin-8(7*H*)-one; 26b and 5,6-dimethyl-2-nitro-8-((4-(trifluoromethoxy)benzyl)oxy)imidazo[1,2-*a*]pyrazine; 26c

Compound **26a** (150 mg, 0.721 mmol) was reacted according to general procedure A with K_2CO_3 and 1-(bromomethyl)4-(trifluoromethoxy)benzene (1.2 eq) at rt overnight. The ratio of **26b**:**26c** in the crude material was 3:1 (NMR). The crude solid was purified over silica gel by MPLC (Grace Reveleris X2, 0–7% MeOH in DCM gradient) to yield **26b** as a yellow solid (178 mg, 69%) and **25c** as a yellow solid (57 mg, 21%). **Major isomer imidazopyrazinone 26b**: LCMS: R_t = 3.61 min, 99 A% @ 254 nm, $[M + H]^+$ = 383.1. ^{1}H NMR (600 MHz, DMSO-d_6) δ 8.93 (s, 1H), 7.38 – 7.31 (m, 4H), 5.37 (s, 2H), 2.43 (q, *J* = 1.0 Hz, 3H), 2.23 (q, *J* = 1.0 Hz, 3H). ^{13}C NMR (150 MHz, DMSO-d_6) δ 153.2, 148.1, 147.4, 136.3, 133.9, 128.2, 126.3, 121.4, 120.1 (q, *J* = 256.1 Hz), 115.3, 112.5, 45.7, 14.9, 13.9. HRMS (ESI): *m/z* calcd for $C_{16}H_{14}F_3N_4O_4$ $[M + H]^+$, 383.0962; found, 383.0958. **Minor isomer imidazopyrazine 26c**: LCMS: R_t = 3.94 min, 99 A% @ 254 nm, $[M + H]^+$ = 383.0. ^{1}H NMR (600 MHz, DMSO-d_6) δ 9.03 (s, 1H), 7.70 – 7.65 (m, 2H), 7.45 – 7.40 (m, 2H), 5.56 (s, 2H), 2.54 (q, *J* = 0.9 Hz, 3H), 2.40 (q, *J* = 0.9 Hz, 3H).^{13}C NMR (150 MHz, DMSO-d_6) δ 150.8, 148.5, 148.1, 135.6, 132.8, 130.5, 129.4, 121.1, 120.6, 120.1 (q, *J* = 255.5 Hz), 113.2, 66.8, 19.6, 13.7. HRMS (ESI): *m/z* calcd for $C_{16}H_{14}F_3N_4O_4$ $[M + H]^+$, 383.0962; found, 383.0961.

5,6-Dimethyl-7-(4-methylbenzyl)-2-nitroimidazo[1,2-*a*]pyrazin-8(7*H*)-one; 26d and 5,6-dimethyl-8-((4-methylbenzyl)oxy)-2-nitroimidazo[1,2-*a*]pyrazine; 26e

Compound **24a** (65 mg, 0.312 mmol) was reacted according to general procedure A with Cs_2CO_3 and 4-methylbenzyl bromide (1.2 eq) with heating (μW 80 °C, 20 min then μW 90 °C, 10 min) followed by stirring overnight at rt, work up B. The ratio of **26d**:**26e** in the crude material was 1.5:1 by LC-MS (UV

254 nm). The crude was purified over silica gel by MPLC (Biotage Isolera, 0-4% DCM/MeOH) to yield **26d** as a yellow powder (39 mg, 40%) and **26e** as a light yellow powder (18 mg, 19%). **Major isomer imidazopyrazinone 26d**: LCMS: R_t = 3.45 min, 99 A% @ 254 nm, $[M+H]^+$ = 313.1. ^{1}H NMR (600 MHz, DMSO-d_6) δ 8.90 (s, 1H), 7.14 (d, J = 7.9 Hz, 2H), 7.08 (d, J = 8.1 Hz, 2H), 5.30 (s, 2H), 2.42 (d, J = 1.0 Hz, 3H), 2.27 (s, 3H), 2.22 (d, J = 1.0 Hz, 3H). ^{13}C NMR (150 MHz, DMSO-d_6) δ 153.2, 148.1, 136.4, 133.9, 133.7, 129.3, 126.5, 126.1, 115.2, 112.3, 46.0, 20.6, 14.8, 13.8. HRMS (ESI): *m/z* calc for $C_{16}H_{16}N_4O_3Na$ $[M+Na]^+$: 335.1115, found 335.1116. **Minor isomer imidazopyrazine 26e**: R_t = 3.81 min, 99 A% @ 254 nm, $[M+H]^+$ = 313.1. ^{1}H NMR (600 MHz, DMSO-d_6) δ 9.01 (s, 1H), 7.44 – 7.40 (m, 2H), 7.25 – 7.20 (m, 2H), 5.48 (s, 2H), 2.55 – 2.52 (m, 3H), 2.40 (d, J = 1.0 Hz, 3H), 2.32 (s, 3H). ^{13}C NMR (150 MHz, DMSO-d_6) δ 151.0, 148.4, 137.5, 132.9, 132.8, 129.4, 128.9, 128.7, 120.3, 113.1, 67.7, 20.8, 19.6, 13.6. HRMS (ESI): *m/z* calc for $C_{16}H_{16}N_4O_3Na$ $[M+Na]^+$: 335.1115, found 335.1115.

5,6-Dimethyl-2-nitro-7-(3-(trifluoromethoxy)benzyl)imidazo[1,2-*a*]pyrazin-8(7*H*)-one; 26f and 5,6-dimethyl-2-nitro-8-((3-(trifluoromethoxy)benzyl)oxy)imidazo[1,2-*a*]pyrazine; 26g

Compound **26a** (120 mg, 0.576 mmol) was reacted according to general procedure A with Cs_2CO_3 and 1-(bromomethyl)-3-(trifluoromethoxy)benzene (1.2 eq) with heating (μW 100 °C) for 10 min. The ratio of **26f**:**26g** in the crude material was 1.2:1 by LC-MS (UV 254 nm). The crude material was purified over silica gel by MPLC (Biotage Isolera, 0-4% dichloromethane/methanol) to yield **26f** as a light brown solid (131 mg, 60%) and **26g** as a yellow gel (66 mg, 30%). **Major isomer imidazopyrazinone 26f**: LCMS: R_t = 3.56 min, 99 A% @ 254 nm, $[M+H]^+$ = 383.1. ^{1}H NMR (600 MHz, DMSO-d_6) δ 8.93 (s, 1H), 7.51 – 7.43 (m, 1H), 7.29 (s, 1H), 7.28 – 7.21 (m, 2H), 5.39 (s, 2H), 2.43 (d, J = 1.1 Hz, 3H), 2.24 – 2.20 (m, 3H). ^{13}C NMR (150 MHz, DMSO-d_6) δ 153.3, 148.6, 148.1, 139.7, 133.9, 130.7, 126.2, 125.1, 120.0 (q, J = 256.2 Hz), 119.6, 119.0, 115.2, 112.4, 45.8, 14.9, 13.9. HRMS (ESI): *m/z* calc for $C_{32}H_{26}F_6N_8O_8Na$ $[2M+Na]^+$: 787.1678, found 787.1670. **Minor isomer imidazopyrazine 26g**: LCMS: Rt = 3.88 min, 99 A% @ 254 nm, $[M+H]^+$ = 383.1. ^{1}H NMR (600 MHz, DMSO-d_6) δ 9.03 (s, 1H), 7.61

– 7.51 (m, 3H), 7.40 – 7.35 (m, 1H), 5.58 (s, 2H), 2.54 (s, 3H), 2.39 (s, 3H). ^{13}C NMR (150 MHz, DMSO-d_6) δ 150.7, 148.5, 148.3, 138.8, 132.7, 130.5, 129.4, 127.5, 120.9, 120.9, 120.7, 120.0 (q, J = 256.2 Hz), 113.2, 66.8, 19.6, 13.7. HRMS (ESI): *m/z* calc for $C_{16}H_{13}F_3N_4O_4Na$ $[M+Na]^+$: 405.0797, found 405.0781.

5,6-Dimethyl-2-nitro-7-(2-(trifluoromethoxy)benzyl)imidazo[1,2-*a*]pyrazin-8(7*H*)-one; 26h and 5,6-dimethyl-2-nitro-8-((2-(trifluoromethoxy)benzyl)oxy)imidazo[1,2-*a*]pyrazine; 26i

Compound **26a** (120 mg, 0.576 mmol) was reacted according to general procedure A with Cs_2CO_3 and 2-(trifluoromethoxy)benzyl bromide (1.2 eq) with heating (μW 100 °C) for 10 min. The ratio of **26h**:**26i** in the crude material was 1:2.1 by LC-MS (UV 254 nm). The crude material was purified over silica gel by MPLC (Biotage Isolera, 0-4% DCM/MeOH) to yield **26h** as a light yellow powder (46 mg, 21%) and **26i** as a light yellow powder (97 mg, 44%). **Minor isomer imidazopyrazinone 26h**: LCMS: R_t = 3.15 min, 99 A% @ 254 nm, $[M+H]^+$ = 383.1. ^{1}H NMR (600 MHz, DMSO-d_6) δ 8.95 (s, 1H), 7.48 – 7.41 (m, 2H), 7.35 – 7.29 (m, 1H), 7.06 (dt, J = 8.0, 1.0 Hz, 1H), 5.36 (s, 2H), 2.45 (d, J = 1.0 Hz, 3H), 2.19 (d, J = 1.0 Hz, 3H). ^{13}C NMR (150 MHz, DMSO-d_6) δ 153.1, 148.1, 145.6, 133.8, 129.2, 128.9, 127.9, 127.1, 126.1, 120.9, 120.3 (q, J = 256.8 Hz), 115.3, 112.6, 41.7, 14.5, 13.9. HRMS (ESI): *m/z* calc for $C_{16}H_{13}N_4O_4F_3Na$ $[M+Na]^+$: 405.0781, found 405.0796. **Major isomer imidazopyrazine 26i**: LCMS: R_t = 3.44 min, 99 A% @ 254 nm, $[M+H]^+$ = 383.1. ^{1}H NMR (600 MHz, DMSO-d_6) δ 9.03 (s, 1H), 7.74 (dd, J = 7.6, 1.8 Hz, 1H), 7.55 (td, J = 7.8, 1.8 Hz, 1H), 7.50 – 7.43 (m, 2H), 5.61 (s, 2H), 2.54 (d, J = 0.9 Hz, 3H), 2.39 (d, J = 1.0 Hz, 3H). ^{13}C NMR (150 MHz, DMSO-d_6) δ 150.6, 148.5, 146.8, 132.7, 131.3, 130.5, 129.3, 128.5, 127.7, 120.8, 120.6, 120.2 (q, J = 256.8 Hz), 113.2, 62.2, 19.6, 13.6. HRMS (ESI): *m/z* calc for $C_{16}H_{13}N_4O_4F_3Na$ $[M+Na]^+$: 405.0781, found 405.0793.

4-Nitro-1-(2-oxo-2-phenylethyl)-1*H*-imidazole-2-carboxamide; 27a

Compound **16a** (1.20 g, 5.53 mmol), K_2CO_3 and 2-bromoacetophenone (1.1 eq) were reacted according to general procedure A at rt for 1 h. The crude was purified over silica gel by MPLC (Grace Reveleris

X2 15–100% EtOAc in pet. spirits gradient) to yield an orange oily-solid (907 mg, 60%). LCMS: R_t = 3.15 min, 98 A% @ 254 nm, $[M + H]^+$ = 274.9. ^{1}H NMR (600 MHz, DMSO-d_6) δ 8.52 (s, 1H), 8.24 (s, 1H), 8.08 – 8.02 (m, 2H), 7.78 – 7.72 (m, 2H), 7.66 – 7.59 (m, 2H), 6.13 (s, 2H). Minor impurities in ^{1}H NMR. ^{13}C NMR (150 MHz, DMSO-d_6) δ 191.9, 159.3, 144.5, 137.7, 134.3, 134.0, 129.1, 128.0, 126.4, 55.7. HRMS (ESI): *m/z* calcd for $C_{12}H_{10}N_4NaO_4$ $[M + Na]^+$, 297.0594; found, 297.0592.

Minimum Inhibition Concentration (MIC) Assay

All compounds were tested for activity against *C. difficile* bacteria (630, ATCC BAA-1382) and representative ESKAPE pathogens *S. aureus* (MRSA, ATCC 43300), *E. coli* (FDA control strain, ATCC 25922), *K. pneumoniae* (MDR, ATCC 700603), *A. baumannii* (type strain, ATCC 19606) and *P. aeruginosa* (quality control strain, ATCC 27853) and fungi *C. albicans* (CLSI reference, ATCC 90028) and *C. neoformans* (H99 type strain, ATCC 208821) using a standard broth microdilution assay essentially as previously described.[49] MICs for each strain were determined as the lowest concentration without visible growth. Variance between replicates was typically within one 2-fold dilution. Median MICs are reported with a range given when the median MIC was between two tested concentrations.

***M. tuberculosis* H37Rv Minimum Inhibition Assays**

The potency of the inhibitors was measured by a resazurin reduction microplate assay as previously described[50,51] with some alterations. *M. tuberculosis* (H37Rv) was grown in Middlebrook 7H9 broth medium supplemented with ADC (Difco Laboratories), 0.5% glycerol, and 0.02% Tyloxapol. Freshly seeded cultures were grown at 37 °C for approximately 14 days to mid-exponential phase (OD_{600} 0.4−0.8) for use in the inhibition assays. Assay plates (96-well microtiter) were prepared with compound serially diluted in 100 μL of 7H9S media (7H9 with 10% ADC, 0.5% glycerol, 0.05% Tween-80 and 1% tryptone). Mid-exponential phase culture of *M. tuberculosis* (OD_{600} 0.4−0.8) was diluted to OD_{600} 0.001

in 7H9S media and 100 μL (representing ~2 x 10^4 CFU/mL) was added to each well. For normoxic conditions, the plates were incubated for 5 days at 37 °C in a humidified incubator prior to the addition of 30 μL of a 0.02% resazurin solution and 12.5 μL of 20% Tween-80 to each well. After 24 h incubation (37 °C), sample fluorescence was measured on a Fluorostar Omega fluorescent plate reader (BMG) with an excitation wavelength of 530 nm and emission read at 590 nm. Percent fluorescence relative to the positive control wells (H37Rv without compound) minus the negative control wells (without H37Rv) was plotted for the determination of the MIC (≤90% reduction in growth). The assays were performed in replicate on independent occasions (n = 3–6). For hypoxic assays the same method was used except assay plates were incubated for 5 days at 0.1% oxygen and after addition of the resazurin solution the fluorescence was measured after a prolonged incubation time of 48 h.

Antiparasitic Assay: *G. lamblia* and *E. histolytica*

Compounds were screened for antiparasitic activity in a 96-well plate using an ATP-bioluminescence based assay for cell growth and survival as previously described.[49] Briefly, trophozoites of *G. lamblia* (WB line[52]) and *E. histolytica* (HM1:IMSS) were axenically maintained in TYI-S-33 medium supplemented with penicillin (100 U/mL) and streptomycin (100 μg/mL).[53] All experiments were performed using trophozoites harvested during the logarithmic phase of growth. Two-fold serial dilutions were prepared from compound stocks (10 mM in DMSO) yielding a concentration range of 78 μM–10 mM. From this dilution plate, 0.5 μL from each well was transferred into 96-well microtitre plates followed by addition of 99.5 μL of trophozoites (5000 parasites) to yield a final 8-point concentration range spanning 0.39–50 μM. Assay plates were incubated for 24–48 h at 37 °C in the GasPak™ EZ Anaerobe Gas Generating Pouch Systems (VWR, West Chester, PA) to maintain anaerobic condition throughout the incubation period. Viable cell numbers were determined in triplicate using the CellTiter-Glo Luminescent Cell Viability Assay.[54]

Antiparasitic Assay: *T. b. brucei*

Compounds were screened for antitrypanosomal activity against *T. b. brucei* (strain 427, BS427) using an established 384-well resazurin viability assay, as previously described.[55-57] Briefly, 55 μL of HMI-9 media supplemented with 10% FCS containing 1200 cells/mL of logarithmic phase *T. b. brucei* bloodstream parasites were added to a 384-well microtiter plate (BD biosciences, USA) and incubated for 24 hrs at 37 °C/5% CO_2. Serial compound concentrations were prepared in 100% DMSO and diluted 1:21 in DMEM media. Five microliters of these dilutions were subsequently added to assay plates to give final compound concentrations ranging from a top final assay concentration of 40 or 20 μM, to $4x10^{-3}$ μM or $2x10^{-3}$ μM, respectively. Plates were incubated for 48 hrs at 37 °C/5% CO_2. Ten microlitres of 0.49 mM resazurin (Sigma-Aldrich, USA) in HMI-9 media +10% FCS was added to assay plates and incubated for a further 2 hrs at 37 °C/5% CO_2 followed by 22 hrs at room temperature. Final assay concentrations of puromycin (5 μM) and 0.4% DMSO were used as in-plate controls for all experiments. Assay plates were read at 535 nm excitation/590 nm emission on an Envision® multiplate reader (PerkinElmer, USA). Non-linear sigmoidal dose response curves with no constraints were plotted and IC_{50} values calculated in GraphPad Prism 6. The IC_{50} value was determined for compounds that exhibited a plateau of inhibition (above 90% inhibition at the top two concentrations) and were calculated from two independent experiments.

Antiparasitic Assay: *Leishmania donovani* Intracellular Amastigote

Compounds were screened for antileishmanial activity in an established DD8 intracellular (THP-1) amastigote assay as previously described.[57] Briefly, seven day old *L. donovani* MHOM/IN/80/DD8 (ATCC50212) culture containing metacyclic promastigotes were added to the 384-well assay plates containing the transformed THP-1 cells (ATCC TIB202) at 72 hrs after the initial cell seeding with a multiplicity of infection (MOI) of 1:5 (ratio host cells : parasites). Assay plates were incubated 24 hrs at 37˚C / 5% CO_2. Non-internalised parasites were removed by washing 6 times in PBS before the addition

of 45 μL RMPI (10% FBS and 25 ng/mL phorbol 12-myristate 13-acetate). Five microliters of compounds were added to wells to give final assay concentrations ranging from 80 to $4x10^{-3}$ μM. Final assay concentrations of 2 μM of amphotericin B and 0.4% DMSO were used as in-plate controls for all experiments. Plates were incubated for 96 hr at 37˚C / 5% CO_2, fixed with 4% paraformaldehyde and stained with SYBR® green and CellMask™ Deep Red plasma membrane dye. Images were acquired on an Opera high-content imaging system (PerkinElmer). Healthy host (THP-1) cells were identified based on fluorescent staining with CellMask Deep Red to characterize the cytoplasm in which the parasite resides and SYBR green to identify both host and parasite nuclei. An infected cell was defined as a host cell containing >3 parasites within the cytoplasm boundary. Non-linear sigmoidal dose response curves with no constraints were plotted and IC_{50} values calculated in GraphPad Prism 6. The IC_{50} value was determined for compounds that exhibited a plateau of inhibition (above 90% inhibition at the top two concentrations) and were calculated from two independent experiments.

Mammalian Cytotoxicity Assay

Human HEK293 and HepG2 cells were seeded at 3000 and 5000 cells per well in 384-well plates, respectively. Cells were cultured in Dulbecco's modified Eagle's medium with 10% FBS for 24 h at 37 °C, 5% CO_2. A dilution series of compounds was added, with the highest concentration of 100 μM. The final concentration of DMSO in culture media was 0.5%, which showed no effect on cell growth. After 24 h incubation with the compounds, 5 μM resazurin was added into each well and incubated at 37 °C for 2 h. As a negative control, 1% Triton X-100 was added into the culture media to lyse all of the cells. The fluorescence intensity was read using Polarstar Omega with excitation/emission 560/590 nm. Data were analyzed with GraphPad Prism 6 software (La Jolla, California USA) to calculate CC_{50} values.

Microsome Stability

Metabolic stability was determined using pooled human (HMMC-PL, Lot# PL050B-B, Thermo Fisher Scientific USA) and mouse (CD-1) (MCMCPL, Lot#MS033D, Thermo Fisher) liver microsomes. Test compound (3 μM, final DMSO concentration 0.2%) and liver microsomes (1 mg/mL) were mixed in 100 mM potassium phosphate buffer, pH 7.4 preincubated at 37 °C (500 μL volume). The reaction was initiated by addition of NADPH solution (cofactor) in 0.1 M potassium phosphate buffer at a final NADPH concentration of 1 mM. The reaction was incubated in a shaking incubator at 37 °C, 150 rpm. Aliquots (90 μL) from the reaction mixture were withdrawn (t = 0, 10, 30, 60 and 120 min) and quenched by adding ice-cold precipitating solution (270 μL) comprising 0.5 μM carbutamide internal standard in acetonitrile: methanol: formic acid (1: 1: 0.001 v/v). Reaction samples were incubated at 4 °C for 30 min, centrifuged at 14,000 × *g* for 8 min and the clear supernatant was analyzed by LC/MS/MS. The percentage of compound remaining at different times was calculated by comparing the peak area ratio of the parent compound (compound peak area/internal standard peak area) at the start of incubation (t = 0 min sample). All samples were tested in triplicate except for the control samples (without NADPH), matrix blank and verapamil standard (time points = 0, 10 and 30 min). LC/MS/MS parameters are detailed in the Supporting Information Table S4.

Plasma Stability

Plasma stability studies were performed using human (HMPLNAHP, Lot#BRH1324758, BioReclamationIVT) and mouse (CD-1) plasma (MSEPLNAHP, Lot#MSE261215, BioReclamationIVT) at five different time points. A solution of plasma and phosphate buffer saline (PBS), pH 7.4 (50:50; v/v) were pre-heated at 37 °C for 30 min (240 μL volume). The reaction was initiated by addition of the test compounds (3 μM, final DMSO concentration 1%) and the reaction was incubated in a shaking incubator at 37 °C, 150 rpm. Aliquots (40 μL) from the reaction mixture were

withdrawn and processed as described for microsome stability assay. All samples were tested in triplicate and eucatropine was used as a positive control.

Plasma Protein Binding

Plasma Protein Binding (PPB) was performed using an Ultrafiltration method.[58,59] Fresh frozen human plasma was pooled from O Positive (Product Number 2799882) and O Negative (Product number 5398256) blood from the R & D division of the Australian Red Cross Blood Services (Brisbane). Test compounds (5 μM) were incubated in 100% human plasma at 37 °C for 30 min (1 mL volume). For unfiltered samples, an aliquot (50 μL) was removed, diluted with PBS (50 μL) and quenched with ice-cold precipitating solution comprising 0.5 μM carbutamide MS internal standard in acetonitrile: methanol: formic acid (1: 1: 0.001). Samples were incubated at 4 °C for 30 min, then centrifuged at 14,000 × *g* for 8 min before the clear supernatant was transferred to a vial for LC/MS/MS analysis. For filtered samples, the plasma sample (250 μL) was filtered using Amicon Ultra-0.5 Centrifugal Filter Devices 30K NMWL at 14,000 × *g* for 7 min and then an aliquot (50 μL) was processed as described for unfiltered samples. The fraction of unbound compound was calculated by determining the concentration of the filtered sample and the concentration of unfiltered sample. All samples were tested in triplicate with sulfamethoxazole as a control.

Caco-2 Permeability Assay

This study was conducted by WuXi AppTec Co. Ltd. (Shanghai). Caco-2 cells from ATCC were seeded onto polystyrene membranes in 96-well insert plate at 1×10^5 cells/cm^2 until the formation of confluent cell monolayer at 21st–28th day. Transport buffer used was HBSS with 10 mM HEPES, pH 7.4. Compounds (2 μM) were tested bidirectionally in duplicate. The plate was incubated for 2 h at 37 °C and 5% CO_2 at saturated humidity without shaking. All samples were then mixed with acetonitrile containing internal standard, centrifuged at 4000 rpm for 20 min and the clear supernatant was diluted 1:1 with water

prior to LC/MS/MS analysis. Test compounds and controls (fenoterol, propranolol and digoxin) in starting solution, donor solution, and receiver solution were quantified using peak area ratio of analyte/internal standard. To confirm the Caco-2 cell monolayer integrity after the transport assay, lucifer yellow rejection assay was performed. The apparent permeability coefficient P_{app} (cm/s) was calculated using the equation: $P_{app} = (dC_r/dt) \times V_r / (A \times C_0)$ where dC_r/dt is the cumulative concentration of compound in the receiver chamber as a function of time (μM/s); V_r is the solution volume in the receiver chamber (0.075 mL on the apical side, 0.25 mL on the basolateral side); A is the surface area for the transport, i.e. 0.0804 cm^2 for the area of the monolayer; C_0 is the initial concentration in the donor chamber (μM). The efflux ratio was calculated using the equation: Efflux Ratio = P_{app} (BA) / P_{app} (AB). Percent recovery was calculated using the equation: % Recovery = 100 x $[(V_r \times C_r) + (V_d \times C_d)] / (V_d \times C_0)$ where V_d is the volume in the donor chambers (0.075 mL on the apical side, 0.25 mL on the basolateral side); C_d and C_r are the final concentrations of transport compound in donor and receiver chambers, respectively.

Solubility Determination

Stock compound solution (20 mM in DMSO) was aliquoted into water and phosphate buffer saline (PBS), pH 7.4 and 0.1 M HCl (pH 1) respectively to a final concentration of 200 μM, 1% DMSO. After 24 hours of incubation in a shaking incubator at room temperature, 130 rpm, solutions were filtered using centrifuge filter tubes (Corning® Costar® Spin-X® centrifuge tube filters, CLS8169) at 8,000 rpm for 1 min. The filtrates were further diluted with acetonitrile (1:1, v/v) prior to analysis using LC/UV as detailed in the general experimental. The solubility was determined based on the peak area at UV absorbance 254 nm, with reference to the standard calibration curve prepared from 20 mM DMSO stock. Compounds and standards (caffeine and pretomanid) were prepared in duplicate and each sample was analyzed in duplicate by LC/UV.

Ancillary Information

Supporting information

^{1}H and ^{13}C NMR Spectra

2D NMR and crystal structure data (Figure S1, Tables S1-S3) for **17a**

LC/MS/MS detection and analysis parameters for plasma protein binding and metabolic stability Table S4

Supplementary biological data Tables S5-S8

Solubility data Table S9

Molecular formula strings (CSV)

Corresponding Author Information

*E-mail: m.cooper@uq.edu.au; m.blaskovich@uq.edu.au Telephone: +61 7 3346 2045; +61 7 3346 2994

Disclosure

MAC currently holds a fractional Professorial Research Fellow appointment at the University of Queensland with his remaining time as CEO of Inflazome Ltd. a company headquartered in Dublin, Ireland that is developing drugs to address clinical unmet needs in inflammatory disease by targeting the inflammasome.

Present Author Addresses

Novasep (Dynamit Nobel Explosivstoff und Systemtechnik GmbH), Leverkusen, Germany

^ Department of Chemical Biology, Helmholtz Centre for Infection Research, Inhoffenstrasse 7, 38124, Braunschweig, Germany

Acknowledgement

We thank Johnny Huang, Geraldine Kaeslin and Janet Reid for assisting with the cytotoxicity assays and the Community for Open Antimicrobial Drug Discovery[40] for performing MIC assays against the ESKAPE bacteria and fungal pathogens. We thank Alan Fairlamb and Stephen Patterson of the University of Dundee for providing the *R*-enantiomer of PA-824. The antimicrobial screening performed by CO-ADD was funded by the Wellcome Trust (UK) and The University of Queensland (Australia). AMJ was supported by an Australian Postgraduate Award, IMB Research Scholarship and QLD Government Smart Futures PhD scholarship and CWA by a Research Training Program scholarship. AD was supported by the National Institutes of Health (grant no.1KL2TR001444). MLS and AJ were supported by ARC grant LP140100560 and NHMRC Project grant APP1067728 awarded to VMA. MAB was supported by Wellcome Trust Strategic Award 104797/Z/14/Z and NHMRC Development Grant APP113719. MAC was supported by an NHMRC Principal Research Fellowship APP1059354.

Abbreviations Used:

Tuberculosis (TB), Minimal Inhibitory Concentration (MIC), structure activity relationships (SAR)

References and Notes

(1) Ang, C. W.; Jarrad, A. M.; Cooper, M. A.; Blaskovich, M. A. T. Nitroimidazoles: Molecular Fireworks That Combat a Broad Spectrum of Infectious Diseases. *J. Med. Chem.* **2017**, *60* (18), 7636–7657.

(2) Schwebke, J. R.; Morgan, F. G.; Koltun, W.; Nyirjesy, P. A Phase-3, Double-Blind, Placebo-Controlled Study of the Effectiveness and Safety of Single Oral Doses of Secnidazole 2 g for the Treatment of Women with Bacterial Vaginosis. *Am. J. Obstet. & Gynecol.* **2017**, *217* (6), 678.e1–678.e9.

(3) FDA Approves Symbiomix Therapeutics' Solosec™ (Secnidazole) Oral Granules for the

Treatment of Bacterial Vaginosis in Adult Women. https://symbiomix.com/fda-approves-symbiomix-therapeutics-solosec-secnidazole-oral-granules-treatment-bacterial-vaginosis-adult-women/ (accessed September 1, 2018).

(4) Traynor, K. Benznidazole Approved for Chagas Disease in Children. *Am. J. Health-Syst. Pharm.* **2017**, *74* (19), 1519.

(5) Simarro, P. P.; Cecchi, G.; Franco, J. R.; Paone, M.; Diarra, A.; Ruiz-Postigo, J. A.; Fèvre, E. M.; Mattioli, R. C.; Jannin, J. G. Estimating and Mapping the Population at Risk of Sleeping Sickness. *PLoS Neglected Trop. Dis.* **2012**, *6* (10), e1859.

(6) Tiberi, S.; Plessis, du, N.; Walzl, G.; Vjecha, M. J.; Rao, M.; Ntoumi, F.; Mfinanga, S.; Kapata, N.; Mwaba, P.; McHugh, T. D.; Ippolito, G.; Migliori, G. B.; Maeurer, M. J.; Zumla, A. Tuberculosis: Progress and Advances in Development of New Drugs, Treatment Regimens, and Host-Directed Therapies. *Lancet Infect. Dis.* **2018**, *18* (7), e183–e198.

(7) Geneva: World Health Organisation. *Global Tuberculosis Report 2017*; 2017; pp 1–262.

(8) Matsumoto, M.; Hashizume, H.; Tomishige, T.; Kawasaki, M.; Tsubouchi, H.; Sasaki, H.; Shimokawa, Y.; Komatsu, M. OPC-67683, a Nitro-dihydro-imidazooxazole Derivative with Promising Action Against Tuberculosis In Vitro and in Mice. *PLoS Med.* **2006**, *3* (11), e466.

(9) Sasaki, H.; Haraguchi, Y.; Itotani, M.; Kuroda, H.; Hashizume, H.; Tomishige, T.; Kawasaki, M.; Matsumoto, M.; Komatsu, M.; Tsubouchi, H. Synthesis and Antituberculosis Activity of a Novel Series of Optically Active 6-Nitro-2,3-dihydroimidazo[2,1-*b*]oxazoles. *J. Med. Chem.* **2006**, *49* (26), 7854–7860.

(10) Nagarajan, K.; Shankar, R. G.; Rajappa, S.; Shenoy, S.; Costa-pereira, R. Nitroimidazoles XXI 2,3-Dihydro-6-nitroimidazo [2,1-*b*] Oxazoles with Antitubercular Activity. *Eur. J. Med. Chem.* **1989**, *24*, 631–633.

(11) Ashtekar, D. R.; Costa-Perira, R.; Nagrajan, K.; Vishvanathan, N.; Bhatt, A. D.; Rittel, W. In Vitro and In Vivo Activities of the Nitroimidazole CGI 17341 Against *Mycobacterium*

tuberculosis. *Antimicrob. Agents Chemother.* **1993**, *37* (2), 183–186.

(12) Upton, A. M.; Cho, S.; Yang, T. J.; Kim, Y.; Wang, Y.; Lu, Y.; Wang, B.; Xu, J.; Mdluli, K.; Ma, Z.; Franzblau, S. G. In Vitro and in Vivo Activities of the Nitroimidazole TBA-354 Against *Mycobacterium tuberculosis*. *Antimicrob. Agents Chemother.* **2015**, *59* (1), 136–144.

(13) Manjunatha, U.; Boshoff, H. I.; Barry, C. E. The Mechanism of Action of PA-824: Novel Insights From Transcriptional Profiling. *Commun. Integr. Biol.* **2009**, *2* (3), 215–218.

(14) Singh, R.; Manjunatha, U.; Boshoff, H. I. M.; Ha, Y. H.; Niyomrattanakit, P.; Ledwidge, R.; Dowd, C. S.; Lee, I. Y.; Kim, P.; Zhang, L.; Kang, S.; Keller, T. H.; Jiricek, J.; Barry, C. E. PA-824 Kills Nonreplicating *Mycobacterium tuberculosis* by Intracellular NO Release. *Science* **2008**, *322* (5906), 1392–1395.

(15) Wayne, L. G.; Hayes, L. G. An In Vitro Model for Sequential Study of Shiftdown of *Mycobacterium tuberculosis* Through Two Stages of Nonreplicating Persistence. *Infect. Immun.* **1996**, *64* (6), 2062–2069.

(16) Patterson, S.; Wyllie, S.; Stojanovski, L.; Perry, M. R.; Simeons, F. R. C.; Norval, S.; Osuna-Cabello, M.; De Rycker, M.; Read, K. D.; Fairlamb, A. H. The *R* Enantiomer of the Antitubercular Drug PA-824 as a Potential Oral Treatment for Visceral Leishmaniasis. *Antimicrob. Agents Chemother.* **2013**, *57* (10), 4699–4706.

(17) Wyllie, S.; Roberts, A. J.; Norval, S.; Patterson, S.; Foth, B. J.; Berriman, M.; Read, K. D.; Fairlamb, A. H. Activation of Bicyclic Nitro-Drugs by a Novel Nitroreductase (NTR2) in *Leishmania*. *PLoS Pathog.* **2016**, *12* (11), e1005971.

(18) Wyllie, S.; Patterson, S.; Stojanovski, L.; Simeons, F. R. C.; Norval, S.; Kime, R.; Read, K. D.; Fairlamb, A. H. The Anti-Trypanosome Drug Fexinidazole Shows Potential for Treating Visceral Leishmaniasis. *Sci. Transl. Med.* **2012**, *4* (119), 119re1.

(19) Thompson, A. M.; Marshall, A. J.; Maes, L.; Yarlett, N.; Bacchi, C. J.; Gaukel, E.; Wring, S. A.; Launay, D.; Braillard, S.; Chatelain, E.; Mowbray, C. E.; Denny, W. A. Assessment of a

Pretomanid Analogue Library for African Trypanosomiasis: Hit-to-Lead Studies on 6-Substituted 2-Nitro-6,7-dihydro-5*H*-imidazo[2,1-*b*][1,3]thiazine 8-oxides. *Bioorg. Med. Chem. Lett.* **2018**, *28* (2), 207–213.

(20) Thompson, A. M.; Bonnet, M.; Lee, H. H.; Franzblau, S. G.; Wan, B.; Wong, G. S.; Cooper, C. B.; Denny, W. A. Antitubercular Nitroimidazoles Revisited: Synthesis and Activity of the Authentic 3-Nitro Isomer of Pretomanid. *ACS Med. Chem. Lett.* **2017**, *8* (12), 1275–1280.

(21) Kim, P.; Kang, S.; Boshoff, H. I.; Jiricek, J.; Collins, M.; Singh, R.; Manjunatha, U. H.; Niyomrattanakit, P.; Zhang, L.; Goodwin, M. Structure−Activity Relationships of Antitubercular Nitroimidazoles. 2. Determinants of Aerobic Activity and Quantitative Structure−Activity Relationships. *J. Med. Chem.* **2009**, *52* (5), 1329–1344.

(22) Lakshminarayana, S. B.; Boshoff, H. I. M.; Cherian, J.; Ravindran, S.; Goh, A.; Jiricek, J.; Nanjundappa, M.; Nayyar, A.; Gurumurthy, M.; Singh, R.; Dick, T.; Blasco, F.; Barry, C. E.; Ho, P. C.; Manjunatha, U. H. Pharmacokinetics-Pharmacodynamics Analysis of Bicyclic 4-Nitroimidazole Analogs in a Murine Model of Tuberculosis. *PLoS One* **2014**, *9* (8), e105222.

(23) Thompson, A. M.; Blaser, A.; Anderson, R. F.; Shinde, S. S.; Franzblau, S. G.; Ma, Z.; Denny, W. A.; Palmer, B. D. Synthesis, Reduction Potentials, and Antitubercular Activity of Ring A/B Analogues of the Bioreductive Drug (6*S*)-2-Nitro-6-{[4-(trifluoromethoxy)benzyl]oxy}-6,7-dihydro-5 *H*-imidazo[2,1-*b*][1,3]oxazine (PA-824). *J. Med. Chem.* **2009**, *52* (3), 637–645.

(24) Drugs for Neglected Diseases *initiative*. Nitroimidazoles (VL) – DND*i*. https://www.dndi.org/diseases-projects/portfolio/nitroimidazole/. (accessed September 1, 2018).

(25) Thompson, A. M.; O'Connor, P. D.; Marshall, A. J.; Yardley, V.; Maes, L.; Gupta, S.; Launay, D.; Braillard, S.; Chatelain, E.; Franzblau, S. G.; Wan, B.; Wang, Y.; Ma, Z.; Cooper, C. B.; Denny, W. A. 7-Substituted 2-Nitro-5,6-dihydroimidazo[2,1-*b*][1,3]oxazines: Novel Antitubercular Agents Lead to a New Preclinical Candidate for Visceral Leishmaniasis. *J. Med. Chem.* **2017**, *60* (10), 4212–4233.

(26) Thompson, A. M.; O'Connor, P. D.; Marshall, A. J.; Blaser, A.; Yardley, V.; Maes, L.; Gupta, S.; Launay, D.; Braillard, S.; Chatelain, E.; Wan, B.; Franzblau, S. G.; Ma, Z.; Cooper, C. B.; Denny, W. A. Development of (6*R*)-2-Nitro-6-[4-(trifluoromethoxy)phenoxy]-6,7-dihydro-5*H*-imidazo[2,1-*b*][1,3]oxazine (DNDI-8219): A New Lead for Visceral Leishmaniasis. *J. Med. Chem.* **2018**, *61* (6), 2329–2352.

(27) Thompson, A. M.; Blaser, A.; Palmer, B. D.; Anderson, R. F.; Shinde, S. S.; Launay, D.; Chatelain, E.; Maes, L.; Franzblau, S. G.; Wan, B.; Wang, Y.; Ma, Z.; Denny, W. A. 6-Nitro-2,3-dihydroimidazo[2,1-*b*][1,3]thiazoles: Facile Synthesis and Comparative Appraisal Against Tuberculosis and Neglected Tropical Diseases. *Bioorg. Med. Chem. Lett.* **2017**, *27* (11), 2583–2589.

(28) Jarrad, A. M.; Debnath, A.; Miyamoto, Y.; Hansford, K. A.; Pelingon, R.; Butler, M. S.; Bains, T.; Karoli, T.; Blaskovich, M. A. T.; Eckmann, L.; Cooper, M. A. Nitroimidazole Carboxamides as Antiparasitic Agents Targeting *Giardia lamblia*, *Entamoeba histolytica* and *Trichomonas vaginalis*. *Eur. J. Med. Chem.* **2016**, *120*, 353–362.

(29) Goodacre, S. C.; Hallett, D. J.; Carling, R. W.; Castro, J. L.; Reynolds, D. S.; Pike, A.; Wafford, K. A.; Newman, R.; Atack, J. R.; Street, L. J. Imidazo[1,2-*a*]pyrazin-8-ones, Imidazo[1,2-*d*][1,2,4]triazin-8-ones and Imidazo[2,1-*f*][1,2,4]triazin-8-ones as Alpha2/Alpha3 Subtype Selective GABAA Agonists for the Treatment of Anxiety. *Bioorg. Med. Chem. Lett.* **2006**, *16* (6), 1582–1585.

(30) Mignani, S.; Aloup, J. C.; Barreau, M. Synthesis and Pharmacological Properties of 5*H*, 10*H*-Imidazo[1,2-*a*]indeno[1,2-*e*]pyrazine-4-one, A New Competitive AMPA/KA Receptor Antagonist. *Drug Dev. Res.* **1999**, *48*, 121–129.

(31) Stutzmann, J.-M.; Bohme, G. A.; Boireau, A.; Damour, D.; Debono, M.-W.; Genevois-Borella, A.; Imperato, A.; Jimonet, P.; Pratt, J.; Randle, J. C. R.; Ribeill, Y.; Vuilhorgne, M.; Mignani, S. 4,10-Dihydro-4-oxo-4*H*-imidazo[1,2-*a*]indeno[1,2-*e*]pyrazin-2-carboxylic Acid Derivatives.

Bioorg. Med. Chem. Lett. **2000**, *10* (10), 1133–1137.

(32) Plouvier, B. M. C.; Fedida, D.; Beatch, G. N.; Chou, D. T. H.; Yifru, A. S.; Jung, G. Imidazo Compounds and Uses Thereof. WO 2005/034837. April 21, 2005.

(33) Couturier, C.; Silve, S.; Morales, R.; Pessegue, B.; Llopart, S.; Nair, A.; Bauer, A.; Scheiper, B.; P verlein, C.; Ganzhorn, A.; Lagrange, S.; Bacqu, E. Nanomolar Inhibitors of *Mycobacterium tuberculosis* Glutamine Synthetase 1: Synthesis, Biological Evaluation and X-Ray Crystallographic Studies. *Bioorg. Med. Chem. Lett.* **2015**, *25* (7), 1455–1459.

(34) Rao, A. K. S. B.; Rao, C. G.; Singh, B. B. Regioselective Alkylation of 4(5)-Nitro-1*H*-imidazoles in Acidic Media: Study of Temperature Effects. *J. Chem. Soc., Perkin Trans. 1* **1994**, No. 17, 2399–2402.

(35) Prevot, I.; Leumann, C. J. Evaluation of Novel Third-Strand Bases for the Recognition of a C· G Base Pair in the Parallel DNA Triple-Helical Binding Motif. *Helv. Chim. Acta* **2002**, *85* (2), 502–515.

(36) Plettenburg, O.; Hofmeister, A.; Kadereit, D.; Brendel, J.; Loehn, M. Cyclohexylamin Isoquinolone Derivatives as Rho-Kinase Inhibitors. WO2007012422A1. February 1, 2007.

(37) Singh, B.; Cavalluzzo, C.; De Maeyer, M.; Debyser, Z.; Parmar, V.; Van der Eycken, E. Microwave-Assisted Silver(I)-Mediated Selective *O*-Alkylation of Aromatic Imidate Systems. *Synthesis* **2009**, *16*, 2725–2728.

(38) Semple, G.; Andersson, B.-M.; Chhajlani, V.; Georgsson, J.; Johansson, M. J.; Rosenquist, Å.; Swanson, L. Synthesis and Biological Activity of Kappa Opioid Receptor Agonists. Part 2: Preparation of 3-Aryl-2-pyridone Analogues Generated by Solution- and Solid-Phase Parallel Synthesis Methods. *Bioorg. Med. Chem. Lett.* **2003**, *13* (6), 1141–1145.

(39) Gurumurthy, M.; Mukherjee, T.; Dowd, C. S.; Singh, R.; Niyomrattanakit, P.; Tay, J. A.; Nayyar, A.; Lee, Y. S.; Cherian, J.; Boshoff, H. I.; Dick, T.; Barry, C. E., III; Manjunatha, U. H. Substrate Specificity of the Deazaflavin-Dependent Nitroreductase from *Mycobacterium tuberculosis*

Responsible for the Bioreductive Activation of Bicyclic Nitroimidazoles. *FEBS J.* **2011**, *279* (1), 113–125.

(40) Blaskovich, M. A. T.; Zuegg, J.; Elliott, A. G.; Cooper, M. A. Helping Chemists Discover New Antibiotics. *ACS Infect. Dis.* **2015**, *1* (7), 285–287.

(41) Kim, P.; Zhang, L.; Manjunatha, U. H.; Singh, R.; Patel, S.; Jiricek, J.; Keller, T. H.; Boshoff, H. I.; Barry, C. E., III; Dowd, C. S. Structure−Activity Relationships of Antitubercular Nitroimidazoles. 1. Structural Features Associated with Aerobic and Anaerobic Activities of 4- and 5-Nitroimidazoles. *J. Med. Chem.* **2009**, *52* (5), 1317–1328.

(42) Liu, X.; Wright, M.; Hop, C. E. C. A. Rational Use of Plasma Protein and Tissue Binding Data in Drug Design. *J. Med. Chem.* **2014**, *57* (20), 8238–8248.

(43) de Angelis, I.; Turco, L. Caco-2 Cells as a Model for Intestinal Absorption. *Curr. Protoc. Toxicol.* **2011**, *47*, 20.6.1–20.6.15.

(44) Xavier, A. S.; Lakshmanan, M. Delamanid: A New Armor in Combating Drug-Resistant Tuberculosis. *J. Pharmacol. Pharmacother.* **2014**, *5* (3), 222–224.

(45) Katsuno, K.; Burrows, J. N.; Duncan, K.; Hooft van Huijsduijnen, R.; Kaneko, T.; Kita, K.; Mowbray, C. E.; Schmatz, D.; Warner, P.; Slingsby, B. T. Hit and Lead Criteria in Drug Discovery for Infectious Diseases of the Developing World. *Nat. Rev. Drug Discovery* **2015**, *14* (11), 751–758.

(46) Blaser, A.; Palmer, B. D.; Sutherland, H. S.; Kmentova, I.; Franzblau, S. G.; Wan, B.; Wang, Y.; Ma, Z.; Thompson, A. M.; Denny, W. A. Structure–Activity Relationships for Amide-, Carbamate-, and Urea-Linked Analogues of the Tuberculosis Drug (6*S*)-2-Nitro-6-{[4-(tifluoromethoxy)benzyl]oxy}-6,7-dihydro-5*H*-imidazo[2,1-*b*][1, 3]oxazine (PA-824). *J. Med. Chem.* **2011**, *55* (1), 312–326.

(47) Sutherland, H. S.; Blaser, A.; Kmentova, I.; Franzblau, S. G.; Wan, B.; Wang, Y.; Ma, Z.; Palmer, B. D.; Denny, W. A.; Thompson, A. M. Synthesis and Structure-Activity Relationships

of Antitubercular 2-Nitroimidazooxazines Bearing Heterocyclic Side Chains. *J. Med. Chem.* **2010**, *53* (2), 855–866.

(48) Dreier, L.; Wider, G. Concentration Measurements by PULCON Using X-Filtered or 2D NMR Spectra. *Magn. Reson. Chem.* **2006**, *44*, S206–S212.

(49) Jarrad, A. M.; Karoli, T.; Debnath, A.; Tay, C. Y.; Huang, J. X.; Kaeslin, G.; Elliott, A. G.; Miyamoto, Y.; Ramu, S.; Kavanagh, A. M.; Zuegg, J.; Eckmann, L.; Blaskovich, M. A. T.; Cooper, M. A. Metronidazole-Triazole Conjugates: Activity Against *Clostridium difficile* and Parasites. *Eur. J. Med. Chem.* **2015**, *101*, 96–102.

(50) Tran, A. T.; West, N. P.; Britton, W. J.; Payne, R. J. Elucidation of *Mycobacterium tuberculosis* Type II Dehydroquinase Inhibitors Using a Fragment Elaboration Strategy. *ChemMedChem* **2012**, *7* (6), 1031–1043.

(51) Taneja, N. K.; Tyagi, J. S. Resazurin Reduction Assays for Screening of Anti-Tubercular Compounds Against Dormant and Actively Growing *Mycobacterium tuberculosis*, *Mycobacterium bovis* BCG and *Mycobacterium smegmatis*. *J. Antimicrob. Chemother.* **2007**, *60* (2), 288–293.

(52) Townson, S. M.; Laqua, H.; Upcroft, P.; Boreham, P. F.; Upcroft, J. A. Induction of Metronidazole and Furazolidone Resistance in *Giardia*. *Trans. R. Soc. Trop. Med. Hyg.* **1992**, *86* (5), 521–522.

(53) Diamond, L. S.; Harlow, D. R.; Cunnick, C. C. A New Medium for the Axenic Cultivation of *Entamoeba histolytica* and Other *Entamoeba*. *Trans. R. Soc. Trop. Med. Hyg.* **1978**, *72* (4), 431–432.

(54) Debnath, A.; Parsonage, D.; Andrade, R. M.; He, C.; Cobo, E. R.; Hirata, K.; Chen, S.; García-Rivera, G.; Orozco, E.; Martínez, M. B.; Gunatilleke, S. S.; Barrios, A. M.; Arkin, M. R.; Poole, L. B.; McKerrow, J. H.; Reed, S. L. A High-Throughput Drug Screen for *Entamoeba histolytica* Identifies a New Lead and Target. *Nat. Med.* **2012**, *18* (6), 956–960.

(55) Sykes, M. L.; Avery, V. M. Development of an Alamar Blue™ Viability Assay in 384-Well Format for High Throughput Whole Cell Screening of *Trypanosoma brucei brucei* Bloodstream Form Strain 427. *Am. J. Trop. Med. Hyg.* **2009**, *81* (4), 665–674.

(56) Sykes, M. L.; Baell, J. B.; Kaiser, M.; Chatelain, E.; Moawad, S. R.; Ganame, D.; Ioset, J.-R.; Avery, V. M. Identification of Compounds with Anti-Proliferative Activity Against *Trypanosoma brucei brucei* Strain 427 by a Whole Cell Viability Based HTS Campaign. *PLoS Neglected Trop. Dis.* **2012**, *6* (11), e1896.

(57) Duffy, S.; Sykes, M. L.; Jones, A. J.; Shelper, T. B.; Simpson, M.; Lang, R.; Poulsen, S.-A.; Sleebs, B. E.; Avery, V. M. Screening the Medicines for Malaria Venture Pathogen Box Across Multiple Pathogens Reclassifies Starting Points for Open-Source Drug Discovery. *Antimicrob. Agents Chemother.* **2017**, *61* (9).

(58) Zhang, F.; Xue, J.; Shao, J.; Jia, L. Compilation of 222 Drugs' Plasma Protein Binding Data and Guidance for Study Designs. *Drug Discovery Today* **2012**, *17* (9-10), 475–485.

(59) Di, L.; Kerns, E. H. Plasma Protein Binding Methods. In *Drug-like Properties: Concepts, Structure Design and Methods*; Academic Press: San Diego, CA, 2008; pp 372–377.

Table of Contents Graphic

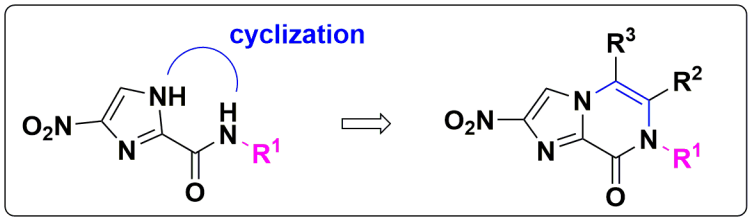

- Active against *G. lamblia*, *T. b. brucei* and *M. tuberculosis*
- Non-cytotoxic against mammalian cells
- Good ADME properties

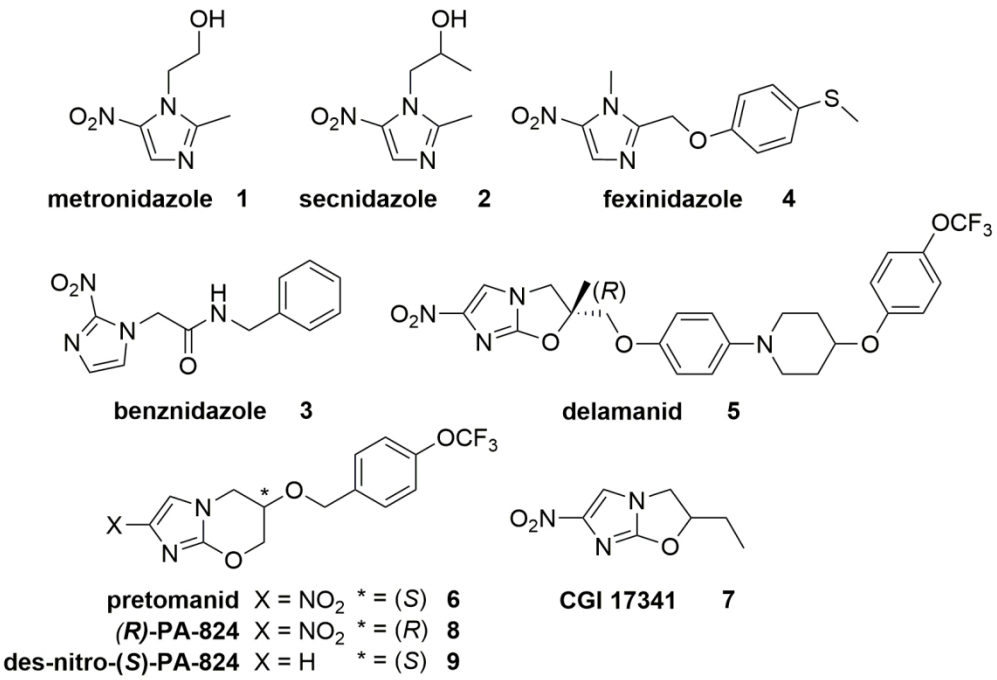

Figure 1

144x98mm (300 x 300 DPI)

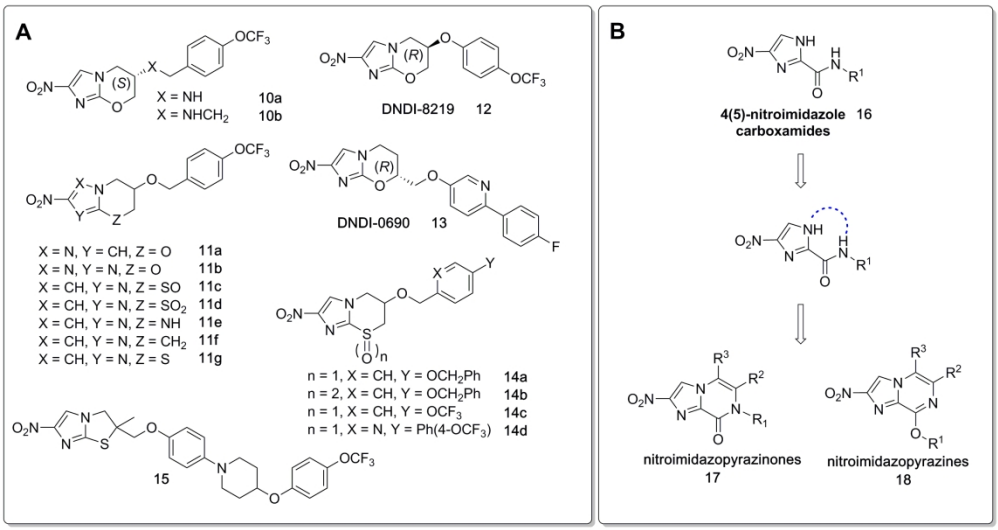

Figure 2

250x132mm (300 x 300 DPI)

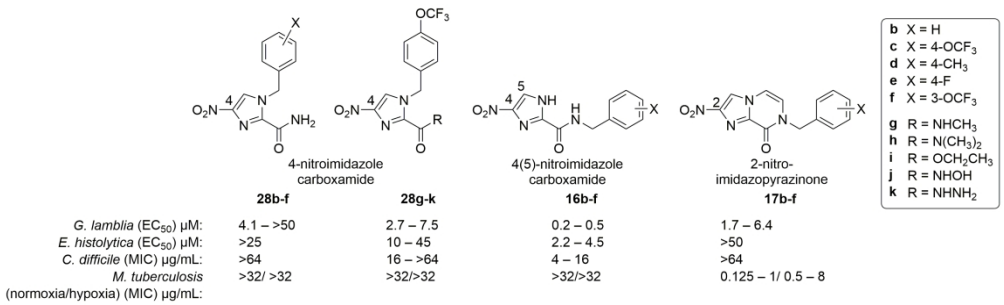

Figure 3

262x79mm (300 x 300 DPI)

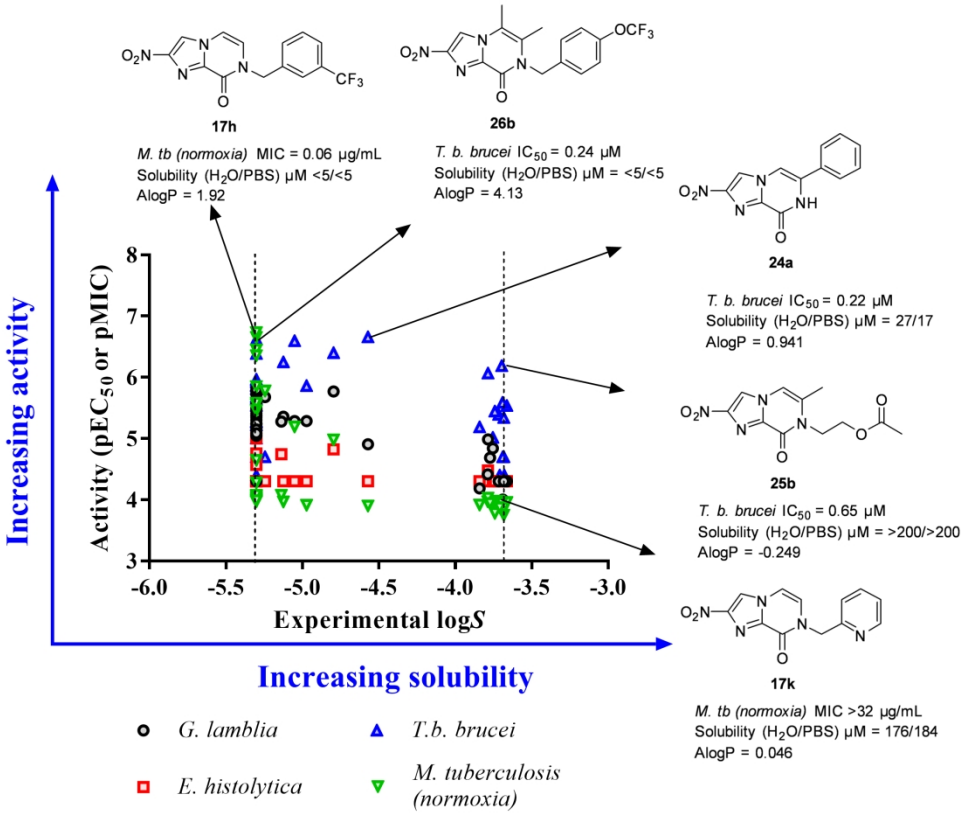

Figure 4

224x193mm (300 x 300 DPI)

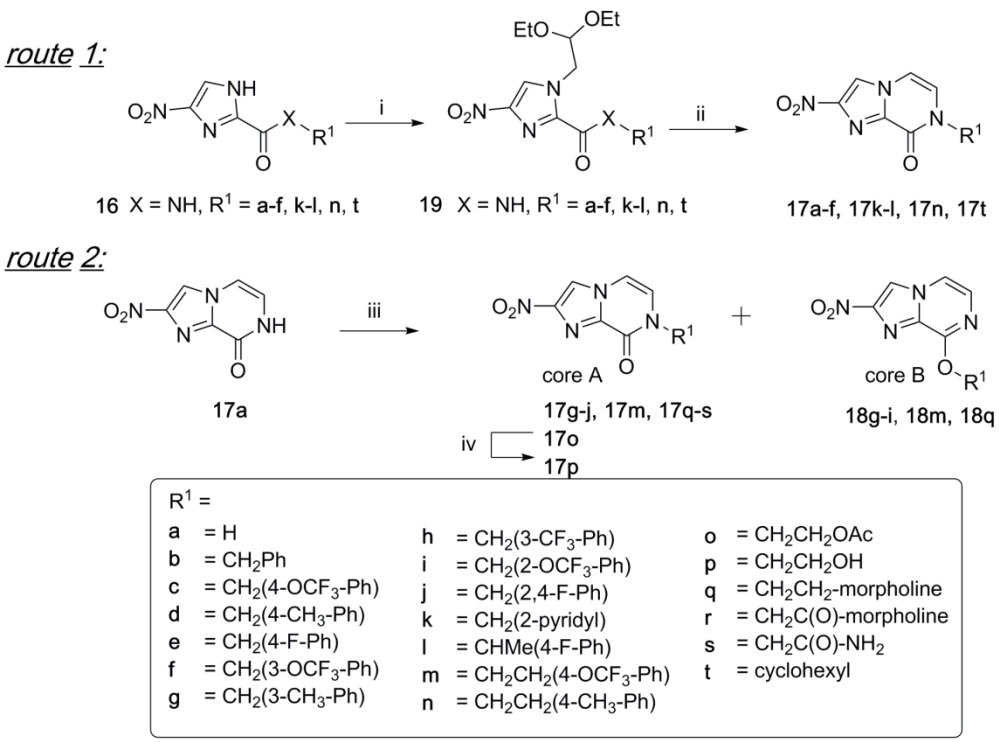

Scheme 1

168x124mm (300 x 300 DPI)

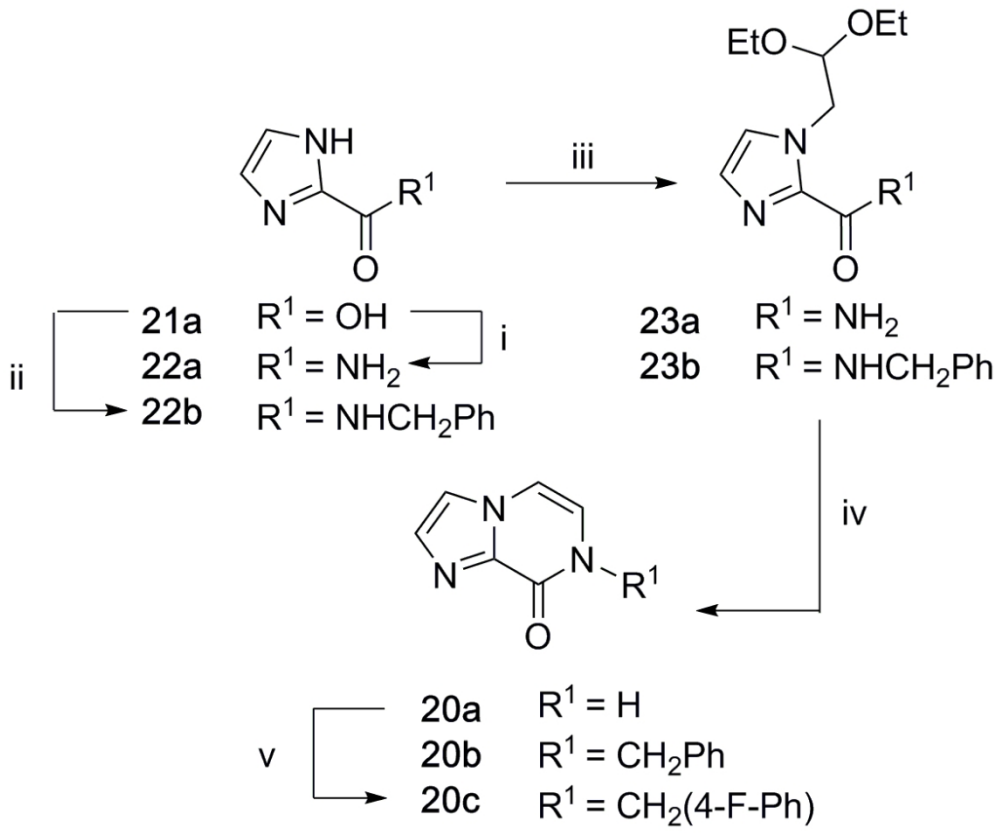

Scheme 2

99x82mm (300 x 300 DPI)

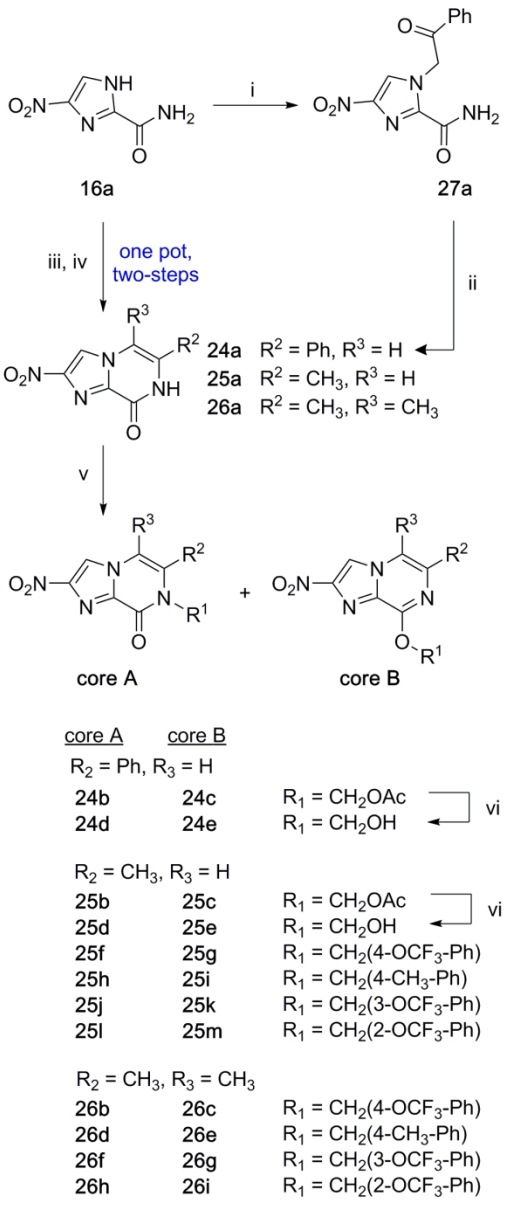

Scheme 3

88x208mm (300 x 300 DPI)

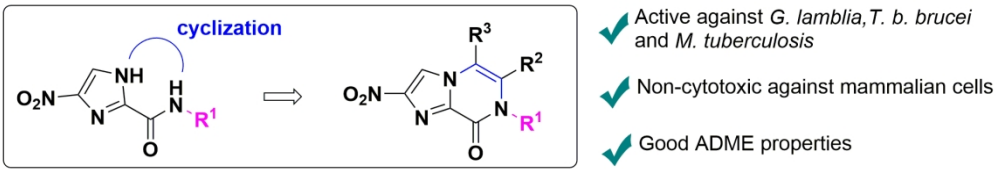

Graphical abstract

171x29mm (300 x 300 DPI)